MODELING THE EFFECTS OF CLIMATE CHANGE ON STREAMFLOW IN A SUB-BASIN OF THE LOWER CHURCHILL RIVER LABRADOR

AMY PRYSE-PHILLIPS

MODELING THE EFFECTS OF CLIMATE CHANGE ON STREAMFLOW IN A SUB-BASIN OF THE LOWER CHURCHILL RIVER, LABRADOR

by

© Amy Pryse-Phillips

A thesis submitted to the

School of Graduate Studies

in partial fulfilment of the

requirements for the degree of

Master of Engineering

Faculty of Engineering and Applied Science

Memorial University of Newfoundland

October 2010

St. John's, Newfoundland & Labrador

Abstract

Future streamflow in the Churchill River is of great interest to Nalcor Energy, the Newfoundland and Labrador energy corporation that is currently planning the development of a 3,074 MW hydroelectric project in Labrador. The current study investigates the potential impacts of climate change on streamflow in a sub-basin of the lower Churchill River.

In this study, a dynamically downscaled future climate scenario is used to drive a hydrological model of the Pinus River basin to assess climate change impacts on localized streamflow between current (1969-2000) and future (2039-2070) periods. The WATFLOOD hydrological model has been selected for this purpose while the North American Regional Climate Change Assessment Program has served as the source of regional climate model (RCM) data.

Biases were detected in RCM temperature and precipitation and non-linear bias-correction procedures were applied prior to simulation in the hydrological model. The results indicated a 13 percent increase in mean annual flow, concentrated in the winter and spring seasons.

Acknowledgements

I thank the following individuals and groups for their support and contributions over the past one and a half years, without which the completion of this work would not have been possible.

Dr. Kenneth Snelgrove (Faculty of Engineering and Applied Science, Memorial University) for his suggestions, teachings, support, and encouragement throughout the project. His detailed explanations and big-picture rationalizations provided essential enlightening.

Dr. Nicholas Kouwen (Distinguished Professor Emeritus at the University of Waterloo, Ontario, Canada) for sharing his expertise related to the WATFLOOD hydrological model set-up and calibration portion of the research.

Hatch Limited in St. John's for making it possible for me to undertake this project.

Nalcor Energy (Lower Churchill Project) for funding this research.

Table of Contents

List of Tables

List of Figures

List of Abbreviations

AHCCD	Adjusted Historical Canadian Climate Database
AR4	IPCC Fourth Assessment Report
CF	Churchill Falls
CGCM3	Coupled General Circulation Model version 3
CRCM	Canadian Regional Climate Model
CV	Coefficient of Variation
DEM	Digital Elevation Model
EC	Environment Canada
GB	Goose Bay
GCM	General Circulation Model/ Global Climate Model
GDP	Gross Domestic Product
GHG	Greenhouse Gas Emissions
GIS	Geographical Information System
GRU	Grouped Response Unit
IPCC	Intergovernmental Panel on Climate Change
MAR	Mean Annual Runoff
NARCCAP	North American Regional Climate Change Assessment Program
NASA	National Aeronautics and Space Administration
NCEP	National Centre for Environmental Prediction
NGA	National Geospatial-Intelligence Agency
NL	Newfoundland and Labrador
NTDB	National Topographic Database
NWP	Numerical Weather Prediction
RCM	Regional Climate Model
SRES	Special Report on Emissions Scenarios
SRTM	Shuttle Radar Topographical Mission
UNEP	United Nations Environment Programme
WMO	World Meteorological Association
WSC	Water Survey of Canada

List of Appendices

Chapter 1 Introduction

1.1 Background

This research forms an early part of a broader study being conducted at Memorial University of Newfoundland and funded by Nalcor Energy (Nalcor), Newfoundland and Labrador's (NL) energy corporation. The main objective of the overall research project is to assess the impact of climate change on the hydroelectric potential of the proposed Lower Churchill Hydroelectric Development in Labrador, Canada.

The hydroelectric potential of the Churchill River has yet to be fully developed. The Churchill Falls generating station, which began producing electricity in 1971, harnesses about 65 percent of the total hydroelectric potential of the river. Development of the remaining 35 percent is being proposed by Nalcor as the Lower Churchill Project. The project, which consists of two dams (at Gull Island and Muskrat Falls), has a total installed capacity of 3,074 MW and is considered one of the most attractive undeveloped hydro projects in North America on a number of fronts. The cost of this development is estimated at between six and nine billion dollars, depending on the development options chosen. Planning and operational considerations for the project are paramount, as this development will continue to produce power well into the future. Figure 1.1 illustrates the project location.

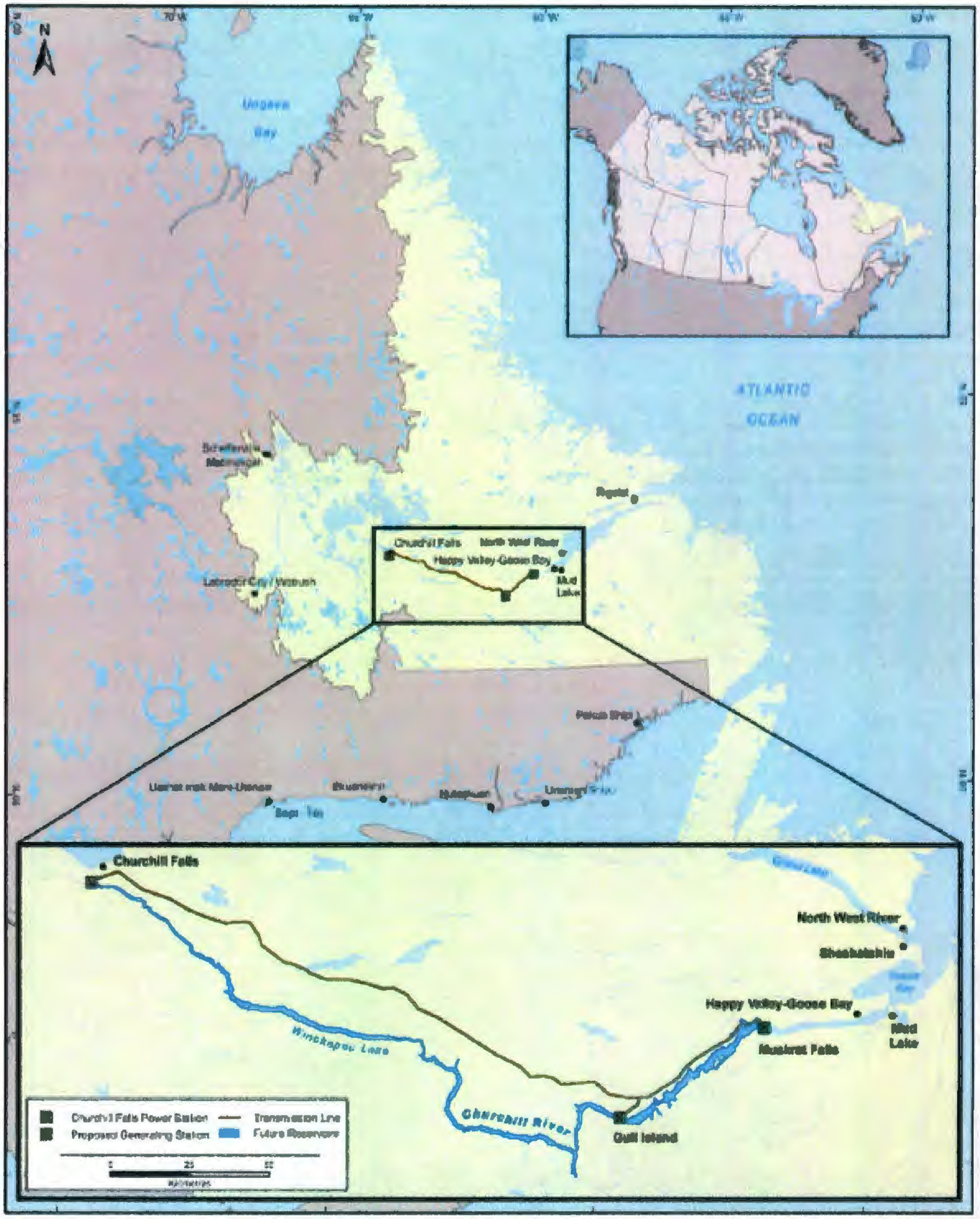

Figure 1.1 Location of the Lower Churchill Hydroelectric Project (Nalcor, 2009)

The Lower Churchill Project has the potential to significantly reduce the greenhouse gas emissions (GHG) from within and outside the Province through the displacement of thermal generation sources. Renewable energy from the Lower Churchill Project could displace over 16 megatonnes of carbon dioxide emissions every year from thermal, coal and fossil fuel power generation – equivalent to the annual greenhouse gas emissions from 3.2 million automobiles (Government of NL, 2010). The Province already produces the largest quantity of electricity per capita than any other jurisdiction in the world and hydroelectricity is the predominant source (NL Provincial Energy Plan, 2007). Figure 1.2 presents the key electricity assets in the Province including hydro plants, thermal plants, gas turbines, and proposed wind developments. The locations of the proposed Gull Island and Muskrat Falls hydro plants are shown in this figure.

Forecasting of reservoir inflows is an important part of the operation and planning of any hydroelectric development. Hourly forecasts are often required to make short term decisions related to the efficient operation of the system; longer term forecasts are also very important, especially for systems with large reservoirs having multi-year storage potential. These longer term hydrologic forecasts, at climate time scales, are also fundamental for planning future hydroelectric developments such as the Lower Churchill Project. As climate and hydrology are inextricably linked, it is essential that climate change impacts on basin hydrology are considered in the planning stages of the project.

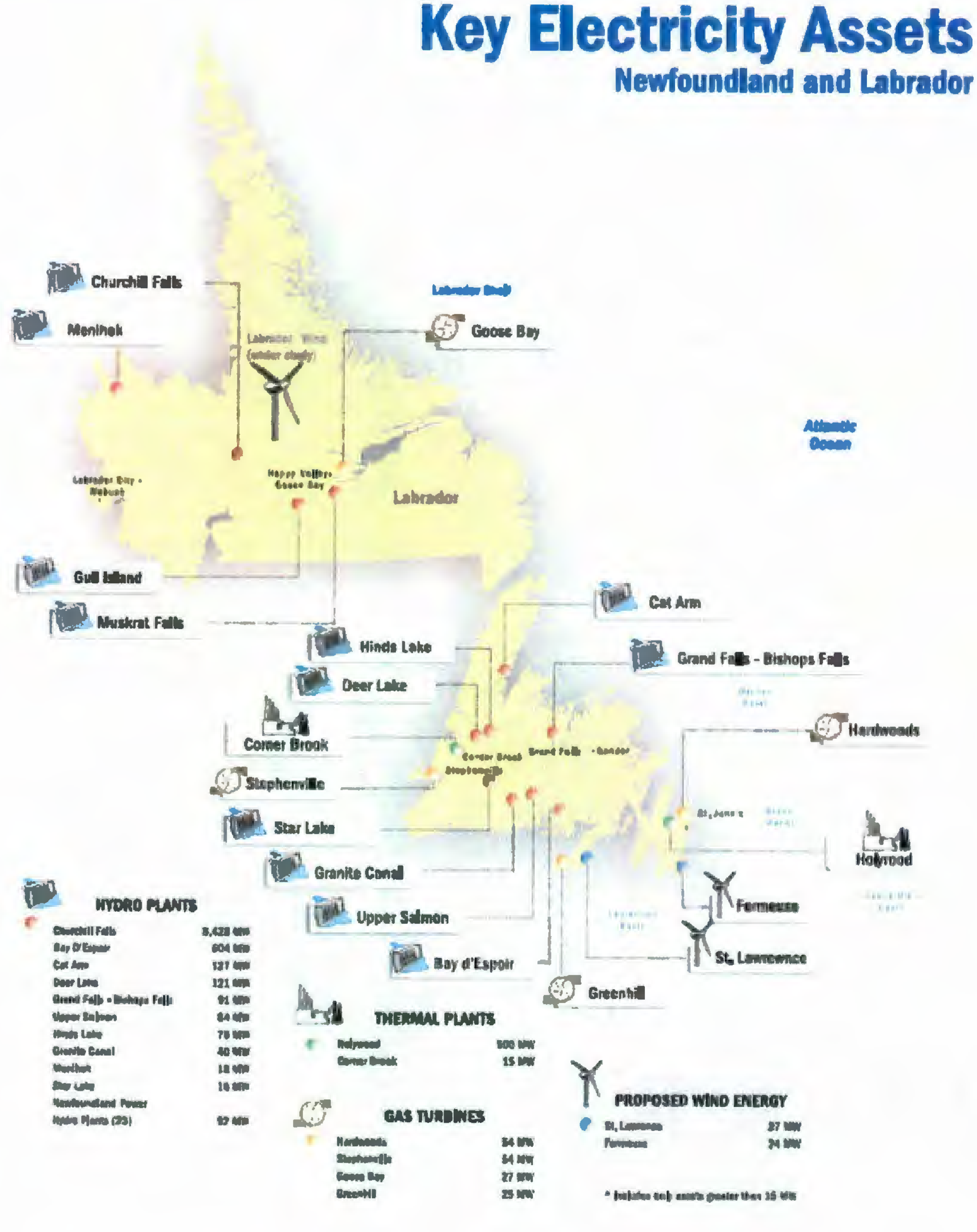

Figure 1.2 Key Electricity Assets of Newfoundland and Labrador (Government of NL, 2007)

The Intergovernmental Panel on Climate Change (IPCC) is a scientific body that was established in 1988 by the United Nations Environment Programme (UNEP) and the World Meteorological Association (WMO) to provide the world with a clear scientific view on the current state of climate change and its potential environmental and socio-economic consequences (IPCC, 2010). In the IPCC Technical Paper VI "Climate Change and Water" (IPCC, 2008), it is stated that "Observational records and climate projections provide abundant evidence that freshwater resources are vulnerable and have the potential to be strongly impacted by climate change, with wide-ranging consequences for human societies and ecosystems". In the same report, the IPCC present the image shown in Figure 1.3 which illustrates the mean of the runoff projections of fifteen different general circulation models (GCMs). These results are based on the A1B emission scenario and illustrate the simulated annual change in runoff for the period 2080-2099 relative to 1980-1999.

Results presented in Figure 1.3 are based on coarse-scale modeling and are therefore not expected to be highly accurate for any region in particular, but nonetheless they do show the general direction and magnitude of expected changes. In Labrador, runoff is expected to increase by between 10 and 20 percent. Stippled regions of the map (of which Labrador is one) indicate areas for which at least 80 percent of the models agree with the direction of the change.

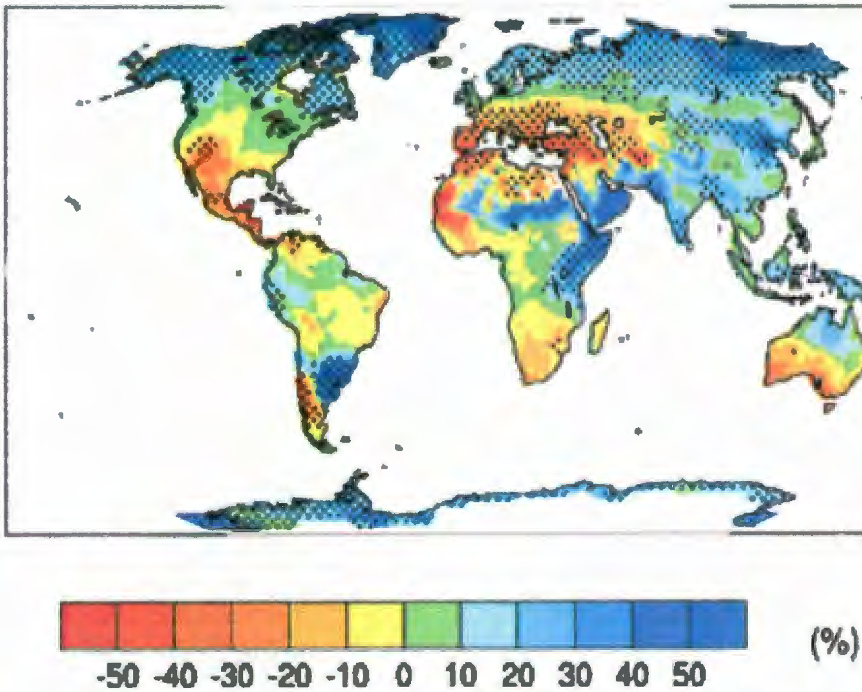

Figure 1.3 Projected Runoff Changes (IPCC, 2008) (black dots indicate regions for which at least 80% of the models agree with the direction of change)

Based on the extensive variability and the magnitude of projected runoff changes, it would be prudent for any hydroelectric developer to conduct further research to investigate local influences and details related to the time evolution of these changes. The current research attempts to do just that, as detailed further in the following section.

1.2 Objectives

The main objectives of the research program include the following:

1. To develop and implement a method for relating changes in surface climate to changes in runoff regimes for the Lower Churchill river system.

2. To develop an initial assessment of how climate change will affect the Lower Churchill river system using regionally downscaled climate data.

The expected outcome of the current research is not to provide a definitive result but rather to test various data sets and methods and develop an approach for the assessment of climate change impacts on the hydroelectric potential of the Lower Churchill Project. As with any good engineering study, the problem should be considered from multiple points of view, and this study presents one possible method of examining the research question. The research is expected to be extended in the future to include regional climate modeling reservoir operational modeling, energy consumption forecasting, and other related studies.

The research which is summarized in this thesis consisted of the following steps.

- Set-up and calibrate a numerical hydrological model for the Pinus River Basin (a sub-basin of the Lower Churchill River watershed).

- Obtain and analyse regionally downscaled climate data (temperature and precipitation) for both current and future climate periods.

- Assess the error contributions associated with the downscaling methods versus the total model error through the assessment of downscaled reanalysis data.

- Use the calibrated hydrological model to simulate current and future period streamflow scenarios.

- Analyse the results of the hydrological simulations to assess the impact of climate change on seasonal and average annual river flow.

Climate change is likely to affect extreme flows (floods and droughts) as well as average flows. The magnitude of extreme events is an important consideration for hydroelectric power producers, especially as it relates to dam safety and assurance of sufficient spillway capacity to safely pass the design flood. Flow peaks can also affect hydroelectric potential but this is less important for large reservoirs such as Gull Island and Muskrat Falls that are able to attenuate and store high inflows. This research has not considered extreme events and is limited to an analysis of average flow in the Pinus River, a tributary of the Churchill River.

1.3 Organization of Thesis

This thesis has been organized into eight sections as follows. Section 2 describes a review of the literature related to climate change and water resources, and in particular, climate downscaling methods and the use of hydrological models as a means of translating climate inputs into streamflow impacts. Section 3 describes data collection and provides a description of the study basin including climate, topography, physiographic characteristics, and streamflow. Section 4 describes the WATFLOOD hydrological model which was used in this study to simulate long term flow in the Pinus River. Section 5 describes the downscaled climate data used, compares downscaled and observed climate, and illustrates bias-correction methods used to pre-process climate data prior to simulation in the hydrological model. Section 6 summarizes the results of the hydrological simulations of the current and future climate periods, and the changes in simulated streamflow between the two periods. Also discussed in this section is an analysis of model error through the simulation of downscaled reanalysis data. Section 7 presents a discussion of the research approach and outcomes, and Section 8 summarizes some recommended areas to be the subject of future research.

Chapter 2 Literature Review

2.1 Climate Change and Water Resources

As the impacts of a changing climate become increasingly evident around the world, the focus of many scientists has shifted from analyzing the occurrence of climate change to mitigation and adaptation measures. With changes in global temperature and precipitation patterns, water availability will be affected, both in magnitude and in timing. Some hydrological trends observed in North America during the 20th century are likely attributable to climate change. These include earlier snowmelt peaks, decreased proportion of frozen precipitation, decreased duration and extent of snow cover, increased and decreased annual precipitation, increased and decreased summer runoff, increased thawing of permafrost, increased water temperatures, decreased glacial mass, and increased drought (Wilby, 2008). As water is the "fuel" of hydroelectric generation projects, such changes in the hydrologic cycle are of utmost interest to hydropower producers.

The effect of climate change on streamflow has been studied for numerous basins around the world. The results of a study for the Lule River basin in Northern Sweden indicated an overall increase in streamflow, earlier spring peak and an increase in hydropower potential (Graham, 2006). A study of the Chaudière River basin in Québec, Canada suggested a slight decrease in annual runoff (Quilbé, 2008). The impact of climate change on the Chute-du-Diable watershed, also in Québec, indicate an earlier spring flood with most scenarios suggesting increases in winter, spring, and fall discharge, and decreases in summer discharge. An assessment of the impact of climate change on low flow in the River Thames in the United Kingdom suggests that substantial reduction in summer precipitation leads to reduced flow in late summer and autumn (Diaz-Nieto, 2005).

Ouranos is a private non-profit research and development consortium based in Québec, Canada that focuses on climate sciences and impacts/adaptation research. Their vision is to provide Québec and all of Canada with the means to effectively adapt to climate change impacts. Ouranos is an important partner in the continued development of the Canadian Regional Climate Model (CRCM) and is a major source of North American regional climate simulations. Hydro Québec was a founding member of Ouranos. As a result, Ouranos has focused several studies on the topic of water supply for the utility, including the Churchill Falls hydroelectric development in Labrador in which Hydro Québec participates as a minority shareholder and primary customer. In one such study, Ouranos considered an ensemble of five CRCM simulations and predicted an increase in annual runoff in the Churchill Falls basin of 21 percent between simulation periods of 1961-1990 and 2041-2070 (Musy, 2008).

In 2004, a study was conducted by SGE Acres Limited with support from the two major hydroelectric utilities in the Province of NL (Newfoundland Power and Newfoundland and Labrador Hydro) to assess the impact of climate change on hydroelectric generation in the province (Richter, 2004). Watershed and operational routing was undertaken for four hydroelectric systems on the island of Newfoundland to examine the impacts of five different climate change scenarios on generation. These climate change scenarios were developed from GCM output using the delta method (a method where future climate change is superimposed on current weather patterns). The results indicated that future annual average inflows ranged between two percent less and 12 percent more than the present-day baseline, translating into annual power generation of between two percent less and 11 percent more than baseline. A major recommendation of that study was to repeat simulations using more refined temperature and precipitation change estimates coming from downscaled GCM results.

Results of these impacts studies vary dramatically, due in part to the interplay in local climate and hydrology, but also due to the methods used to assess the impact of climate change on hydrology. There is uncertainty inherent in all models and within all analysis methods used; this uncertainty is discussed further in the following section.

2.2 Uncertainty in Climate Change Impacts Analysis

A common theme in the literature of climate change impacts assessment is the uncertainty in the various steps of the process. Wilby (2008) introduced the concept of an "Uncertainty Cascade"; which is depicted in Figure 2.1.

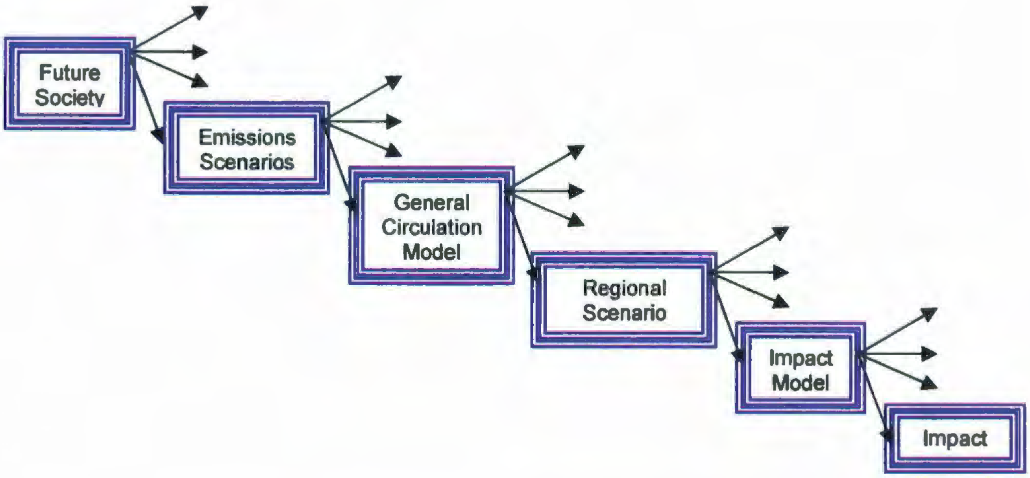

Figure 2.1 Uncertainty Cascade (adapted from Wilby, 2008)

The uncertainty cascade illustrates some of the steps required in a typical climate change impacts analysis. At each step, there are alternative assumptions, methods, and models that can be used, and there is uncertainty associated with each.

A common method that is used to manage this uncertainty in impacts analysis is to consider various alternative inputs in the assessment, resulting in an "uncertainty envelope" or range of likely outcomes. For example, Minville et al. considered a combination of five GCMs and two GHG emissions scenarios and developed probability distribution functions of future hydrologic variables in the Chute-du-Diable watershed in Québec (Minville, 2008). Similarly, fifteen climate change simulations (considering various emissions scenarios, GCMs and RCMs) were included in studies on the Lule River basin in Northern Sweden (Graham, 2007). In a study completed in 2007, the performance of 10 RCMs was assessed based on the ability to reproduce present-day climate in Europe (Jacob, 2007). Model biases were identified and compared and it was determined that the mean of the ensemble of models performed better than any individual model. Pierce came to the same conclusion in his regional climate detection and attribution study of winter temperatures in the western United States (Pierce, 2009). Although good results have been achieved using the mean of an ensemble of climate models, a probabilistic approach is often preferred, especially for the case of climate change risk assessments. With this approach, the range of plausible outcomes may be quantified by gauging the relative importance of the various sources of uncertainty. Minville et al (2008) used a multi-model, multi-projection approach to generate probability distribution functions of future hydrologic variables. Tebaldi et al (2008) used a similar approach to assess climate change impacts on global crop yields. Thorne and Fenner (2009) describe a tool developed to help engineers interpret GCM output and calculate probabilistic distributions of future climate changes as required for risk-based impact assessments.

In the current research the focus was on the development of a methodology to assess climate change impacts on streamflow and not as much on the assessment of uncertainty of the results. It is expected that future research at Memorial University will be conducted in this area.

2.3 Climate Model Comparison

There are several categories of Earth simulation model, each with a specific function in climate impact analysis and/or weather prediction. These models are often similar in form, but each sacrifices a different physical dimension associated with the problem of future prediction as a result of computation power limitations. Table 2.1 compares GCMs, RCMs, numerical weather prediction (NWP) models, and reanalysis models in terms of domain, resolution, timeframe, and typical application. The sacrificial dimension of each model is highlighted in bold and italic font.

Table 2.1 Comparison of Climate Models

	General Circulation Model	**Regional Climate Model**	**Numerical Weather Prediction Models**	**Reanalysis Models**
Domain	Global	***Regional***	Global	Regional or Global
Timeframe	Long (decades)	Long (decades)	***Short (typically** 7 **days)***	Long (decades) ***(Hindcast only)***
Resolution	***Large (~300 km)***	Small (~20-50 km)	Small	Small or Large
Typical Application	Simulate climate response to change in global emissions	Simulate local climate for impacts assessment	Weather prediction	Simulate past climate to provide accurate record of atmospheric fields

As mentioned above, each of the models is essentially the same but each one represents a trade-off given that there are computational power limitations.

GCMs essentially simulate weather over long decadal time frames for the entire globe. Results are typically averaged from these long runs to provide an indication of climate. The sacrificial dimension of GCMs is the low spatial resolution and hence large grids (typically in the order of 300 km). This low resolution makes it difficult for GCMs to provide accurate predictions of localized weather/ climate since local effects of topography and cloud cover are not well represented.

RCMs also simulate weather over long time frames but at a much higher spatial resolution (grid size in the order of 50 km). The sacrificial dimension of RCMs is the areal extent of the simulation or domain. GCM output is often used to provide the boundary conditions of RCMs so that the local effects of global emissions can be modeled inside the RCM. This process of zooming-in on a local area is called dynamic downscaling and is further discussed in Section 2.6.

NWP models use the same physical processes as climate models and simulate weather at high resolution over the entire globe. Due to computational power limitations, NWP models must limit integration time and are therefore only able to provide short term weather predictions. Another difference between NWP models and GCMs lies in the use of initial conditions. NWP models always start from a "measured" state of the atmosphere. Weather balloons and remote sensing and weather station data are all combined with the previous day's forecast to generate a best guess of the state of the atmosphere. From this best guess (also called an "analysis"), the weather model is started and run (also called integrated) ahead in time to produce a forecast (usually for 7-days). New forecasts are usually initialized every 12 hours. After the forecast model has run for approximately seven days it's predictive power decreases since the "memory" from the initial measurements (the analysis) diminishes and the errors and omissions of the model begin to dominate the model output. Results of long runs of weather models do not correspond very well with specific observations; however, the climate (weather averaged over a long period) is preserved.

A climate model is essentially a weather model that is run for a long time. To run it for long enough to generate meaningful statistics, the resolution of the model is forced to decrease. Climate models are run for an initial time period (called the spin-up period) to eliminate the influence (also called forcing) of the initial conditions. When the spin-up period is completed, the climate model runs in essentially an equilibrium producing, statically, the same average climate conditions (but different weather each day) year after year. The "forcing" that is introduced in climate models is an increase in GHGs which influences the radiation balance in the model and nudges the weather in the climate model to take on a slightly different character. This influence is very weak when compared to the forcing associated with changing the initial conditions in weather models; however, in the climate model the influence persists and also influences other aspects (known as feedbacks) of the model.

Reanalysis projects are very similar to the weather modeling process except that the initial conditions are generated from historic observations rather than currently measured data. To generate the reanalysis, all of the historic forecasts have to be regenerated. However, these forecasts are different from their original form since they are now performed with the newest model improvements in a consistent and rigorous way. Using past analysis from achieved forecasts is problematic since the models have been continually changing and improving so that newer analysis simulations are superior in quality. To generate a 30-year reanalysis in a timely way (within a year or two), the spatial resolution of the new reanalysis runs often have to be sacrificially reduced.

In the current study several forecasting methodologies were considered, originating from three of the four Earth simulation model types listed in the above table. The primary method for the assessment of climate change impacts used climate data generated by a RCM forced with GCM output at its boundaries. In the investigation of climate model error, climate data were also obtained from a RCM forced with reanalysis output. NWP models were not used in this research. Further details about these model types including how they are used in a typical climate change impact assessment are provided in the proceeding sections.

2.4 Future Society and Emissions Scenarios

In 2000, the IPCC published the Special Report on Emissions Scenarios (SRES) which provided an updated set of scenarios covering a wide range of the main driving forces of future emissions, from demographic to technological and economic development (IPCC, 2000). Forty scenarios were identified, categorized into four scenario families or storylines, described by the IPCC (2010) as follows.

* A1 storyline and scenario family: a future world of very rapid economic growth, global population that peaks in mid-century and declines thereafter, and rapid introduction of new and more efficient technologies.

* A2 storyline and scenario family: a very heterogeneous world with continuously increasing global population and regionally oriented economic growth that is more fragmented and slower than in other storylines.

* B1 storyline and scenario family: a convergent world with the same global population as in the A1 storyline but with rapid changes in economic structures toward a service and information economy, with reductions in material intensity, and the introduction of clean and resource-efficient technologies.

* B2 storyline and scenario family: a world in which the emphasis is on local solutions to economic, social, and environmental sustainability, with continuously increasing population (lower than A2) and intermediate economic development.

These storylines are used to develop future emissions scenarios and represent the first box in Wilby's uncertainty cascade from Figure 2.1. These emissions scenarios are used to drive GCMs which provide the basis for the development of climate change scenarios. The SRES scenarios are the standard used in current climate change research.

Figure 2.2 presents the projected global carbon dioxide emissions as a multiple of 1990 levels for each of the forty SRES scenarios. These scenarios are classified into six illustrative groups drawn from the four scenario families; the range of emissions in 2100 corresponding to each of these illustrative scenarios is shown to the right of the diagram.

As shown in Figure 2.2, there is significant spread in future emissions scenarios and this spread increases with forecast horizon. Engineering projects such as the Lower Churchill Project have a finite timeline from a financial and life expectancy perspective and thus benefit from the smaller amount of uncertainty in the shorter term. It is hoped that climate change predictions corresponding to the expected lifespan of the project will provide the basis for economically beneficial decisions. After this time there will be an opportunity to adapt based on additional observations, better models, and the benefit of hindsight.

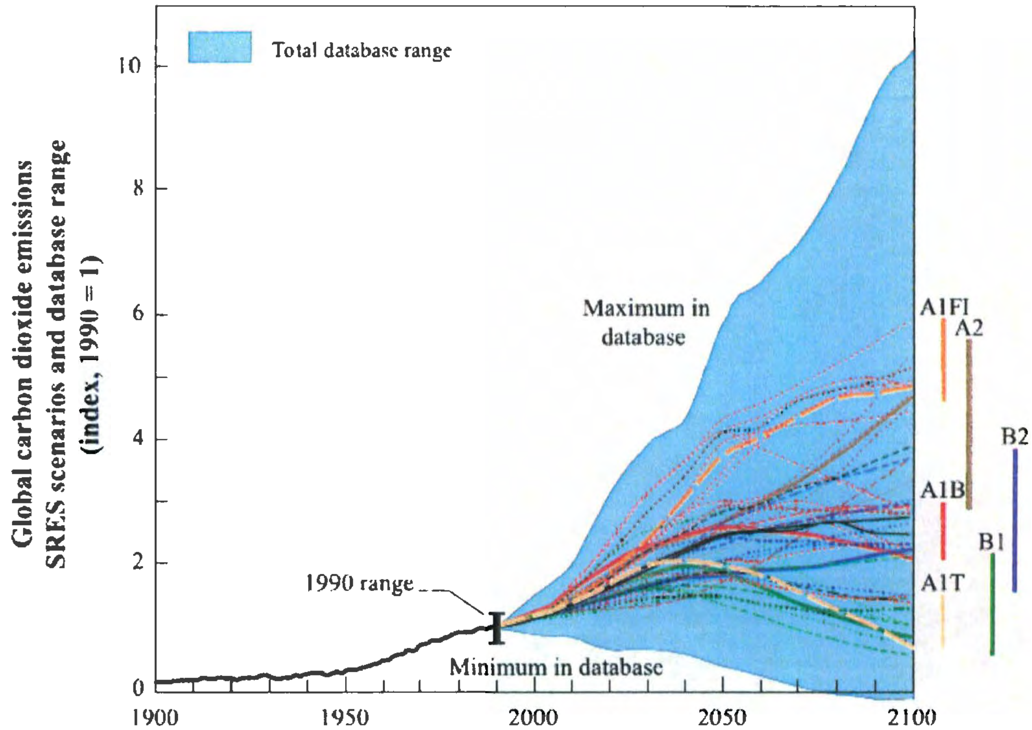

Figure 2.2 Global Carbon Dioxide Emissions for SRES Emissions Scenarios (IPCC, 2000)

There has been some criticism of the SRES scenarios based on the method used to convert national Gross Domestic Product (GDP) data to a common measure using market exchange rates. The result is projections of GDP for developing regions which are improbably high (Castles, 2003). There are also some concerns about the validity of these emissions scenarios in recent years based on a comparison of projected and observed emissions over the past decade. The growth of carbon dioxide emissions since 2000 has been at a rate of over three percent annually; the SRES scenarios projected an annual rate of between 1.4 percent and 3.4 percent between 2000 and 2010 (van Vuuren, 2008).

Despite the criticisms noted above, the SRES emissions scenarios continue to be considered the standard for use in climate change research today.

2.5 General Circulation Models

GCMs are the most sophisticated tools available for the simulation of the Earth's climate system. These complex mathematical models apply physically-based differential equations to calculate the interactions between the ocean, the atmosphere, the land, hydrologic and cryospheric processes, terrestrial and oceanic carbon cycles, and atmospheric chemistry (NOAA, 2010).

GCMs are commonly used in seasonal weather forecasting and also in assessing the sensitivity of the Earth's climate to forcings such as anthropogenic and natural GHG emissions. This type of modeling is a necessary step in the development of climate change scenarios used in climate change impacts research. Unfortunately, due to the complexity of these GCMs and the associated computational requirements, the horizontal resolution is coarse, typically in the order of 300 km. Therefore, GCMs are restricted in their usefulness for local impact studies since they are unable to resolve important sub-grid scale features such as clouds and topography (Wilby, 2002). As such, GCM output is not typically used directly for developing climate change scenarios for regional impact studies, but rather it is translated into useful predictions at a regional scale using one of several available methods, some of which are discussed in the following section.

The IPCC makes reference to 23 GCMs which are widely used in their Fourth Assessment Report (AR4), published in 2007. These 23 models come from 11 different countries, and each model differs in how it computes the interactions of the Earth's climate systems. The climate change forecasts from each of these models is different, and the choice of GCM becomes a major source of uncertainty in the climate change analysis. It has been suggested that the choice of GCM for providing boundary conditions for RCMs plays a more important role in assessing hydrological change than the choice of emissions scenario (Graham, 2007). The research conducted in Québec with the primary focus of evaluating the uncertainty in the assessment of climate change impacts on the hydrology of a watershed, suggested that of all sources of uncertainty considered, the largest comes from the choice of GCM (Minville, 2008).

In the current study the selection of GCM was based primarily on data availability with the expectation that a range of GCMs would be used in future studies to help define the uncertainty related to this input.

2.6 Regional Scenario

As discussed above, GCMs are unable to accurately predict regional climates due to their coarse resolution which is a product of computational power limitations. Hence, the next step in typical climate change impact studies involves transferring the results of GCMs to a scale appropriate for hydrological modeling. There are several options which can generally be grouped into two categories: statistical downscaling and regional climate modeling (also known as dynamic downscaling). A third option is the change factor or delta method. The objective of these methods is to bridge the spatial and temporal resolution gaps between what climate modellers are currently able to provide and what impact assessors require (Wilby, 2002). Each method is described in further detail in the following sections.

2.6.1 Statistical Downscaling

Statistical downscaling involves developing empirical relationships, or transfer functions, between large scale climate variables from GCMs (i.e. predictors) and station-scale observations (i.e. predictands). Various methods have been used to derive these relationships, including linear and non-linear regression, artificial neural networks, canonical correlation, and principal component analyses (Wilby, 2002). These relationships are assumed to hold true in a future climate, and therefore are used to translate GCM predictions for future periods into station-scale surface weather. The assumption that the statistical relationships developed for the present day climate holds true under a different forcing condition of a future climate is one of the main theoretical weaknesses of this method (Gachon, 2007). However, the method has the advantage that it is relatively easy to apply and therefore can be used in cases where RCM output is not available or a more rapid assessment is required. Also, due to its relative ease of application it is often possible to evaluate an ensemble of climate scenarios, thereby permitting a better evaluation of uncertainty.

2.6.2 Dynamic Downscaling (Regional Climate Modeling)

Dynamic downscaling or regional climate modeling is more computationally demanding than statistical downscaling and this is one of its most noteworthy drawbacks. Similar to GCMs, RCMs are physically based models, applying the conservation laws of mass, energy, and momentum to simulate the Earth's climate. Where GCMs sacrifice horizontal resolution due to computational power limitations, RCMs sacrifice domain size. The resolution of a RCM is typically in the range of 20-50 km which allows RCMs to resolve local atmospheric processes and enables the prediction of local-scale weather. RCMs are nested within GCMs such that time-varying atmospheric forcings from the GCMs are applied at the RCM boundaries providing a transfer of information from one model to another. Figure 2.3 provides a schematic depiction of an RCM nested within a GCM.

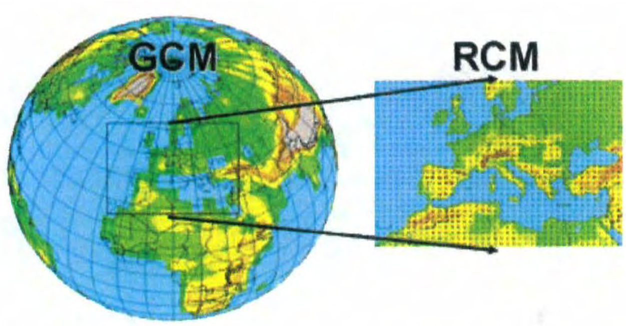

Figure 2.3 Schematic Depiction of RCM Nesting Approach (Giorgi, 2008)

Reanalysis data can also be used to provide the atmospheric forcing to the boundaries of a RCM. This type of data is generated from numerical weather models which simulate past global weather using historical observations as both initial conditions and to reset the model back to observed conditions throughout the simulation. These models are therefore able to provide a more accurate representation of the past atmosphere than a GCM that typically use no climate observations during their simulations. Since reanalysis output is essentially a physically based interpolation of past weather observations, it removes much of the uncertainty in the boundary conditions of a RCM. Using reanalysis data instead of a GCM to force the boundaries of a RCM for a historic period is a useful method to differentiate between errors resulting from the GCM and those introduced by the RCM.

As with any model, RCMs cannot reproduce observations without error. Research in Denmark identified a distinct systematic bias in simulated monthly mean temperature and precipitation for an ensemble of thirteen RCMs forced with the European Centre for Medium Range Weather Forecasting Reanalysis (ERA40) (Christensen, 2008). Temperature and precipitation biases were also found in downscaled ERA15 data for the Rhine basin in Western Europe (Terink, 2009). In the current study, temperature and precipitation biases were identified in the output of the CRCM forced with both the Canadian Coupled Global Climate Model (CGCM) and reanalysis data from the U.S. National Centre for Environmental Prediction (NCEP).

It is often necessary to apply a bias-correction to RCM data to achieve a good match with observed climate (Terink, 2009; Minville, 2008; Leander, 2007; Christensen, 2008). It is assumed that the skill of the model in reproducing the observed climate (after bias-correction) will be carried over to future climate conditions.

2.6.3 Change Factor Approach

An unsophisticated yet practical alternative to climate downscaling in the development of regional climate change scenarios is called the change factor approach, also known as the delta method. This is a relatively straightforward procedure which allows for rapid impact assessment; however, there are fundamental drawbacks with this method. In general, the procedure involves comparing GCM output for baseline and future periods and calculating change factors for climate variables of interest to quantify the difference between the two periods. For example, in assessing the impact of climate change on hydroelectric generation in Newfoundland, a 3.3 degrees C increase in temperature (Warmest scenario) and an 22.7 percent increase in precipitation (Wettest scenario) were determined for the month of February (Richter, 2004). These factors are then applied to the observed climatology to estimate future climatology. The primary drawbacks of this method include the following.

- Only the mean, maxima, and minima of the climate changed variables are different from the baseline case. The range and variability of the two scenarios remain the same.

- The rate of occurrence of precipitation is unchanged in the climate change scenario. This is a concern in studies related to the length of wet/dry spells.

- This method requires that equivalent observed and modeled climate variables exist.

2.7 Impact Model

Hydrology and climate are tightly interrelated and as such, climate models typically include a representation of hydrological processes such as precipitation, interception, evaporation, infiltration, and local runoff. These processes are included in climate models so that the transfers of energy, moisture, and momentum between the land/ocean and the atmosphere are reasonably captured. Although runoff and soil moisture are included in climate models, the lateral transfer of this water between the grid cells is often ignored. Therefore, for the assessment of local climate change impacts on water resources, a hydrological model is typically used.

Like each of the steps in a typical climate change impact assessment, there is uncertainty in the selection and use of a hydrological model. The research conducted under a Québec-Bavarian pilot study on integrative catchment modeling in the context of climate change applied three hydrological models of varying complexity to model current and future climate scenarios over an alpine basin in Germany (Ludwig, 2009). The models included in the analysis were PROMET, a spatially distributed model; HYDROTEL, a semi-distributed model; and HSAMI, a lumped conceptual model. The observations arising from this work suggested that uncertainties introduced by the hydrological models can be of the same magnitude as the climate scenario inputs. The importance of having physically based model processes to maintain the predictive power of the hydrological model was also noted. This conclusion relates to the underlying assumption that the calibration of the hydrological model to local conditions will hold true under a future changed climate. This is another major assumption associated with this research and many other studies using hydrological models to assess climate change impacts on water resources. Minville (2008) investigated this assumption by examining the performance of her hydrological model over the existing record and looking for differences in the performance for colder/wetter years and hotter/dryer years. None were identified suggesting that the model may be acceptable for use in a future climate.

The WATFLOOD distributed hydrological model has been used to assess climate change impacts within the Peace and Athabasca catchments and deltas. The model was successfully calibrated based on historic measurements of climate and streamflow. Climate change simulations of future periods, assessed using

WATFLOOD, generally indicate an earlier melt season and lower winter flow. Some modeling challenges and areas for water resource modeling improvements were identified, including uncertainties in input data, calibration of gauged basins, and the imperfect representation of physical processes, particularly involving snow and phase change (Toth, 2006).

The importance of proper representation of physical processes is echoed by Bingeman (2006). In this paper on the validation of hydrological processes in a hydrological model, it was suggested that hydrological model evaluation must go beyond the usual examination of the output hydrograph to include a thorough review of the model's internal behaviour.

Most hydrological models used in impact assessments use a combination of simplified physically-based and conceptual equations to represent hydrological processes. Just as climate models provide a simplification of hydrological processes (e.g. by ignoring the lateral movement of water across the grid), most hydrological models tend to simplify climate processes. In fact, many of the hydrological models used in impact assessments have only temperature and precipitation as inputs and ignore other climate variables such as short wave radiation, long wave radiation, humidity, wind speed, and atmospheric pressure which are likely to be influenced by future change and are known to influence hydrologic processes. Modern land surface schemes such as CLASS (Canadian Land Surface Scheme) are sophisticated hydrological models that do take these complex energetic processes into account, but they are much more difficult to set up because of the lack of available measured data. In fact, even simple observations of temperature and precipitation are not always available at locations of interest and those measured often exhibit large measurement biases.

Despite the limitations noted above related to simplified hydrological models, they continue to be used for climate change impact analyses. Calibration to observed streamflow remains a necessity, and it is wise to include calibration to other internal variables when available. As with any modeling exercise, the choice of hydrological model cannot capture the full complexity of nature; however, it is important that the model capture reasonably well the main features of the system dynamics relevant to the particular study (Dibike, 2007).

The WATFLOOD hydrological model was selected for use in the current study based on its relatively low input data requirement, its transferability to other watersheds without re-calibration, and its successful application in other similar watersheds in Canada. The advantages and some of the limitations of the WATFLOOD model are further discussed in Section 4.

Chapter 3 Study Basin and Data Acquisition

This section describes the selection of the Churchill River sub-basin that was modeled in this study as well as providing hydrologically-relevant information about the basin. These data include physiographic characteristics, climate data, and streamflow data from within or near the study basin. Appendix A includes a table which summarizes the sources of the data collected as part of this research. Appendix B provides a flowchart of the research steps.

3.1 Basin Selection

Streamflow data are paramount in the validation of a hydrological model. As such, the basins considered for this climate change impact analysis included only those basins having an active hydrometric station within them. There are five Water Survey of Canada (WSC) hydrometric stations in the lower Churchill River watershed for which flow data are available. Table 3.1 summarizes the drainage area and period of record of each of these stations and indicates whether the flow regime in the basin is natural or regulated.

Due to the regulation of the two stations on the Churchill River, they are not good candidates for hydrological modeling since considerable effort would be required to de-regulate the flow to correspond with hydrological model predictions of natural flow.

Table 3.1 Hydrometric Stations in Churchill River Watershed

Station Name	Station ID	Drainage Area	Period of Record	Regulation Type
[1]Pinus River	03OE011	770 km^2	1998-Present	Natural
East Metchin River	03OD007	1,750 km^2	1998-Present	Natural
Minipi River	03OE003	2,330 km^2	1979-Present	Natural
[2]Churchill River at Churchill Falls Powerhouse	03OD005	69,200 km^2	1972-Present	Regulated
Churchill River above Upper Muskrat Falls	03OE001	92,500 km^2	1948-Present	Regulated

[1] The Pinus River basin drainage area is not published; basin delineation based on 1:50,000 NTDB mapping.
[2] Flow data are contributed by CF(L)Co based on operations at Churchill Falls.

The three other stations are in natural basins within the Churchill River watershed. The Minipi River station is located downstream of Minipi Lake which provides significant attenuation to streamflow. Although the attenuation effect might be negligible over long time frames, this station was ruled out for the study since details on the elevation-volume relationship and the outflow characteristics of the lake are not known. Although published, the drainage area of the East Metchin station is suspect based on a mean annual runoff (MAR) review. The headlands of this basin are very flat and the drainage divide is difficult to delineate based on 1:50,000 scale National Topographic Database (NTDB) mapping and digital elevation data. Therefore, this basin was also excluded from the analysis. The Pinus River basin does not have either of these complications and therefore it was chosen as the study basin for the current research.

The confluence of the Pinus and Churchill Rivers is just downstream of Gull Lake, between the two proposed hydroelectric projects. Figure 3.1 illustrates the location of each of the hydrometric stations listed in Table 3.1, their respective basins as well as the overall Churchill River basin. Also shown on this figure is the location of the Churchill Falls hydroelectric generation station and the two proposed hydroelectric developments which make up the Lower Churchill Project.

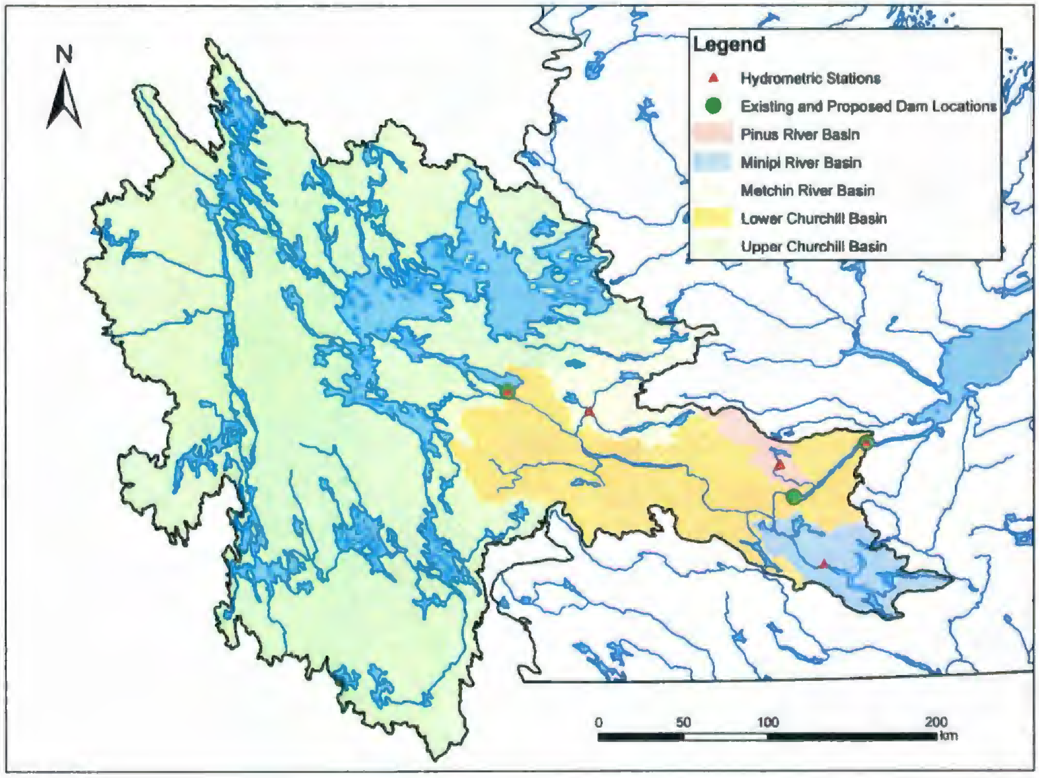

Figure 3.1 Churchill River Basin and Hydrometric Station Locations

3.2 Physiographic Characteristics

The Pinus River basin lies within the lower Churchill River watershed which is in an area of transition between Arctic and sub-Arctic climates. Vegetation is typical of Boreal and Taiga ecosystems which are adapted to nutrient-poor conditions and extremes in weather (Nalcor, 2009). Forest covers approximately 65 percent of the Pinus River basin, with black spruce coniferous trees being the dominant type. The remaining land surface consists of water bodies (approximately 20 percent) and wetlands (approximately 15 percent).

3.2.1 Digital Terrain Data

Perhaps the most important part of the development of the hydrological model is the characterisation of the land surface. Digital terrain models, also known as digital elevation models (DEMs), describe the topography, or elevation of the land. They are commonly found in digital raster format whereby the terrain is represented by a grid of squares with each square associated with a single elevation value. DEMs are often used in a geographic information system (GIS) environment where relief maps may be created or the data may be analysed for some other purpose such as the development of a hydrological model.

Topographical information can be developed using survey data, but remote sensing technologies are becoming increasingly popular and offer the important advantages of accuracy, scale, and efficiency. For this study, the Shuttle Radar Topography Mission (SRTM) DEM was used. This international research effort, led by the National Geospatial-Intelligence Agency (NGA) and the National Aeronautics and Space Administration (NASA) in the United States, obtained elevation data on a near-global scale to generate the most complete high-resolution digital topographical database of Earth. SRTM consisted of a specially modified radar system that flew onboard the Space Shuttle Endeavour during an 11-day mission in February 2000 (NASA, 2009). The horizontal resolution of data points is 1 arc-second (approximately 30 m) for the United States and 3 arc-seconds (approximately 90 m) for global coverage between 60 degrees North and 56 degrees South latitude. The product consists of seamless raster data with horizontal and vertical accuracies of 20 m and 16 m, respectively (Hayakawa, 2008).

Based on the SRTM elevation data, the elevation of land in the Pinus River basin ranges from 350 m to 510 m. Figure 3.2 illustrates the DEM of the Pinus River basin and Figure 3.3 illustrates the drainage network.

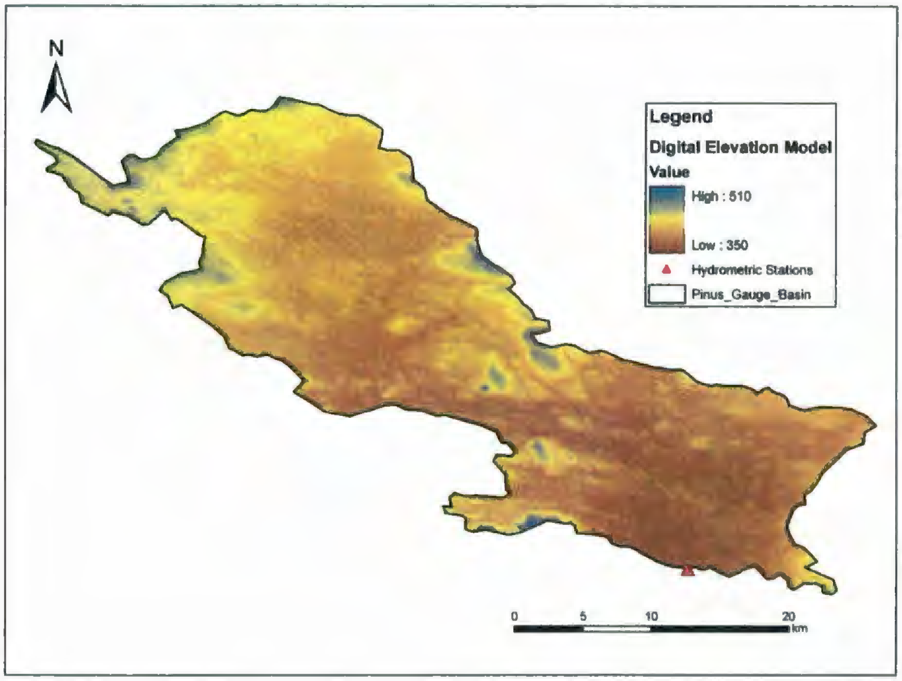

Figure 3.2 Digital Elevation Model of the Pinus River Basin

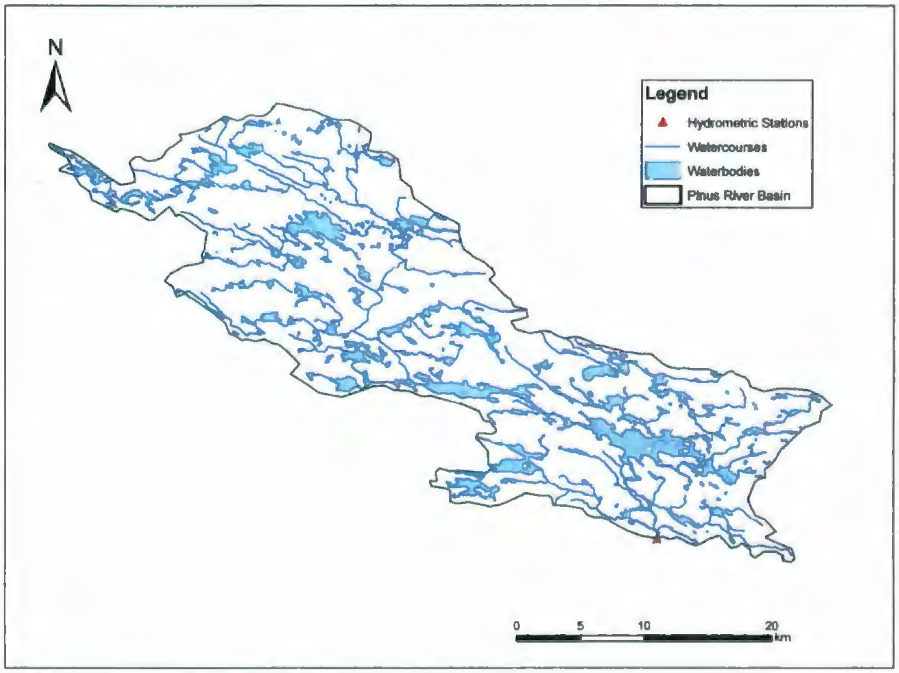

Figure 3.3 Drainage Network of the Pinus River Basin

3.2.2 Land Cover Data

Land cover data were also required as input to the WATFLOOD hydrological model as discussed in Section 4.1.1. Digital NTDB mapping (based on aerial photography acquired in the late 1970s) was used to determine the distribution of the three main land cover types used in the model: forest, water, and wetlands. Figure 3.4 illustrates the distribution of these three land classes in the Pinus River basin. White areas in this figure (which are likely barren or rocky outcrops) were lumped into the forest class.

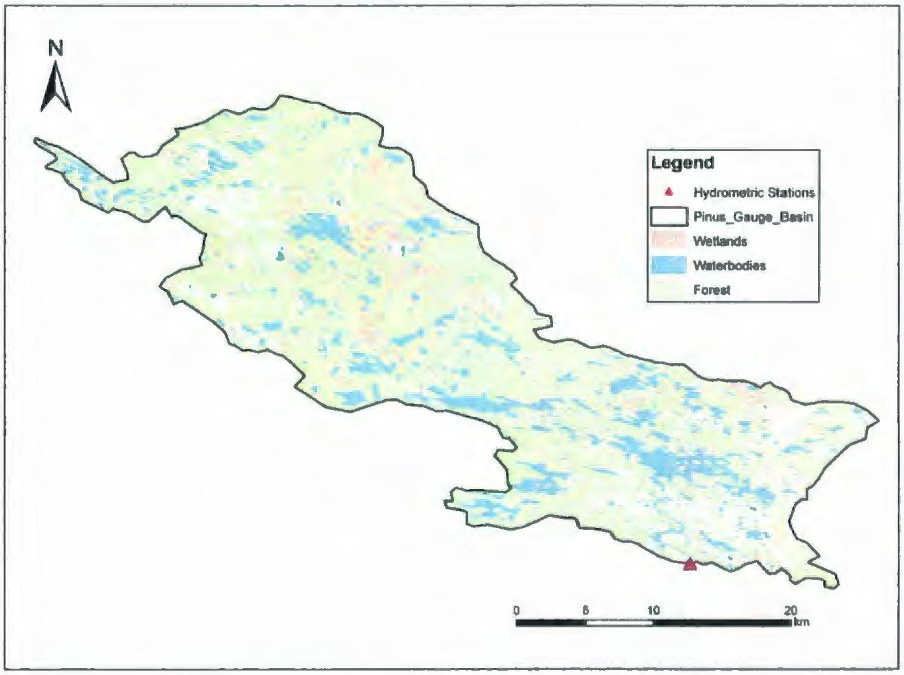

Figure 3.4 Land Cover Map of the Pinus River Basin

(Note: White areas were lumped into the forest class)

WATFLOOD is capable of utilizing a large number of land classes when used in conjunction with remote sensing data. However, the use of additional land classes requires many more calibration parameters and additional model complexity which is not always favourable. Simple models with equal predictive skill are always preferred over more complex ones. Given the lack of climate observations available for the Pinus basin, it was felt that a minimum number of land classes should first be tried with additional land classes used if deemed necessary based on the results of the calibration. As the calibration was successful using the land classes shown in Figure 3.4, no more land classes were added and hence the number of parameters that required calibration was minimized.

3.3 Climate Data

3.3.1 Observed Climate Data

Environment Canada (EC) maintains a network of climate stations across the country. These stations record a range of different climate variables; temperature and precipitation are of most interest in the current study as these were the two variables selected for hydrological model forcing.

There are no climate stations within the Pinus River basin; the two closest stations are located at Goose Bay and Churchill Falls which are located approximately 90 km and 160 km, respectively from the centre of the Pinus River basin. The locations of these climate stations relative to the Pinus River basin are illustrated in Figure 3.5. Figures 3.6 and 3.7 present the EC monthly climate normal temperature and precipitation for Goose Bay and Churchill Falls based on the 1971-2000 period.

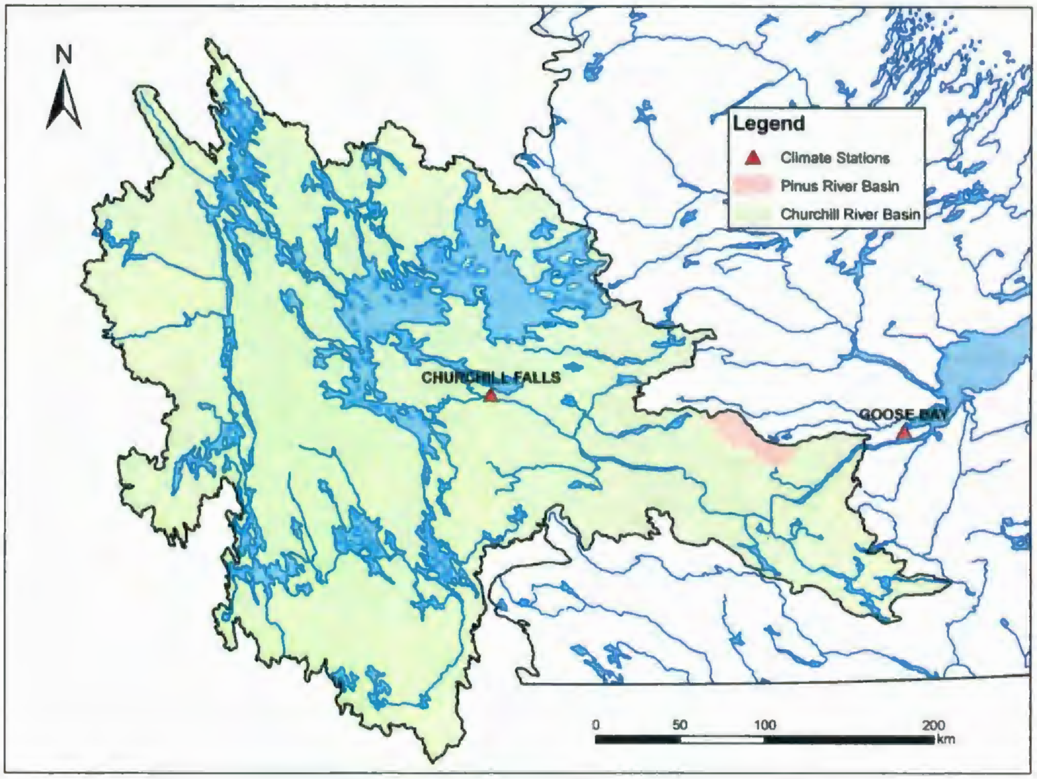

Figure 3.5 Climate Station Location Map

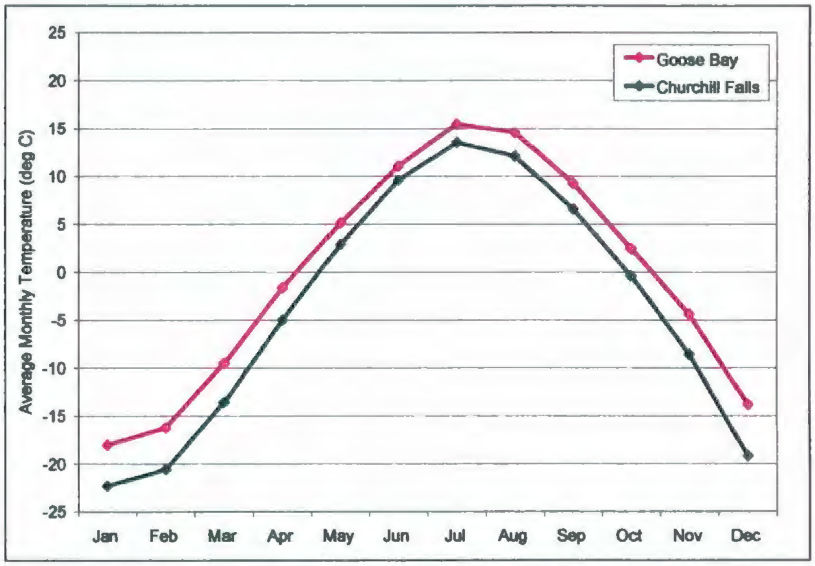

Figure 3.6 Climate Normal Temperature at Goose Bay and Churchill Falls (1971-2000)

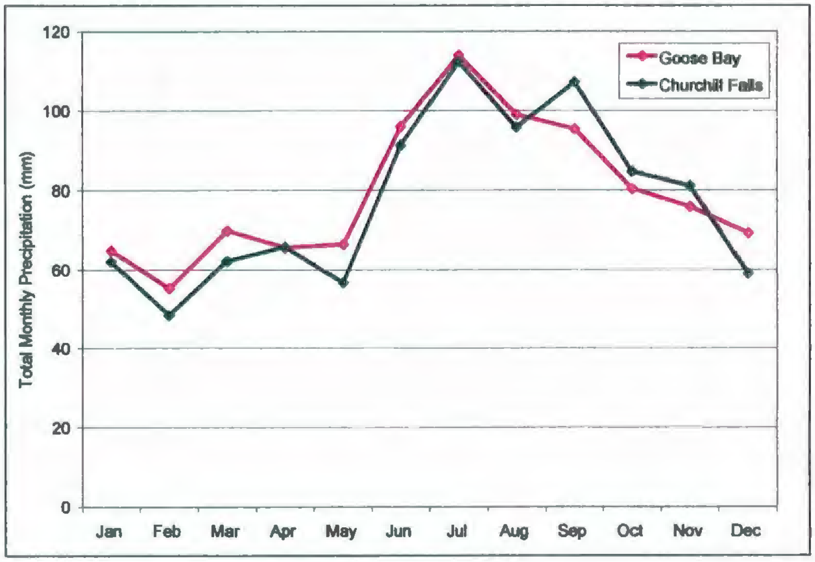

Figure 3.7 Climate Normal Precipitation at Goose Bay and Churchill Falls (1971-2000)

Daily and hourly climate data were obtained from EC for the current research. Table 3.2 summarizes the climate data obtained for the stations at Goose Bay (GB) and Churchill Falls (CF).

There are several methods that can been applied to estimate the climate of a basin for which there are no observed climate data. Simple averaging of data sets from surrounding climate stations can be risky as the stations may not be of equal quality or equally representative of the basin of interest. More sophisticated data assimilation procedures can more objectively combine data sets. In this study, the Goose Bay climate station was preferred based on it's longer period of record and manual precipitation measurements (the Churchill Falls station moved to automatic precipitation measurements which are known to be very inaccurate in the winter). A successful hydrological model calibration was achieved using historical climate data from the Goose Bay station alone (hydrological model calibration is discussed further in Section 4.3).

Table 3.2 Summary of Observed Climate Data

Data Type	Climate Variables	Station	Period of Record
Hourly Climate Data	Ceiling, Visibility, Sea Level Pressure, Dew Point Temperature, Wind Direction, Wind Speed/Gust, Station Pressure, Dry Bulb and Wet Bulb Temperature, Relative Humidity, Cloud Opacity, Cloud Amount, Weather Indicator	GB – Manual (8501900)	1953-2009
		CF – Manual (8501132)	1968-1993
		CF – Auto (8501130)	1994-2009
Daily Climate Data (NOT Quality Assured)	Max/Min Temperature, Total Rainfall, Total Snowfall, Total Precipitation, 6-hour Precipitation	GB – Manual (8501900)	1992-2009
		CF – Manual (8501132)	n/a
		CF – Auto (8501130)	1992-2009
Daily Climate Data (Quality Assured)	Max/Min Temperature, Total Rainfall, Total Snowfall, Total Precipitation, 6-hour Precipitation	GB – Manual (8501900)	1953-2009
		CF – Manual (8501132)	1968-1993
		CF – Auto (8501130)	n/a
Tipping Bucket Rain Gauge Data	Hourly Precipitation	GB – Manual (8501900)	1961-2007
		CF – Manual (8501132)	1969-1992
		CF – Auto (8501130)	n/a

3.3.2 AHCCD Climate Data

Original station climate observations often have inconsistencies related to changes in instruments, observing procedures, and station relocation. The EC Adjusted Historical Canadian Climate Data (AHCCD) provides adjusted and homogenized climate data for Canada that can be used for climate trend analysis. Climate variables currently available through this program include air temperature, precipitation, surface pressure, and surface wind.

Adjusted temperature data consisting of daily mean, maxima and minima were obtained and compared with the raw observed air temperatures at Goose Bay. The methodology used for the adjustment was regression-based and is described by Vincent (1998). The correlation coefficient (r^2) between AHCCD and observed data sets (both monthly and daily) is greater than 0.99. Figure 3.8 illustrates the comparison of mean monthly temperatures for the period 1953-2008.

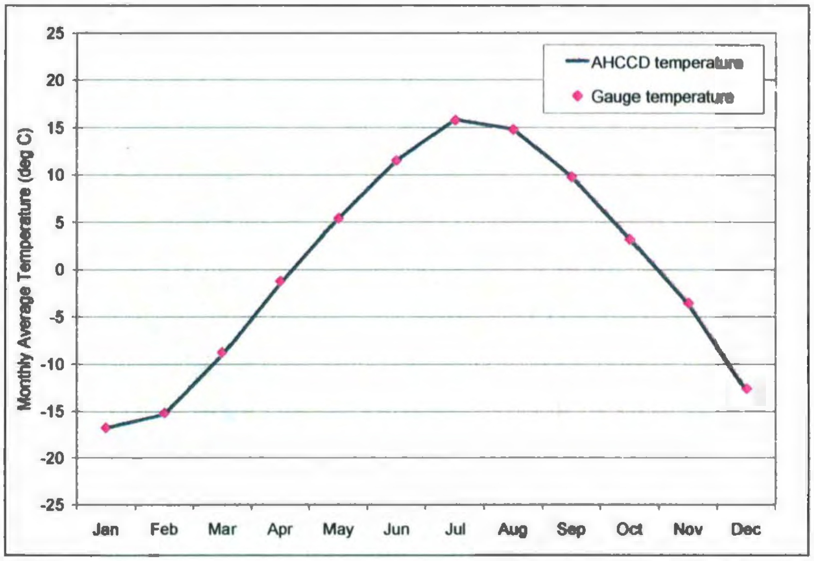

Figure 3.8 AHCCD and Gauge Temperature at Goose Bay (1953-2008)

As is evident, the adjustment had very little effect on the original gauge data; monthly averages are within 0.2 degrees C for all months. The range of temperatures over the day is important to the hydrology and for this reason hourly data are preferred for hydrological modeling. To apply an hourly distribution of temperatures to the AHCCD daily means would be difficult and prone to error. Therefore the original hourly temperatures observed at Goose Bay were used in the current research rather than the AHCCD adjusted data set.

It is well known that climate stations have difficulty in capturing the full amount of precipitation due to factors including wind undercatch (the inability of the gauge to capture the full amount of precipitation falling from the sky), evaporation, and splash. Many different techniques have been applied with varying degrees of success in estimating true amounts, but virtually all have generated underestimates (Mékis, 1999). The AHCCD includes adjusted daily rain, snow and total precipitation amounts for 495 stations in Canada including Goose Bay. The adjustment methodology is described in Mékis and Hogg (1999). This data set was obtained and used in the current research; as expected, gauge observations from Goose Bay were increased in every month by between 7 percent (corresponding to 8 mm in the month of July) and 37 percent (corresponding to 25 mm in the month of January) with an annual average of 15 percent. The WATFLOOD hydrological model typically requires hourly precipitation input; however, there is a smearing function that was used in the current study to distribute the daily precipitation over the day. Figure 3.9 illustrates the comparison of gauge and AHCCD precipitation for the 1953-2008 period.

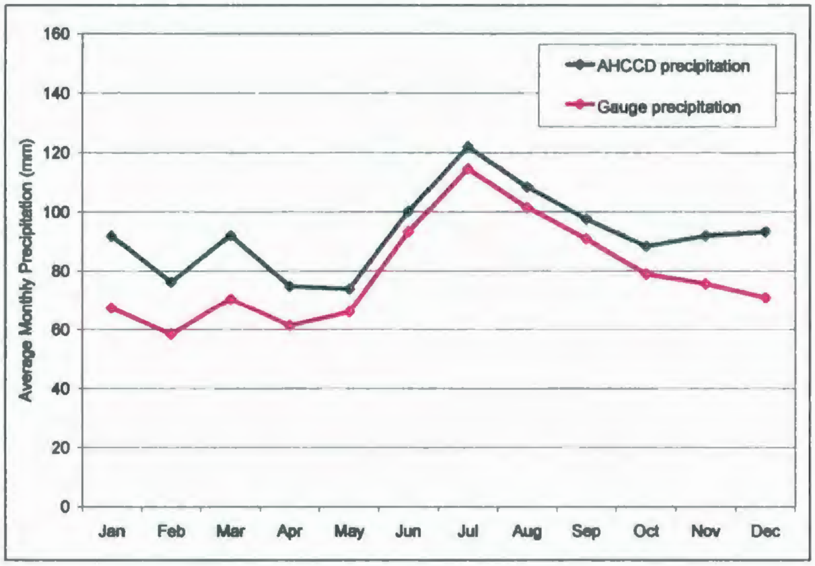

Figure 3.9 AHCCD and Gauge Precipitation at Goose Bay (1953-2008)

Prior to learning of and obtaining this AHCCD daily precipitation data set, hydrological model simulations with observed precipitation resulted in flow that was much lower than observed. A snow adjustment factor of 1.2 was assumed to account for potential gauge undercatch and this brought simulated flow closer in line with observed, but the AHCCD precipitation data set led to an even better agreement. This was an important innovation that contributed to the success of this study.

3.3.3 NARCCAP Climate Data

The North American Regional Climate Change Assessment Program (NARCCAP) is an international program led by the National Centre for Atmospheric Research in the United States. The objective of the program is to provide high resolution climate change scenarios for impacts research in the United States, Canada, and northern Mexico. NARCCAP climate modellers have simulated multiple RCMs nested in a number of different GCMs and forced with NCEP reanalysis data. The domain of the modeling is illustrated in Figure 3.10 which depicts the topography of the continent.

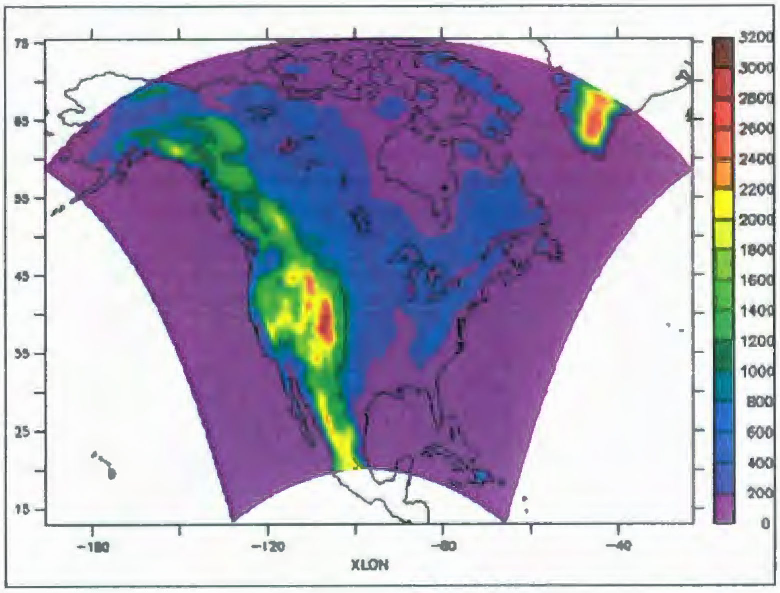

Figure 3.10 NARCCAP Domain (NARCCAP, 2010)

Table 3.3 presents the matrix of planned and completed NARCCAP climate simulations as of June 2010. For the current study only one GCM/RCM combination was considered and this was the CGCM3-CRCM scenario. It is expected that the results of other model combinations will be used as this research is progressed; this will be important to develop an understanding of the range of possible outcomes. The NCEP-CRCM scenario was also used in the current study for the assessment of attribution of error between the GCM and RCM. Both of the combinations used in this thesis are highlighted in Table 3.3 with bold and underlined font.

Table 3.3 NARCCAP Climate Simulations Matrix

Regional Climate Model	General Circulation Model				Reanalysis Data
	GFDL	CGCM3	HADCM3	CCSM	NCEP
CRCM		**<u>Completed</u>**		Planned	**<u>Completed</u>**
ECPC	Planned		Planned		Completed
HRM3	Planned		Completed		Completed
MM5I			Planned	Completed	Completed
RCM3	Completed	Completed			Completed
WRFP		Planned		Planned	Completed

The NARCCAP scenarios were simulated for both current (1971-2000) and future (2041-2070) periods to permit the evaluation of climate change impacts. Looking further into the future would likely be beyond the financing period of the Lower Churchill Project and is therefore not as pertinent for Nalcor. Due to NARCCAP resource limitations, only a single future emissions scenario was considered and that was the SRES A2 scenario. This was one of the 'marker' scenarios developed through the IPCC and was a popular one at the time of NARCCAP program planning (NARCCAP, 2010). As shown in Figure 2.2 (Section 2.4), the

A2 scenario is one of the more pessimistic projections of future emissions; however, these scenarios were developed in 2000 and there has been some concern recently that they are too low. This opinion is based on the fact that the rate of increase of observed emissions over the past decade is at the upper end of the IPCC projections.

For this study, temperature and precipitation data were obtained for the grid point closest to the Goose Bay climate station since the hydrological model was calibrated using observed Goose Bay climate. Monthly average observed and simulated temperature and precipitation at Goose Bay are summarized in Appendix C and D, respectively. Code written to aid with the extraction of the RCM data is included in Appendix E.

3.4 Streamflow Data

As mentioned in Section 3.1, there is a WSC hydrometric gauge on the Pinus River (station 03OE011) which has been in operation since November 1998. The drainage area upstream of this gauge is approximately 770 km^2. At this station, water level data are recorded continuously and are converted into flow based on a rating curve which defines the stage relationship to flow. The rating curve is determined in the field through the measurement of widths, depths, and velocities over a range of water levels. The rating curve is updated periodically to account for changes in the river cross section that occur over time.

Inaccuracies can occur during the measurement of any of the above noted quantities through errors introduced by technique or equipment used. Results of various analyses generally show that streamflow measurement accuracies of within 5 percent are achievable 95 percent of the time provided that the field data have been obtained in accordance with an acceptable standard (Environment Canada, 1981).

Figure 3.11 presents the average monthly hydrographs at the Pinus River hydrometric station for each year and also the average over the entire period of record considering full years only (1999-2008). As shown, the spring peak typically occurs in the month of May, although peak flow has occurred in June in two of the ten years on record.

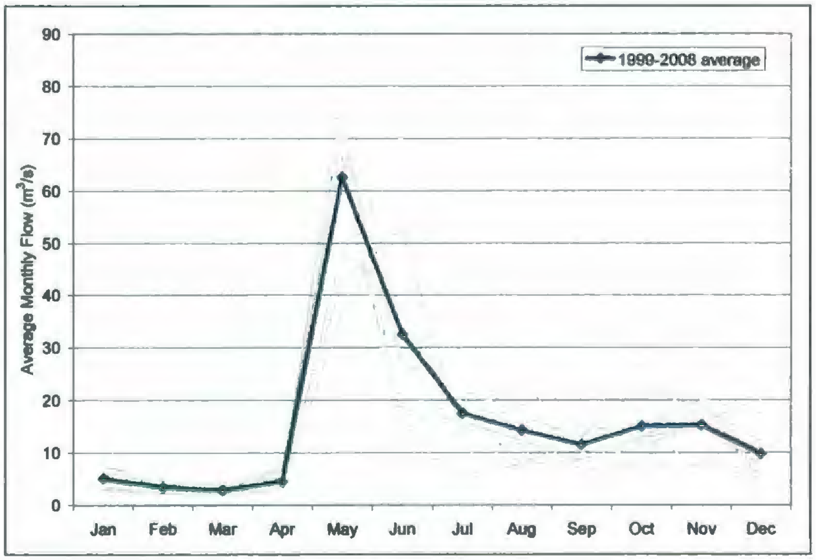

Figure 3.11 Average Monthly Pinus River Flow (1999-2008)

Figure 3.12 presents the daily hydrograph for the entire period of record (October 1998 to December 2008). These daily streamflow data were used in the hydrological model calibration as discussed in Section 4.3.

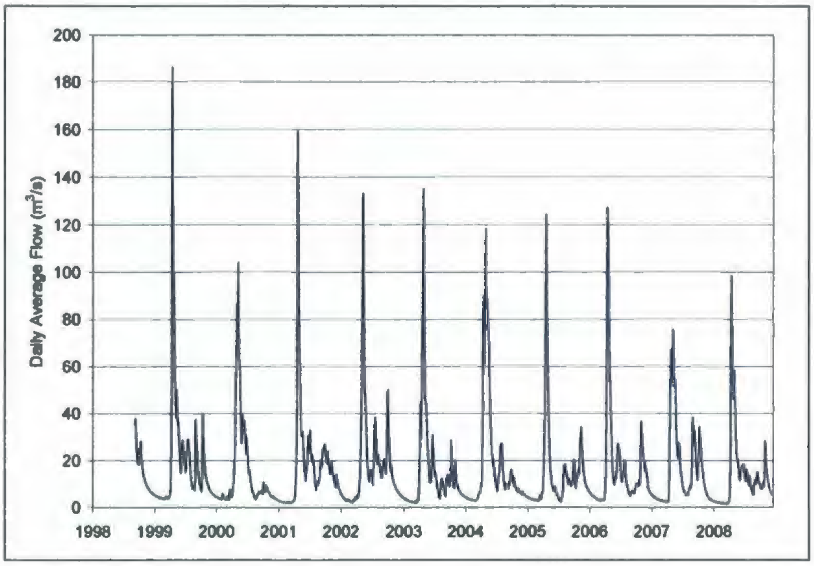

Figure 3.12 Average Daily Pinus River Flow (1998-2008)

The MAR of the Pinus River basin over the 1999-2008 period is 665 mm. This is slightly higher than the MAR calculated for the entire Churchill River basin (as measured at Muskrat Falls) which is 608 mm for the same period; however, this estimate must be used with care as the flow measured at Muskrat Falls is regulated by the Churchill Falls hydroelectric project upstream. There is multi-year storage available in the Upper Churchill reservoirs and therefore it is possible that this estimate could be higher or lower depending on the reservoir levels at the beginning and end of the period.

The average annual precipitation at Goose Bay from the AHCCD for the 1999-2008 period is 1077 mm. Dividing the Pinus Basin MAR by this value gives a runoff ratio of 0.62 which represents the fraction of precipitation that appears as runoff. It can be assumed that the remaining 38 percent of the precipitation is evaporated.

Monthly average observed and simulated Pinus River flows are summarized in Appendix F.

Chapter 4 Hydrological Modeling

4.1 Description of WATFLOOD

The WATFLOOD numerical hydrological model is a set of FORTRAN programs for DOS. The model was developed by Dr. Nicholas Kouwen, Distinguished Professor Emeritus at the University of Waterloo in Ontario, Canada. Model development began in the 1970s and continues to this day. The model is aimed at both short term simulations for the purposes of flood forecasting and multi-year simulations suitable for climate change studies. The following sections describe the model approach and provide a brief discussion of the hydrological processes represented in the model.

4.1.1 Approach

The WATFLOOD model is a combination of a physically based routing model and a conceptual hydrological simulation model of a watershed. In general, the vertical water budget processes in the model are represented by conceptual equations while the horizontal routing processes are modeled using physically-based equations (Bingeman, 2006).

The parameters of the conceptual hydrologic equations are selected for each hydrologically significant sub-group within the simulation area. These sub-groups are typically chosen to correspond to specified land cover classes. The proportion of each land cover in each computational grid can be easily determined from any land cover image including those based on remote sensing data. It is assumed that each pixel belonging to a defined land cover class responds in a similar way with respect to infiltration, surface runoff and interflow, evaporation, snowmelt, and drainage to groundwater (Bingeman, 2006). The runoff response from the grid is calculated for each of these areas individually and then the total runoff is routed in succession first overland to the channel and then downstream to the next grid. This approach is called the grouped response unit (GRU) or pixel grouping approach; Figure 4.1 illustrates the GRU and physically based routing approaches schematically.

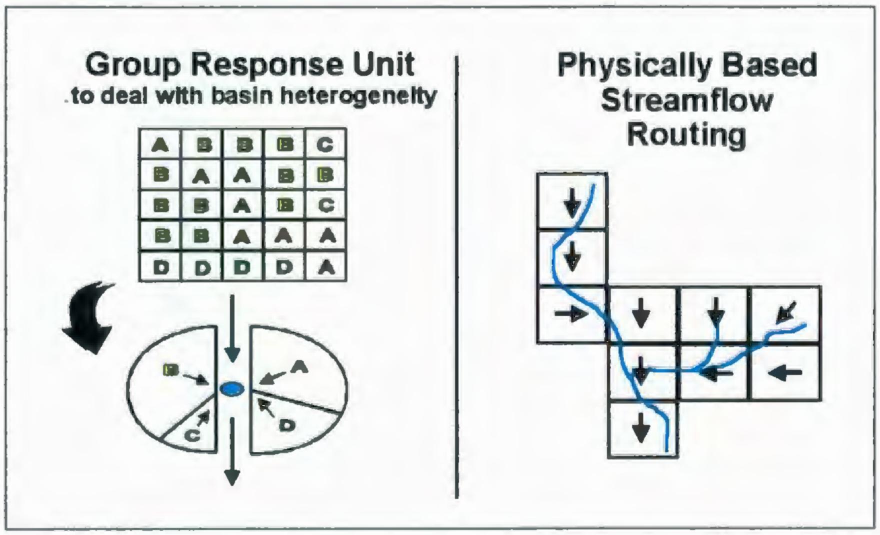

Figure 4.1 Grouped Response Unit and Runoff Routing Concepts (Donald, 1992)

The GRU approach constitutes an important advantage of the WATFLOOD model over more traditional basin-averaging approaches. Not only can the averaging of basin parameters lead to inaccurate runoff estimates, but models of this structure have parameters which are basin-specific and cannot be transferred to other basins. Because the parameters of the WATFLOOD model correspond to the land cover, the parameters can be easily transferred to other physiographically similar watersheds. Further, if the land use of a watershed changes over time, the parameters do not need to be re-estimated, only the land cover map and the fractions in each grid need to be redefined.

4.1.2 Hydrological Processes

Figure 4.2 presents some of the major hydrological processes included in the WATFLOOD model.

In terms of hydrological model complexity, there are simpler models and much more complex models than WATFLOOD. WATFLOOD ensures a good representation of water balance; however it does not represent energy-related processes well. For example, the method of evaporation chosen for this study uses the Hargreaves equation which is based on air temperature only; wind, sunshine, and humidity (all known to influence evaporation) are not considered. Despite the simplification of the hydrological processes in WATFLOOD, a reasonably good result can be achieved for the purpose of comparing average streamflow in different climate periods. An advantage of a less complex model such as WATFLOOD relates to the availability of input data required. It is rare to have observations of all the various climate data required to model hydrological processes in more detail (e.g. short wave radiation, long wave radiation, humidity, wind speed, atmospheric pressure, sunshine and cloud cover). In the current study, temperature and precipitation were the only two climate inputs used to force the hydrological model. Observations of these climate parameters were not available for the Pinus River basin but a reasonable calibration was achieved using Goose Bay climate inputs, as described in Section 4.3.

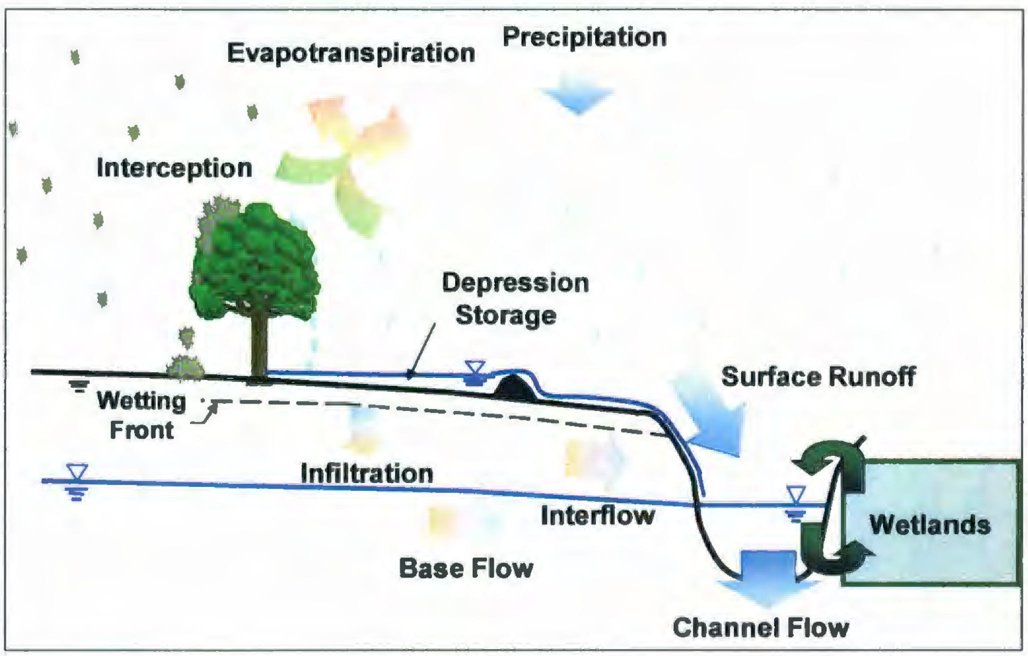

Figure 4.2 Hydrological Processes of the WATFLOOD Model (Stadnyk, 2004)

4.2 Watershed File Setup

The watershed file is a very important WATFLOOD input as it contains the basic geographical and geophysical data necessary to run the hydrological model. Topography and land cover are considered to be the most important physiographic features affecting the outcome of the model (Bingeman, 2006). The watershed file consists of a regular grid of cells with data values for several physiographic attributes assigned to each cell (NRC, 2007). Green Kenue™ (formerly EnSim Hydrologic) is an advanced data preparation, analysis, and visualization tool for hydrologic modellers which permits the automatic generation of the watershed file based on digital elevation and land use data.

SRTM digital elevation data were obtained for the Pinus River watershed as discussed in Section 3.2.1. These data were imported into Green Kenue from which the program delineated the watershed boundary as well as the drainage paths of surface water through the watershed. These delineations were compared with 1:50,000 scale NTDB base mapping and small adjustments were made to ensure an accurate representation of the drainage patterns.

The next step toward development of watershed inputs involved the definition of model grid size and the application of this grid to the study basin. A grid size of approximately 2 km by 2 km was chosen for the Pinus model. Figure 4.3 illustrates the model grid as well as the Green Kenue-delineated watershed boundary and channels. The colour scheme of this figure corresponds to the elevation of the midpoint of the main channel within each cell.

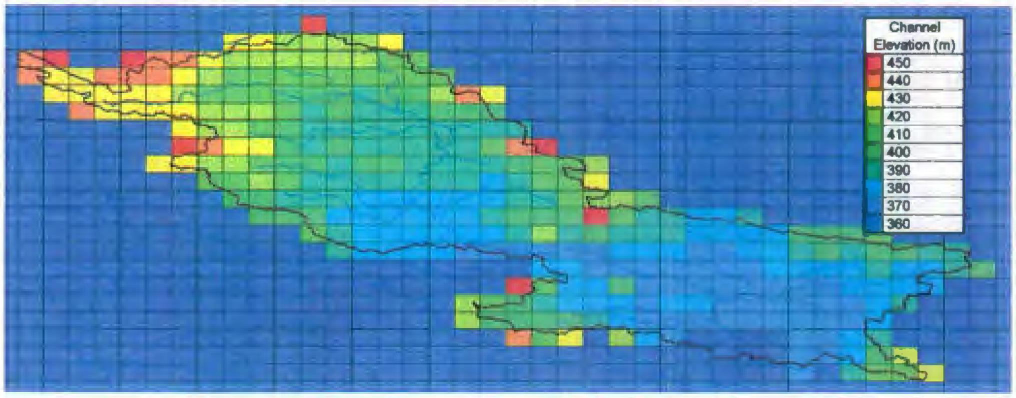

Figure 4.3 Green Kenue Model Grid (Channel Elevation)

(Note: Map projection is lat-lon therefore grids do not appear square)

Table 4.1 summarizes some of the physiographic attributes that are automatically calculated by Green Kenue for each cell in the model grid.

Table 4.1 Green Kenue Watershed Data Attributes

Attribute	Description
Channel elevation (ELV)	Elevation of the midpoint of the main channel with a cell.
Drainage area (FRAC)	Percentage of the cell area that flows in the indicated drainage direction.
Drainage direction (S)	Direction of the majority of the flow out of the cell (possible directions include the 4 cardinal directions and 4 intermediate directions).
River class (IBN)	River roughness class (maximum of 5 may be defined).
Contour density (IROUGH)	Gives an indication of the number of contours in a cell.
Land cover	Percentage of cell area in each land use category.

4.3 Model Calibration

As discussed previously, there are no observed climate data from within the Pinus River basin. The closest climate station is at Goose Bay, approximately 90 km east of the basin centroid. Observed climate data are also available at Churchill Falls, approximately 160 km west of the basin centroid; however these data were not used in the current study. It is recommended that additional research be conducted to assess the potential of using Churchill Falls observed climate data, or some combination of the two stations, for calibration of the Pinus River basin hydrological model. A reasonable calibration was achieved using Goose Bay climate alone; the only adjustment to the Goose Bay climate was made to account for the lower temperatures expected at the higher elevations of the Pinus basin. The Goose Bay climate station is at an elevation of approximately 50 m whereas the Pinus River basin has an elevation range of between 350 m and 510 m. Accordingly, assuming a lapse rate of 0.0041 deg C/m, Goose Bay temperatures were reduced by between 1.2 and 1.4 degrees prior to hydrological model input. This adjustment was somewhat inconsequential since snowmelt parameters such as base temperature were optimized to provide a good fit to measured streamflow; it is likely that the optimal parameter values accounted for any inaccuracy in the lapse rate assumption.

Ten full years of daily streamflow data were available for model calibration (1999 to 2008) as discussed in Section 3.4. Because the climate inputs used to force the hydrological model for the calibration period were measured at the Goose Bay climate station rather than within the Pinus basin, a perfect calibration was not expected. The intent of the calibration was therefore not to fit the measured streamflow exactly but to reproduce the "climate signal" (e.g. monthly average streamflow, timing of spring runoff, baseflow recession periods, etc.).

In the process of calibrating the hydrological model to measured streamflow, the sensitivity of several model parameters was assessed. The base temperature and melt factor were determined to have a significant effect on the timing of the spring hydrograph, and these parameters were set early in the calibration process. Appropriate baseflow recession parameter values were then determined as well as upper zone to lower zone drainage parameters. The model was determined to be very sensitive to the river roughness parameter. The roughness was increased to represent the energy losses through the many lakes in the system and this provided a better match of hydrograph peaks. Once the hydrograph shape was matching closely, evaporation parameters such as maximum interception capacity were adjusted to achieve a better representation of total runoff volume. Overall, the model was determined to be very sensitive to spring temperature inputs, and that biases introduced that affected melt rates (e.g. lapse rate) had a significant influence on hydrograph shape and timing.

As with any model, the chosen hydrological model cannot give a full picture of reality; however, it is important that the model represents well the main features of the system dynamics relevant to the particular study (Dibike and Coulibaly, 2007). In this study, average streamflow is of interest; the calibration of the Pinus basin model led to a good agreement between observed and simulated average streamflow, as shown in Figures 4.4 and 4.5.

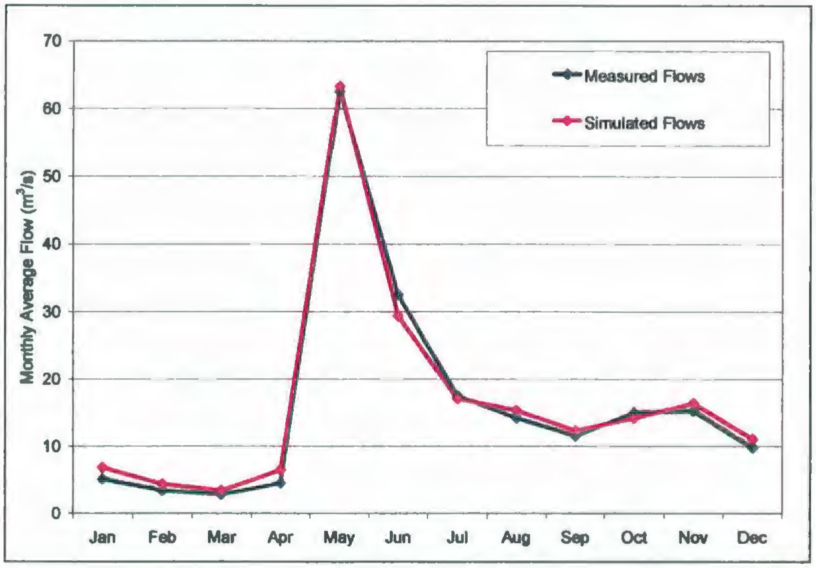

Figure 4.4 Observed and Simulated Monthly Average Pinus River Flow

(Calibration Period, 1998-2008)

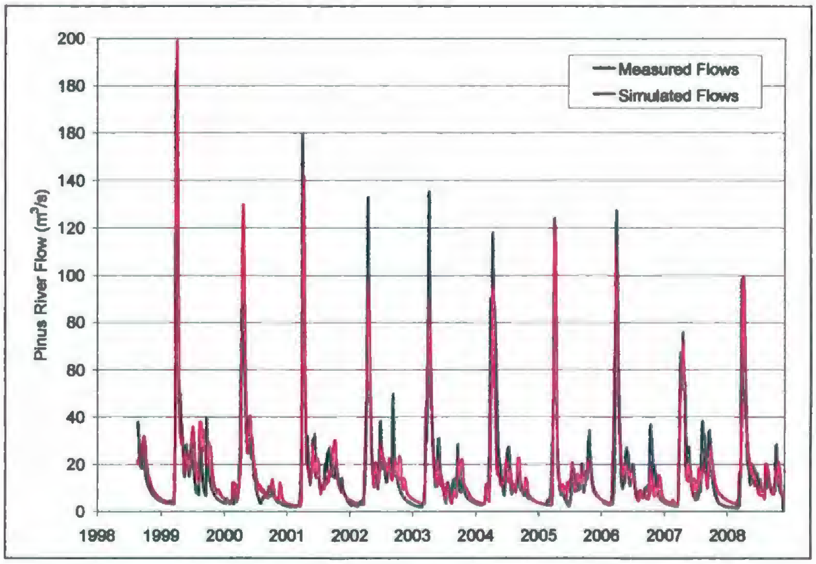

Figure 4.5 Observed and Simulated Daily Average Pinus River Flow

(Calibration Period, 1998-2008)

The Nash-Sutcliffe coefficient N_r is a measure of statistical association between the observed and simulated streamflow which indicates the percentage of the observed variance that is explained by the predicted data. For the daily streamflow over the calibration period (1992-2008), the Nash-Sutcliffe coefficient was 0.80 while the correlation coefficient (r^2) was 0.81. Equations for these statistical measures are provided below where S_i is the simulated flow for each time step, O_i is the observed value, O_i^* is the average measured flow, and N is the total number of values within the period of analysis. These scores were deemed acceptable for the purpose of climate change impacts assessment on average basin flow.

$$N_r = 1 - \frac{\sum_{i=1}^{N} (S_i - O_i)^2}{\sum_{i=1}^{N} (O_i - O_i^*)^2}$$

$$R = \frac{\frac{1}{N} * \sum_{i=1}^{N} (O_i - O_i^*) * (S_i - O_i^*)}{\sqrt{\left(\frac{N * \sum_{i=1}^{N} O_i^2 - \left(\sum_{i=1}^{N} O_i \right)^2}{N * (N-1)} \right)} * \sqrt{\left(\frac{N * \sum_{i=1}^{N} S_i^2 - \left(\sum_{i=1}^{N} S_i \right)^2}{N * (N-1)} \right)}}$$

Typical hydrological model studies split the observed data into two data sets. The first is used to select model parameters and the second is used to test these parameters for a different time period. In the current study the entire observed data set was used for model calibration. Since the climate inputs used were observed 90 km away from the modeled basin, the goal was to produce a model that was climatologically representative rather than being able to match individual events. Hydrological model calibration is often be influenced greatly by individual event flows; without observed climate from within the basin it is more important to use all of the observed data to generate such a model. If this model continues to be used for impacts research, additional years of streamflow data should be used for model validation.

Appendix G contains the calibrated WATFLOOD parameter file.

4.4 Model Limitations and Possible Improvements

The WATFLOOD hydrological model used in this research was appropriate for the level of complexity of the study. Although the modeling did not include potential changes in cloud cover, wind, humidity and other variables which are important to the hydrological process, the calibration achieved using temperature and precipitation alone was sufficient for this initial study into climate change impacts on the Lower Churchill Project.

It is likely that a better model calibration would have been achieved if there were observed climate data from stations within the study basin. As it was, observed temperature and precipitation from the Goose Bay climate station (approximately

90 km from the centre of the Pinus Basin) were used with a slight temperature adjustment related to the elevation difference between the two locations. Precipitation measurement error was accounted for by using the AHCCD daily precipitation data set for Goose Bay. Temperature data were compared to the AHCCD daily temperature data set and were found to be relatively free of error and so the original gauge temperature data were used.

It is possible that a better calibration would have been achieved if hourly precipitation data were used rather than daily. These data are available for summer months (obtained using a tipping bucket rainfall gauge), but observations are not deemed to be accurate for months in which frozen precipitation exists. It was found that the biggest change with respect to input data related to the use of the AHCCD data for winter snow accumulations. Without AHCCD adjustments, spring runoff was severely underestimated.

Flow measurement errors, more likely during the spring peak, may have affected the model calibration slightly. However, Environment Canada (1981) suggests that accuracies within 5 percent are achievable 95 percent of the time.

Chapter 5 Downscaled Climate Data Assessment and Correction

5.1 Comparison between Modeled and Observed Climate

Prior to using a RCM to predict the future climate, it is important that the model is able to accurately predict the current climate. To this end, average monthly CGCM3-CRCM temperature and precipitation for the Goose Bay grid point were compared with observed temperature and observed (AHCCD) precipitation for the overlapping period (1968-2000). The RCM was found to underestimate temperature by between 2.3 and 7.0 degrees C, and precipitation by between 5 and 53 percent, with the largest difference in the winter period. Figures 5.1 and 5.2 illustrate the comparison between monthly average observed and RCM temperature and precipitation, respectively.

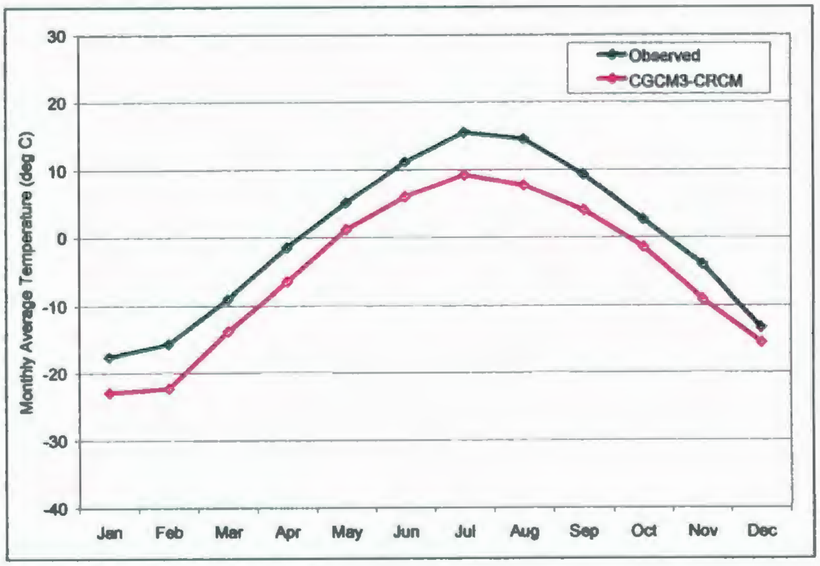

Figure 5.1 Observed and CGCM3-CRCM Temperature at Goose Bay (1968-2000)

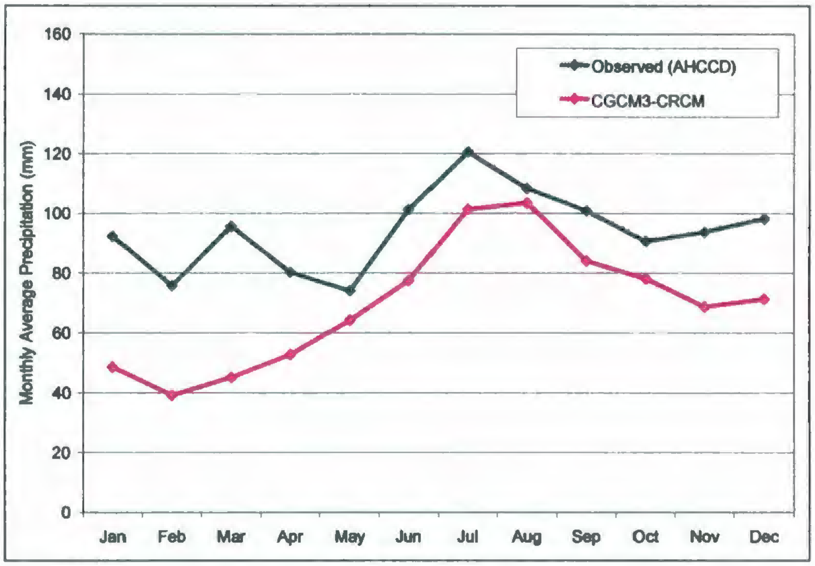

Figure 5.2 Observed and CGCM3-CRCM Precipitation at Goose Bay (1968-2000)

A bias correction method was applied to reduce the biases in both temperature and precipitation, as discussed in the following section.

5.2 RCM Bias Correction

Leader and Buishand (2007) found that a relatively simple nonlinear transformation, correcting both mean and coefficient of variation (CV, equivalent to standard deviation divided by mean) led to a better reproduction of observed precipitation than the commonly used linear scaling correction which has the disadvantage of leaving standard deviation unchanged. They proposed a more straightforward approach for adjusting the mean and variance of RCM temperature. These bias-correction procedures were used in the current study to correct the RCM precipitation and temperature, as described in Sections 5.2.1 and 5.2.2, respectively.

In the current study it is assumed that the future RCM climate suffers from the same problems as the current RCM climate. Accordingly, the measurement-derived bias correction factors were applied equally to both current and future RCM output. This assumption ignores the possible changed seasonality of future climate. For example, if the future winter period is shorter than the current winter period, it may be more appropriate to apply the corrections to this shorter period. In this study the corrections are applied based on Julian day; application of the corrections based on condition rather than time should be considered as an area of future research.

The bias-corrections applied in the current study were based on the comparison between observed and RCM climate from the single grid point closest to the Goose Bay climate station. Leander and Buishand (2007) suggested that basin-averages be used; however, this assumes that there are more than one climate station and RCM grid point within the basin. There are no climate stations within the Pinus River basin. Averaging Goose Bay and Churchill Falls climates was considered; however, an acceptable hydrological model calibration was achieved using Goose Bay climate alone as discussed in Section 4.3. Hence bias-corrections were developed for a single grid point closest to the Goose Bay climate station.

5.2.1 Precipitation Bias Correction

Corrected RCM precipitation values were estimated for every day of the current and future periods using the following equation.

$$P^* = aP^b$$

In this equation P* is the bias-corrected precipitation, P is the uncorrected precipitation, and a and b are the correction parameters corresponding to mean and CV, respectively. To reduce sampling variability, these factors were determined for each 5-day period of the year, including data from 30 days before and after the considered 5-day period, and averaged over the entire current climate period (1968 to 2000). Terink et al. (2009) applied the same bias-correction methodology and developed the charts shown in Figure 5.3 to illustrate the averaging procedure.

The factor b was determined first such that the CV of the corrected precipitation matched that of the observed daily precipitation. Then the factor a (which depends on the value of b) was determined such that the mean of the corrected precipitation matched that of the observed daily precipitation. The values of the correction factors a and b are shown in Figure 5.4.

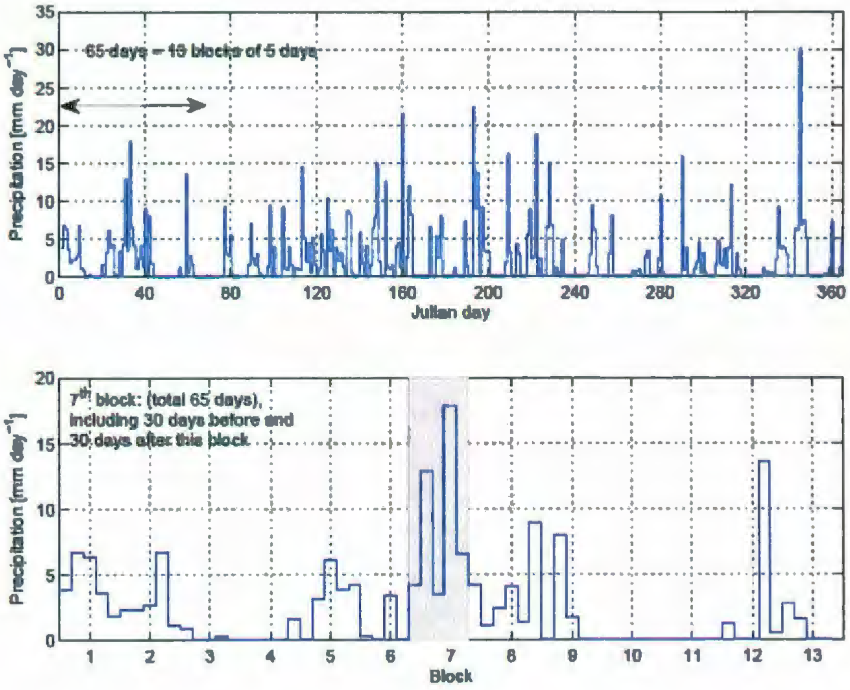

Figure 5.3 Schematisation of the division of a year into 73 blocks of 5 days (Terink, 2009)
Top Panel: daily precipitation throughout the year;
Bottom panel: first 65 days of the year resulting in 13 blocks of 5 days each

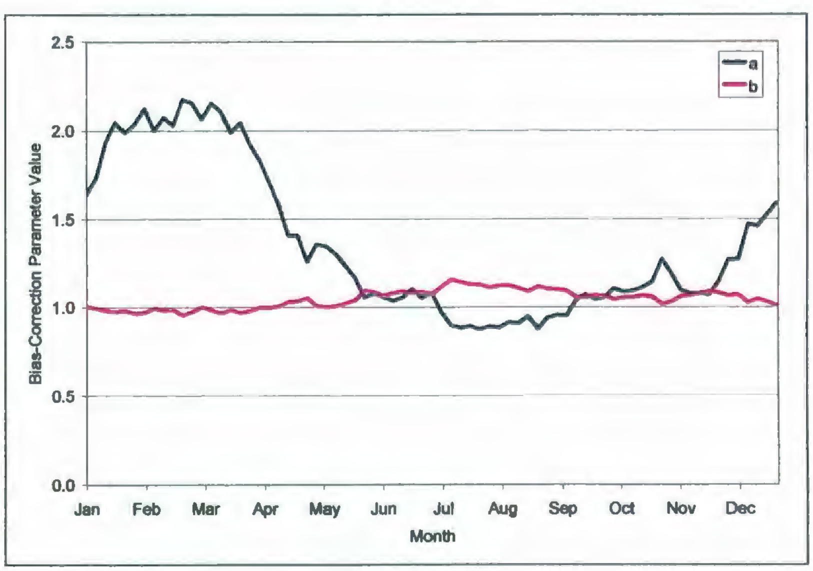

Figure 5.4 Average Precipitation Bias-Correction Parameter Values (1968-2000)

As shown, the a parameter has a value greater than one for all months with the exception of July and August, and it is highest in the winter period where the RCM underestimates the precipitation by the largest percentage. The b parameter has a value less than one in January, February and March and greater than one for the remainder of the year. A value greater than one indicates that the CV of the precipitation is enhanced by the correction.

Figure 5.5 compares observed (AHCCD) average monthly precipitation with uncorrected RCM and bias-corrected RCM from the Goose Bay grid point. Figure 5.6 illustrates the comparison between uncorrected and bias-corrected precipitation for the current (1968-2000) and future (2038-2070) periods.

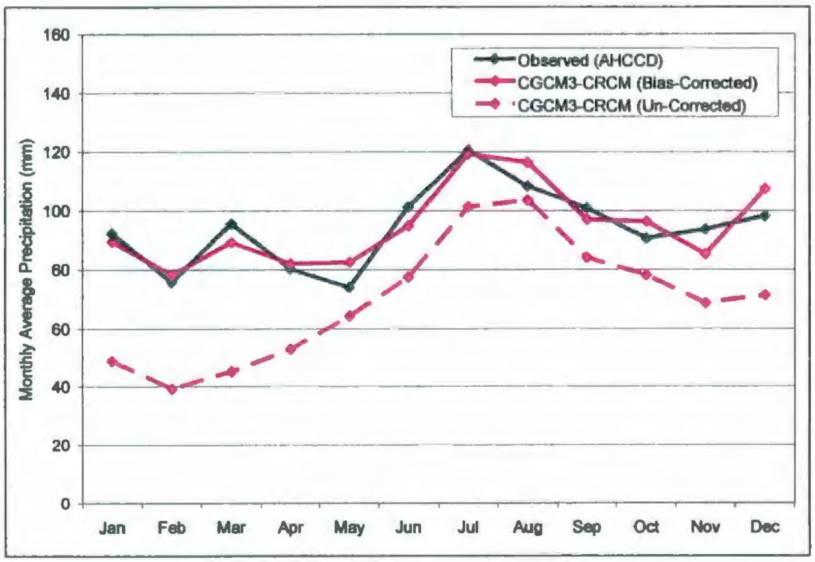

Figure 5.5 Observed and CGCM3-CRCM Precipitation at Goose Bay (1968-2000)

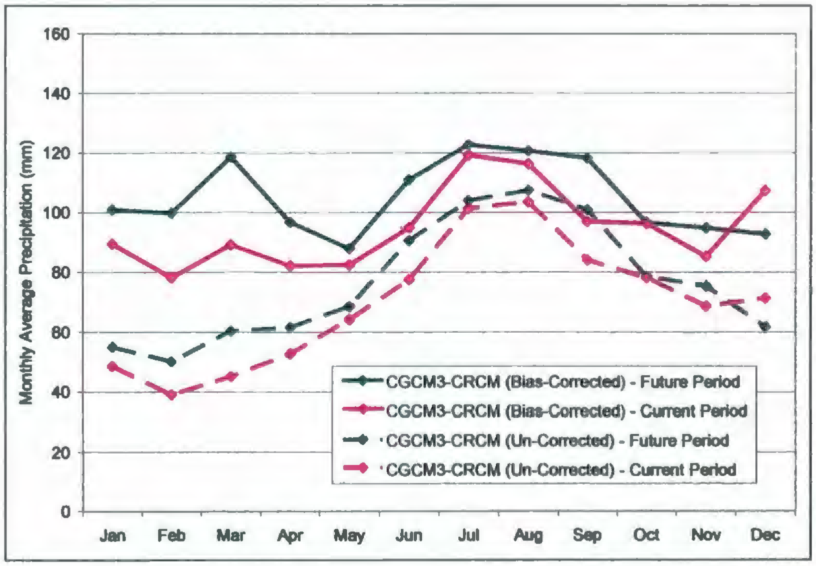

Figure 5.6 Current and Future CGCM3-CRCM Precipitation at Goose Bay

As shown in Figure 5.5, the bias-correction presents a significant improvement in the match with observed precipitation. It is interesting to note the magnitude of the average March precipitation in the future climate period shown in Figure 5.6. As the corrections determined to bring the current period RCM precipitation in line with observed were applied equally to both current and future periods, some seemingly unrealistic future snowfall amounts resulted; other correction methods for winter precipitation should be considered in future studies.

5.2.2 Temperature Bias Correction

The method presented by Leander and Buishand (2007) to correct the mean and variability of RCM temperature uses the following equation.

$$T^* = \overline{T} + (T - \overline{T}) * \frac{\sigma(T_{observed})}{\sigma(T_{RCM})} + (\overline{T}_{observed} - \overline{T}_{RCM})$$

In this equation T^* is the bias-corrected RCM temperature, T is the uncorrected RCM temperature, $\overline{T}$ indicates 30-year average, and σ is the standard deviation. To reduce sampling variability, mean and standard deviation values were determined for each 5-day period of the year, including the 30 days before and after the considered 5-day period, and averaged over the current climate period (1968 to 2000).

Figure 5.7 compares observed average monthly temperature with uncorrected RCM and bias-corrected RCM from the Goose Bay grid point. Figure 5.8 illustrates the comparison between uncorrected and bias-corrected temperature for the current and future periods.

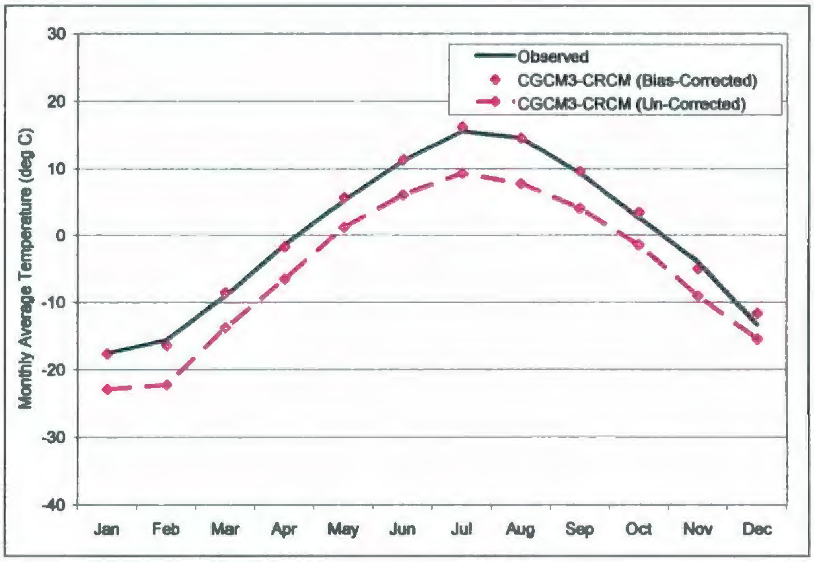

Figure 5.7 Observed and CGCM3-CRCM Temperature at Goose Bay (1968-2000)

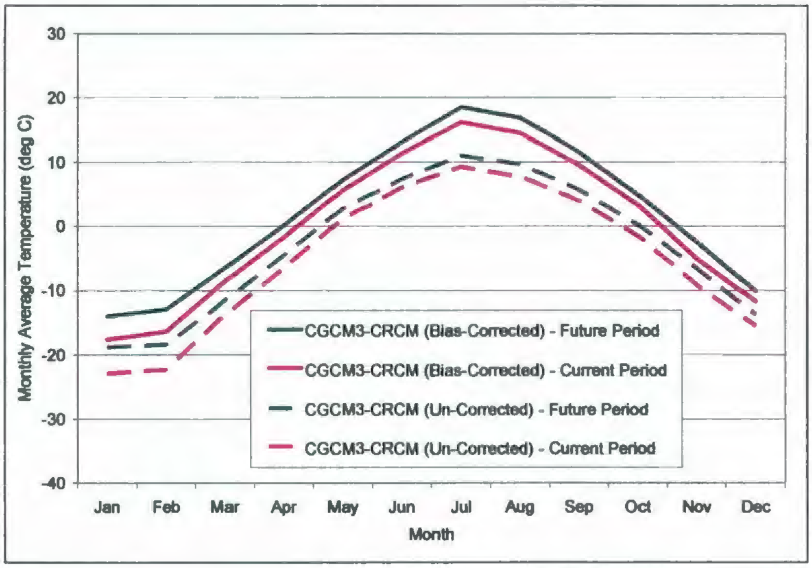

Figure 5.8 Current and Future CGCM3-CRCM Temperature at Goose Bay (data points are removed for clarity)

5.3 Current versus Future Climate

5.3.1 Temperature

The CGCM3-CRCM predicted increase in mean annual temperature at Goose Bay for the future climate period (2038-2070) relative to the current climate period (1968-2000) is 2.4 degrees C. The distribution of this change by month is illustrated in Figure 5.8 for both uncorrected and bias-corrected RCM temperatures (mean annual change is the same for both data sets). Table 5.1 summarizes the monthly temperature difference in the bias-corrected RCM data.

Table 5.1 Current and Future Temperature at Goose Bay

Month	Monthly Average Temperature (deg C)		Difference (Future-Current) (deg C)
	Current Period (1968-2000)	Future Period (2038-2070)	
January	-17.8	-14.0	+3.8
February	-16.5	-12.9	+3.6
March	-8.7	-6.5	+2.2
April	-1.9	0.1	+2.0
May	5.5	7.2	+1.7
June	11.2	13.1	+1.9
July	16.0	18.5	+2.5
August	14.4	16.9	+2.5
September	9.4	11.6	+2.2
October	3.3	4.9	+1.6
November	-5.1	-2.5	+2.6
December	-11.8	-10.1	+1.7
Annual	**-0.1**	**2.3**	**+2.4**

5.3.2 Precipitation

The CGCM3-CRCM predicted increase in mean annual precipitation at Goose Bay for the future climate period relative to the current climate period is 10 percent (uncorrected precipitation) or 11 percent (bias-corrected precipitation). The distribution of these changes by month is illustrated in Figure 5.6. Table 5.2 summarizes the monthly precipitation difference in the bias-corrected RCM data.

Table 5.2 Current and Future Precipitation at Goose Bay

Month	Monthly Average Precipitation (mm)		Difference	
	Current Period (1968-2000)	Future Period (2038-2070)	(mm)	(%)
January	89	101	+12	+13
February	78	100	+22	+28
March	89	119	+30	+33
April	82	97	+15	+18
May	82	88	+6	+7
June	94	111	+17	+17
July	119	123	+4	+3
August	116	121	+5	+4
September	97	118	+21	+22
October	96	96	-	-
November	85	95	+10	+12
December	107	93	-14	-13
Annual	**1134**	**1260**	**+126**	**+11**

5.4 Daily Temperature Range

In addition to comparing the observed and RCM mean temperatures (as discussed in Section 5.1), an investigation of daily temperature ranges was conducted. Observed and CGCM3-CRCM average daily temperature ranges were compared and the influence of daily temperature range on simulated flow was checked. Daily temperature range was calculated based on observed hourly temperatures and RCM 3-hourly temperatures over the period 1968-2000. The temperature bias-correction procedure did not affect the temperature variation within the day and therefore uncorrected and bias-corrected daily ranges were equal. The daily maximum and minimum temperature series from the RCM were also obtained and average daily range compared. The average daily temperature range from each data set was estimated for each 5-day period of the year, considering the 30 days before and after in the calculation of each 5-day period average, similar to the procedure used in the temperature and precipitation bias-correction methods. Figure 5.9 illustrates this comparison.

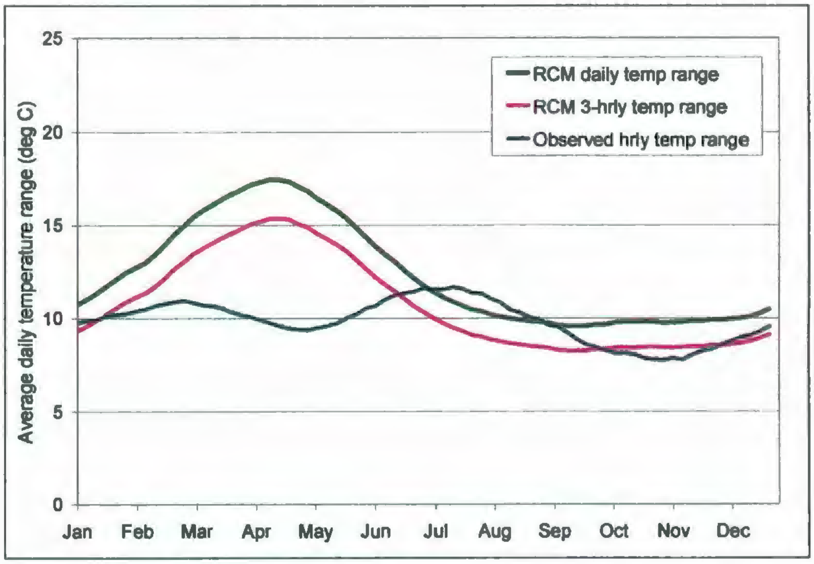

Figure 5.9 Observed and CGCM3-CRCM Daily Temperature Range at Goose Bay (1968-2000)

A comparison between RCM data sets (green and pink curves in Figure 5.9) illustrates the expected result: the average daily range of the 3-hourly RCM data is lower than the actual daily range as predicted by the RCM (daily maximum minus daily minimum). This difference is due to the resolution of the 3-hourly data – the coarser the resolution of the data, the lower the daily range is expected to be.

The largest difference between RCM 3-hrly and observed daily temperature range is in the spring when the RCM range is up to five degrees higher. It is a very revealing diagnostic that the air temperature range of the RCM output increases during the snow melt period while the measured data show a decline. This indicates that energy in the RCM is being used to heat the air during the spring instead of melting snow, evaporating water or thawing the ground.

To assess the sensitivity of the hydrological model to the daily temperature range, the hydrological model was simulated with observed daily average temperatures and the resulting streamflow was compared to that determined using hourly temperatures. Figure 5.10 illustrates the comparison of the monthly average streamflow from these two simulations.

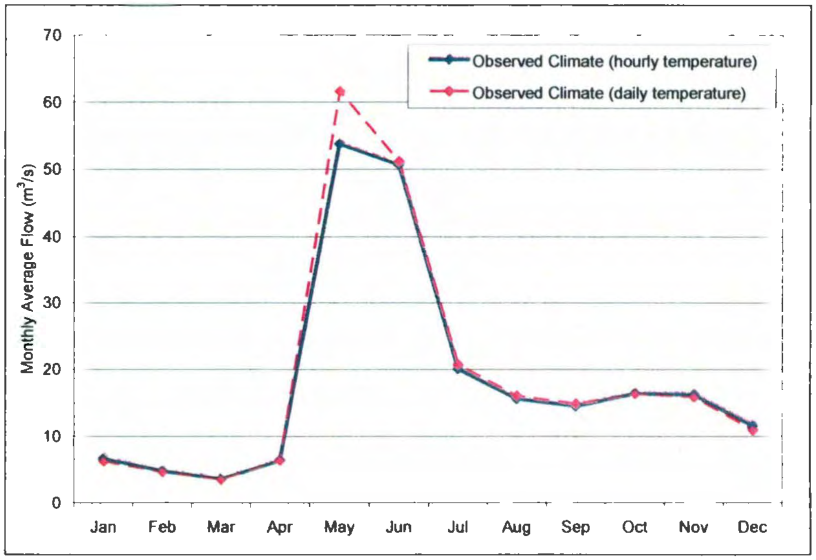

Figure 5.10 Simulated Pinus River Flow under Observed Climate (Daily and Hourly Temperatures)

The results suggest that the hydrological model is not overly sensitive to daily temperature range except for the month of the spring peak (May) where the average streamflow is higher for the daily temperature simulation. The lower May peak in the hourly temperature case could be due to a reduced snowpack resulting from sublimation during the warmest part of the day which is not represented in the daily temperature case.

Daily average temperature by definition have zero daily temperature range. The RCM daily temperature range as shown in Figure 5.9 is closer to observed than zero, and hence it is expected that the sensitivity of the hydrological model to the error in RCM daily temperature range would be less severe than that illustrated in Figure 5.10. Therefore, due to the slight effect anticipated from correction of this characteristic of the RCM data, it was not corrected prior to simulation in the hydrological model.

5.5 NCEP-CRCM Climate

As discussed in Section 2.3, reanalysis models simulate past climate using historical observations and numerical weather forecasts to provide an accurate record of atmospheric fields. As such, reanalysis predictions are expected to be more realistic than those from any GCM. Reanalysis data are often used to provide the boundary conditions for RCMs. The comparison between a GCM-driven run and one driven by reanalysis data provides the potential to discriminate between the bias resulting from the driving GCM and the bias introduced by the

RCM (Leander, 2007). This was the goal in using reanalysis data in the current study.

As discussed in Section 3.3.3, NARCAPP modellers included NCEP reanalysis-driven RCM runs in their climate modeling matrix. Temperature and precipitation data sets from the NCEP-CRCM runs have been used in this research for comparison with CGCM3-CRCM climate predictions, as described in the following sections.

5.5.1 Temperature

Figure 5.11 presents the comparison between observed, uncorrected NCEP-CRCM and uncorrected CGCM3-CRCM average monthly temperature at Goose Bay. The 1979-2000 period was chosen for this comparison as this is the period for which NCEP-CRCM data are available. As shown, the NCEP-CRCM predicted monthly average temperature is generally closer to observed. Table 5.3 summarizes the information numerically.

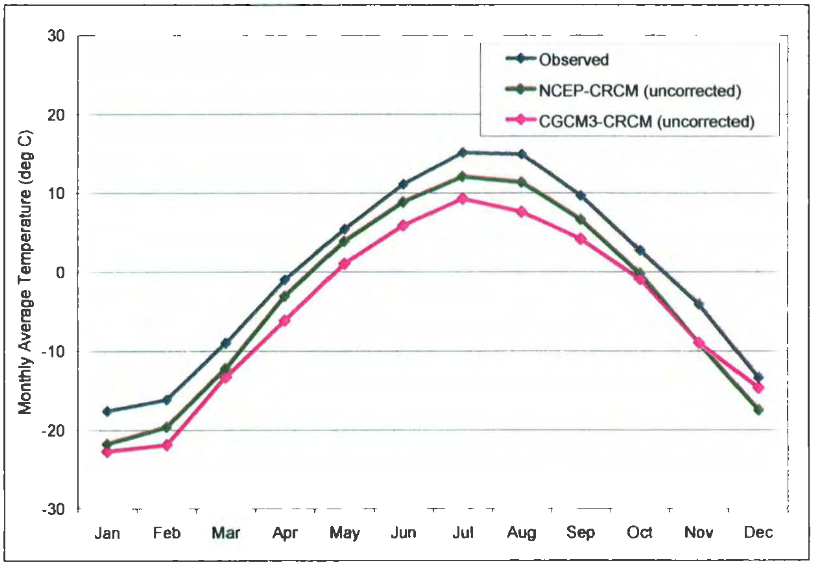

Figure 5.11 Observed and Uncorrected RCM Temperature at Goose Bay (1979-2000)

The NCEP-CRCM temperature predictions are closer to observed for every month with the exception of December. The percentage improvement of the NCEP-CRCM estimate over the CGCM3-CRCM estimate ranges from -192 percent (December) to +64 percent (May) and the annual average is a +35 percent improvement.

The bias-correction procedure described in Section 5.2.2 was applied to the NCEP-CRCM data. The result was a very close match with observed average monthly temperatures, as shown in Figure 5.12.

Table 5.3

Comparison of Temperature between Observed and Uncorrected RCM (1979-2000)

Month	Temperature (deg C)			Difference (deg C) (Modeled - Observed)		*Improvement of NCEP-CRCM over CGCM3-CRCM (%)
	Observed	CGCM3-CRCM	NCEP-CRCM	CGCM3-CRCM	NCEP-CRCM	
January	-17.6	-22.8	-21.8	-5.2	-4.2	+19
February	-16.1	-22.0	-19.7	-5.9	-3.5	+40
March	-9.0	-13.4	-12.3	-4.4	-3.3	+26
April	-1.0	-6.3	-3.1	-5.3	-2.1	+60
May	5.4	0.9	3.8	-4.5	-1.6	+64
June	11.1	5.8	8.8	-5.4	-2.3	+57
July	15.1	9.1	12.0	-6.0	-3.1	+48
August	14.9	7.5	11.3	-7.4	-3.6	+52
September	9.7	4.0	6.6	-5.6	-3.1	+45
October	2.7	-1.0	-0.2	-3.8	-2.9	+22
November	-4.1	-9.1	-9.1	-5.0	-4.9	+1
December	-13.4	-14.8	-17.5	-1.4	-4.1	-192
Annual	**-0.1**	**-5.1**	**-3.3**	**-5.0**	**-3.2**	**+35**

* Improvement calculated as percentage of difference between CGCM3-CRCM and observed.

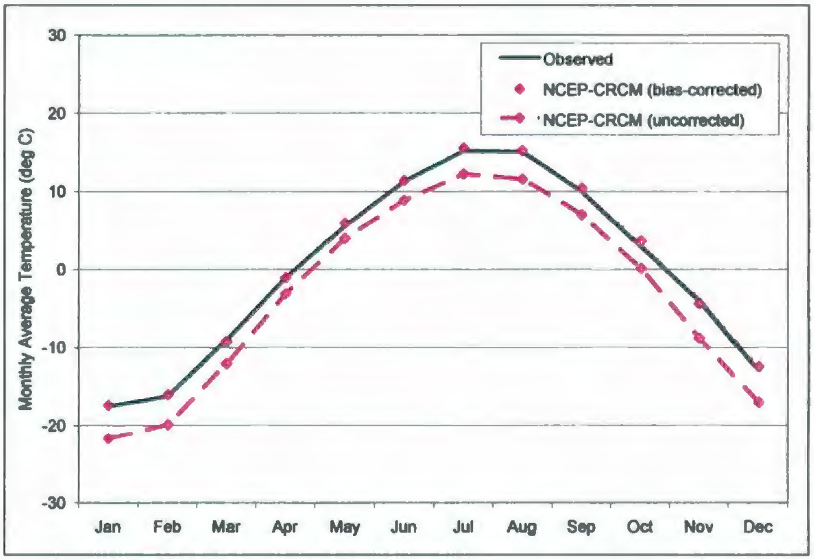

Figure 5.12 Observed and NCEP-CRCM Temperature at Goose Bay (1979-2003)

5.5.2 Precipitation

Figures 5.13 presents a comparison between observed, uncorrected NCEP-CRCM and uncorrected CGCM3-CRCM average monthly precipitation at Goose Bay. As shown, the NCEP-CRCM predicted precipitation is closer to observed for most months. Table 5.4 summarizes the comparison numerically.

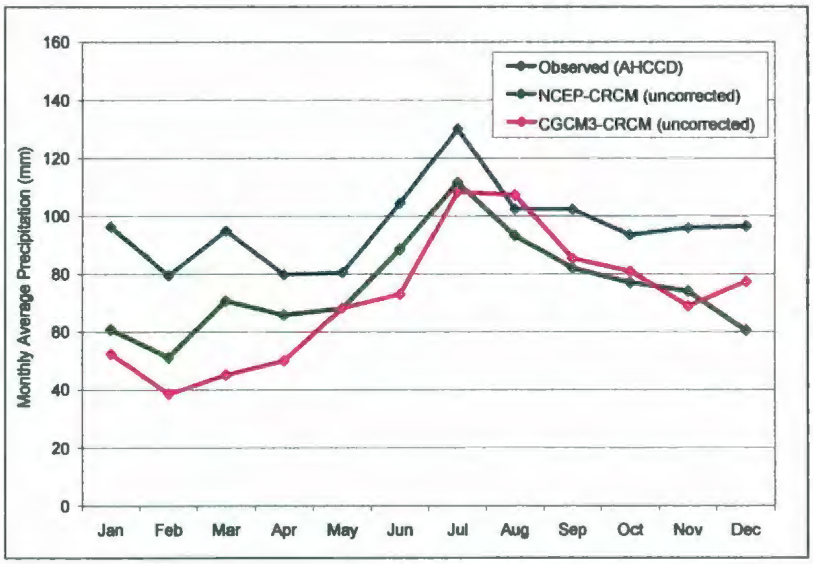

Figure 5.13 Observed and Uncorrected RCM Precipitation at Goose Bay (1979-2000)

The NCEP-CRCM precipitation predictions are closer to observed for every month with the exception of August, September, October, and December. The percentage improvement of the NCEP-CRCM estimate over the CGCM3-CRCM estimate ranges from -105 percent (August) to +53 percent (April) and the annual average is a +17 percent improvement.

Table 5.4

Comparison of Precipitation between Observed and Uncorrected RCM (1979-2000)

Month	Precipitation (mm)			Difference (%)		*Improvement of NCEP-CRCM over CGCM3-CRCM (%)
	Observed (AHCCD)	CGCM3-CRCM	NCEP-CRCM	CGCM3-CRCM	NCEP-CRCM	
January	96.3	52.0	60.7	-46.0	-37.0	+19
February	79.3	38.2	51.0	-51.9	-35.7	+31
March	94.8	44.8	70.5	-52.7	-25.6	+51
April	79.7	49.7	65.6	-37.7	-17.7	+53
May	80.4	67.9	67.9	-15.6	-15.5	+1
June	104.4	72.6	88.3	-30.4	-15.4	+49
July	130.2	108.1	111.5	-17.0	-14.4	+15
August	102.4	107.0	93.0	+4.5	-9.1	-105
September	102.3	85.0	81.8	-16.9	-20.0	-18
October	93.5	80.5	76.9	-13.8	-17.7	-28
November	95.9	68.5	73.9	-28.6	-23.0	+20
December	96.4	76.9	60.3	-20.2	-37.4	-86
Annual	**1155.6**	**851.2**	**901.4**	**-26.3**	**-22.0**	+17

* Improvement calculated as percentage of difference between CGCM3-CRCM and observed.

From a qualitative perspective, the NCEP-CRCM precipitation also appears to have an improved climate signature or phasing when compared to the precipitation from the CGCM3-CRCM. While there is still a significant general underestimate in monthly NCEP-CRCM precipitation when compared to observations, these bias differences appear to have a more constant bias when compared to the CGCM3-CRCM. A simple correlation analysis between uncorrected monthly precipitation with observed (AHCCD) for the overlapping period (1979-2000) gives correlation coefficient (r^2) scores of 0.12 for CGCM3-CRCM and 0.41 for the NCEP-CRCM. This result confirms the qualitative observation.

The precipitation bias-correction procedure described in Section 5.2.1 was applied to the NCEP-CRCM data. Figure 5.14 compares the bias correction parameters for the both simulations. As shown, the NCEP-CRCM mean correction factor (a) is much lower than the CGCM3-CRCM factor in the first six months of the year. The values of a are similar for the month of June and then the NCEP-CRCM factor exceeds that of the CGCM3-CRCM for the remainder of the year, though by a small amount. The bias-correction resulted in monthly average precipitation that was closer to observed, though slightly overestimated, as shown in Figure 5.15.

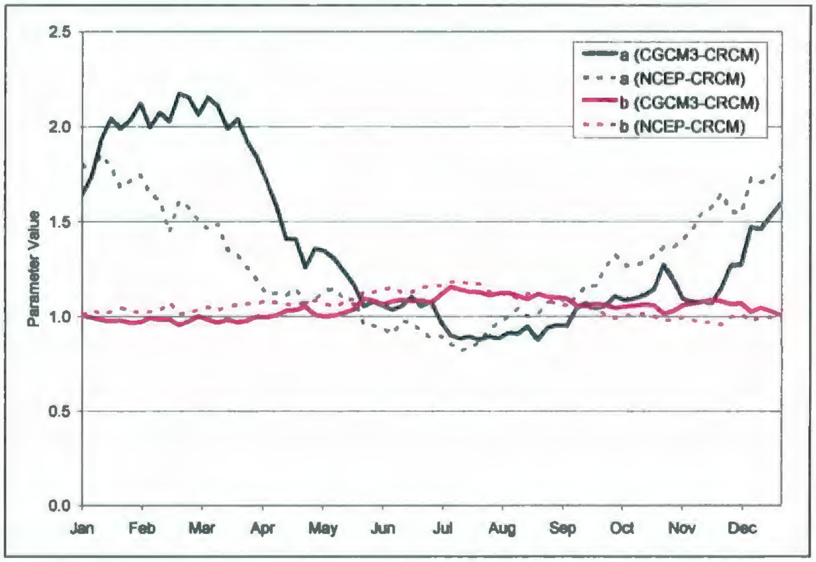

Figure 5.14 Precipitation Bias-Correction Factor Comparison

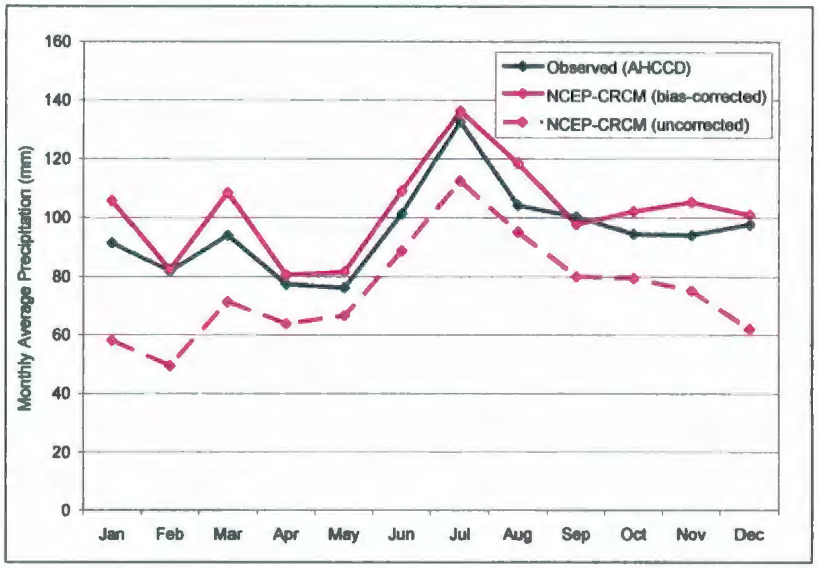

Figure 5.15 Observed and NCEP-CRCM Precipitation at Goose Bay (1979-2003)

5.5.3 GCM vs. RCM Error in Climate Predictions

Since reanalysis predictions of atmospheric fields are more accurate than GCM predictions, the comparison of output from reanalysis-driven RCM runs and GCM-driven RCM runs provides the opportunity to assess the attribution of error between the GCM and RCM. This comparison is useful only under the assumption that errors associated with initial conditions and RCM model forcing (i.e. reanalysis data) are small compared to the error associated with the RCM.

As summarized above, NCEP-CRCM temperatures were more accurate than CGCM3-CRCM temperatures for every month with the exception of December. On average, NCEP-CRCM temperatures were closer to observed than CGCM3-CRCM by 35 percent. Assuming that the error associated with NCEP-CRCM predictions are due solely to the RCM (i.e. the error associated with initial conditions and reanalysis data are negligible), the above noted result suggests that on average, 35 percent of the error in the CGCM3-CRCM temperature predictions is attributable to the GCM, and the remaining 65 percent of the error is attributable to the RCM.

In terms of precipitation, NCEP-CRCM was more accurate than CGCM3-CRCM for each month with the exception of August, September, October, and December. On average, NCEP-CRCM precipitation was closer to observed by 17 percent. Again assuming that the error associated with initial conditions and reanalysis data is negligible compared to that of the RCM, this result suggests that 17 percent of the error in the CGCM3-CRCM precipitation predictions is attributable to the GCM, and the remaining 83 percent of the error is attributable to the RCM.

The above noted error attribution analysis is not exhaustive but nonetheless suggests that RCM bias dominated the overall error and that this error has little dependence on which set of boundary conditions (GCM or NCEP) was used to force the model. Further analysis is required to understand the error structure in light of reanalysis and measurement error data quality, cross-correlation between data error and model error, and the spatial character of the data over a larger study area.

Although using reanalysis data to provide the boundary conditions to the GCM is more accurate than using an RCM to do so, reanalysis data cannot be used for the assessment of climate change impacts since it is only available for historic periods.

Chapter 6 Hydrological Model Simulation Results

6.1 Application of Goose Bay Climate to Pinus River Basin

As discussed in Section 4.3, the Pinus River basin hydrological model was calibrated using Goose Bay climate, with an adjustment for temperature based on the difference in elevation between the two locations. As discussed in Section 5.2, bias-correction factors were developed based on observed and RCM climate from the Goose Bay grid point. Due to an inconsistency in the Goose Bay and the Pinus River basin temperature difference assumed for the purpose of hydrological model calibration (i.e., the lapse rate) and that predicted by the RCM, the hydrological model was not suitable for use with RCM data from the Pinus River grid point. The model was calibrated for an assumed temperature regime corresponding to observed temperature at Goose Bay reduced by between 1.2 and 1.4 degrees depending on the elevation of the model grid cell, whereas the difference in temperature between the Goose Bay and Pinus River RCM grid points was just 0.5 degrees (Pinus River being the cooler of the two locations as expected based on elevation). Because of this difference the model will not produce accurate results for the current period using the temperature regime predicted by the RCM for the Pinus River basin grid point. It should be noted that there was very little difference in the seasonality of the RCM temperatures at Goose Bay and Pinus River. The correlation coefficient of the daily temperatures at these two RCM grid points was over 0.99.

Based on the assumptions described above, RCM climate from the Goose Bay grid point was used in this study for the assessment of the impacts of climate change on Pinus River flow. In essence, this study assumes that the Pinus River basin has the same climate as Goose Bay (with the exception of a slight difference in temperature) and will experience the same change in climate as is predicted to occur at Goose Bay.

6.2 Simulation with Observed Climate

The Pinus River basin hydrological model was calibrated by simulating streamflow using Goose Bay observed temperature and precipitation as input. The results of the calibration are described in Section 4.3 of this thesis.

Once calibrated, the hydrological model was used to simulate streamflow based on a longer period of observed climate (1968-2008). This period overlaps with the RCM current climate period; the comparison of simulated streamflow based on observed and RCM climate is discussed in Section 6.3.

Some interesting trends were noticed in the simulated streamflow based on observed climate. Figure 6.1 compares the simulated streamflow for the model calibration period (1999-2008) and the RCM current climate period (1969-2000).

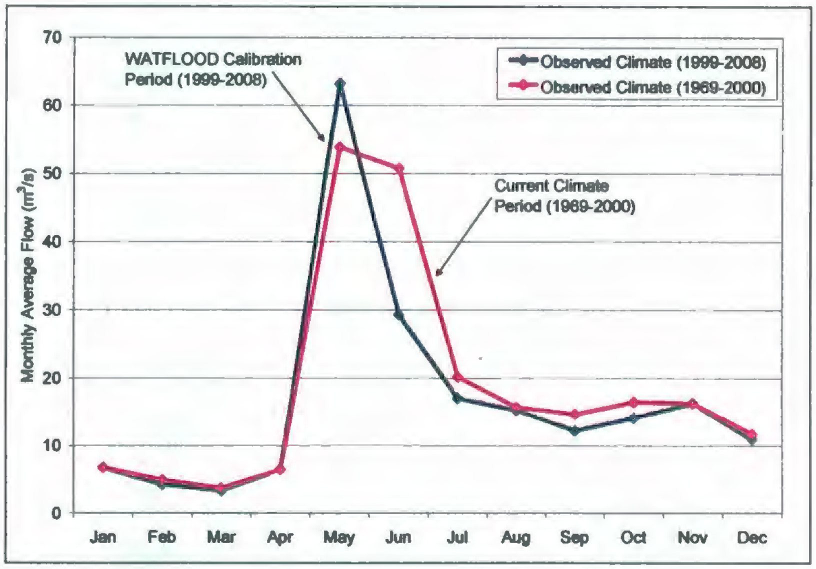

Figure 6.1 Simulated Pinus River Flow under Observed Climate in Calibration Period and CGCM3-CRCM Current Climate Period

As shown, there is a significant difference in May and June flow between the two simulations. In the more recent calibration period, the spring runoff peak occurs in May and the streamflow quickly recedes with the June average flow less than half of the May flow. This is not the case in the longer and earlier simulation of 1969-2000. The spring peak is lower and spans the months of May and June, dropping to summer levels (similar to the calibration period) in July.

Figure 6.2 compares the monthly average simulated Pinus River flow for the following three consecutive but overlapping 20-year periods: 1969-1988, 1979-1998, and 1989-2008.

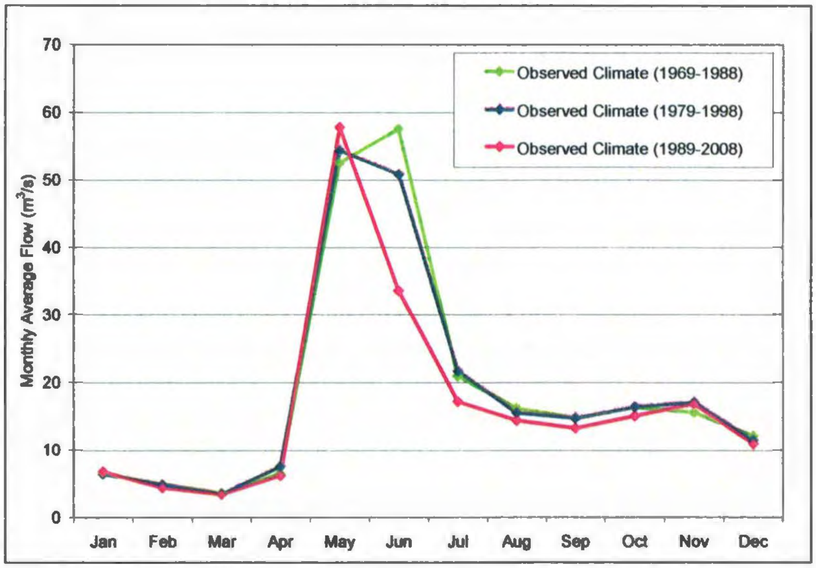

Figure 6.2 Simulated Pinus River Flow under Observed Climate in three consecutive 20-year periods

A similar trend is apparent as that in Figure 6.1; it appears based on the comparison of these 20-year averages that May flow is increasing slightly over time and June flow is decreasing in a much more pronounced fashion. The mean annual flow corresponding to these three periods is also decreasing with time, from 19.1 m^3/s (1969-1988) to 18.8 m^3/s (1979-1998) to 16.7 m^3/s (1989-2008).

This apparent trend is, in fact, consistent with observations from across Canada where hydrologic basins are experiencing earlier and more intense spring melt periods. Burn (2002) detected significant trends in several hydrologic variables implying earlier spring melt conditions. Of the 50-60 hydrometric records from across the country that were used in the analysis, he found that the percentage of stations displaying increasing trends for March and April flows were 38 and 33 percent, respectively, while 28 percent of stations displayed a decreasing trend for June flows. While more data will be required to confirm this finding for the Churchill River basin, it is worth noting that the recent period may already be experiencing a climate signal. A separate study would be warranted to look into whether or not the apparent trends are related to climate change or simply a function of natural variation.

6.3 Simulation with CGCM3-CRCM Modeled Climate

6.3.1 Comparison with Observed Climate Simulations

The hydrology of the 1968-2000 period was simulated with both observed and modeled climate, as illustrated in Figure 6.3. The monthly average simulated flows corresponding to both uncorrected and bias-corrected RCM inputs are shown (dotted and solid pink curves, respectively).

The spring peak of the uncorrected RCM hydrograph is late as a result of the underestimation of temperature which delays the model spring melt. Also the uncorrected RCM simulated flows are lower than observed throughout the year but particularly in the spring; this is a result of the underestimation of precipitation which was most deficient in the winter (approximately 50 percent lower than observed in January, February, and March). The bias-corrected RCM hydrograph is an improvement and represents a plausible condition; however, differences remain with the observed climate hydrograph and these are related to the bias-correction methods applied to the RCM temperature and precipitation. Although simulated flows under RCM climate may not be highly accurate, the comparison of simulated flow under current and future period RCM climate is expected to provide a reasonable indication of the effects of climate change on streamflow.

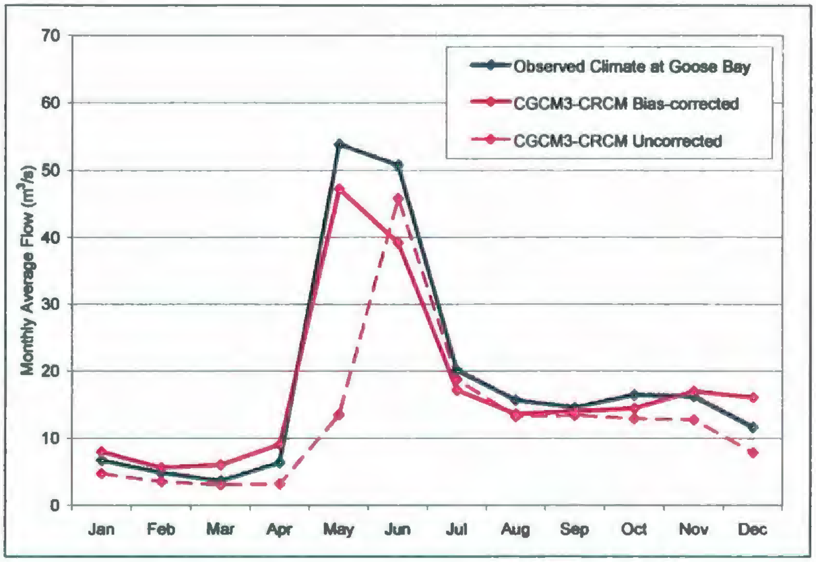

Figure 6.3 Simulated Pinus River Flow under Observed and CGCM3-CRCM Climate (1969-2000)

To further investigate the relative influence of the RCM temperature and RCM precipitation in the differences noted above, additional simulations were conducted. These "mix and match" simulations used observed climate for either temperature or precipitation, and bias-corrected RCM climate for the other.

Figure 6.4 illustrates the resulting simulated monthly average flows from these two simulations.

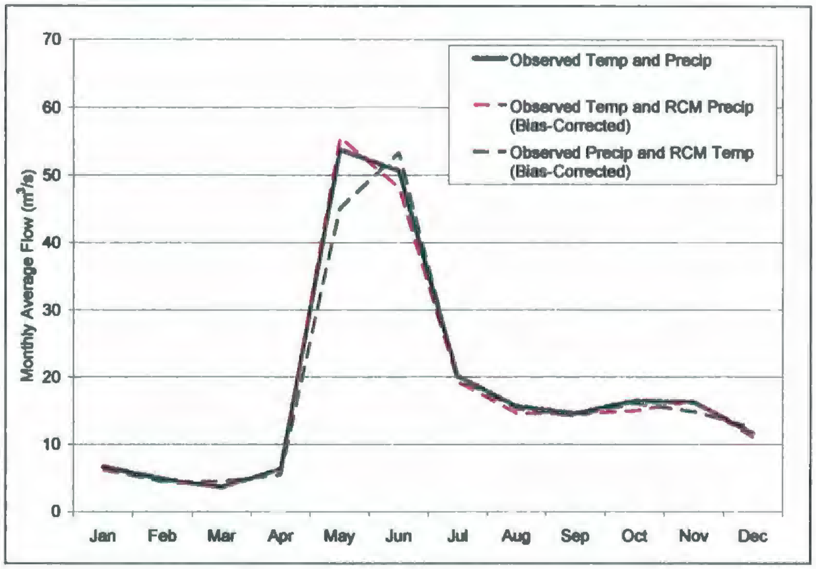

Figure 6.4 Simulated Pinus River Flow under Mix and Match Simulation Scenarios (data points are removed for clarity)

Both of the dotted curves shown in Figure 6.4 are conceivable; however the simulation with observed temperature and RCM precipitation (dotted pink curve) seems to provide a better fit with the observed temperature and precipitation hydrograph (solid blue line). When modeled temperature and observed precipitation are used as input to the hydrological model, the resulting monthly average hydrograph (dotted green curve) does not fit the observed curve as well; the May flow is too low and the June flow is slightly too high. This result suggests that the differences between the solid blue and pink curves in Figure 6.3

are primarily related to the bias-corrected RCM temperature input. Although the bias-correction of the RCM temperatures improved the monthly averages when compared to observed, the differences that remain (possibly including differences in the diurnal temperature variation) lead to differences in the simulated streamflow.

6.3.2 *Current versus Future Streamflow*

The question of how climate change is likely to affect the streamflow of the Churchill River is resolved in this study through the simulation of the Pinus River flow using modeled climate for current and future periods as input. Figure 6.5 presents the monthly average simulated flow for the two periods based on the bias-corrected CGCM3-CRCM temperature and precipitation inputs.

As shown in Figure 6.5, future period streamflow is predicted to be higher in each month with the exception of June, with an average annual increase of 12.8 percent. The greatest increase is expected in the spring period, likely due to increases in February and March precipitation in the order of 30 percent as described in Section 5.3. The percentage increases in monthly average flow are summarized in Table 6.1.

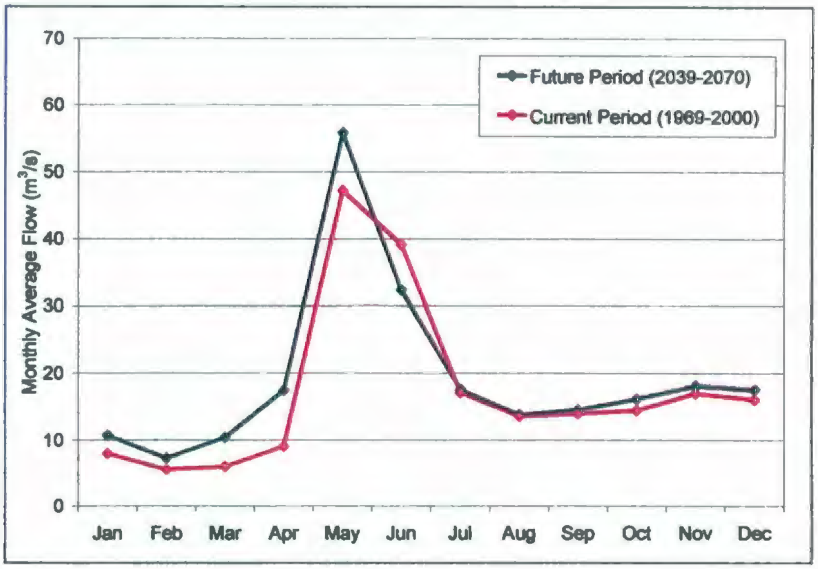

Figure 6.5 Simulated Pinus River Flows under Current and Future Climate (CGCM3-CRCM bias-corrected climate)

Table 6.1 Simulated Pinus River Flow under Current and Future Climate

Month	Monthly Average Flow (m^3/s)		Difference (%)
	Current Climate (1968-2000)	Future Climate (2038-2070)	
January	7.8	10.7	36.7
February	5.4	7.3	33.6
March	5.9	10.4	76.6
April	8.9	17.4	95.8
May	47.1	55.8	18.5
June	39.0	32.4	-17.1
July	17.0	17.6	3.4
August	13.5	13.8	2.6
September	13.8	14.5	5.1
October	14.3	16.1	12.8
November	16.8	18.1	7.4
December	15.9	17.5	10.2
Annual	**17.2**	**19.4**	**12.8**

In comparison with Figure 6.5, Figure 6.6 presents the monthly average simulated flow for the current and future periods based on the raw uncorrected CGCM3-CRCM temperature and precipitation inputs. Although the annual hydrographs are not plausible due to the biases associated with these uncorrected data, it is interesting to see how the predicted changes in temperature and precipitation from the uncorrected RCM data translate to a change in streamflow.

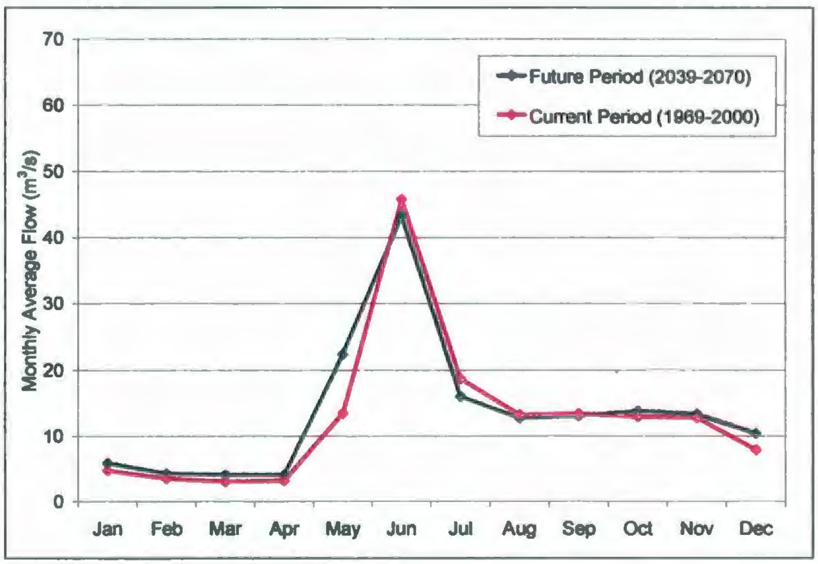

Figure 6.6 Simulated Pinus River Flow under Current and Future Climate (CGCM3-CRCM uncorrected climate)

The increase in streamflow between current and future periods using uncorrected inputs is not as great as the increase predicted using bias-corrected inputs; however on an annual basis, future period streamflow is still predicted to be 8.3 percent higher. The difference between this 8.3 percent estimate and the 12.8

percent estimate derived from the use of bias-corrected inputs is related to the bias-correction methods applied to the original RCM data, and is expected to be within the range of uncertainty of this assessment.

Figure 6.7 presents the comparison of current and future period predicted streamflow (based on bias-corrected temperature and precipitation) as a flow-duration curve. This type of curve illustrates the percentage of time that flow can be expected to equal or exceed a specified value. For example, it is expected that a flow of 11.1 m^3/s will be equalled or exceeded 50 percent of the time in the current period, whereas the corresponding flow in the future period is 13.4 m^3/s. This type of plot is believed to have been first used by the American engineers in the late 1800s. It is most frequently used for determining water-supply potentials in planning and design of water resource projects, particular hydroelectric ones (Chow, 1964). It should be noted that there is considerable inaccuracy in the simulated flows under RCM climate; however the relative change between current and future simulated streamflow is expected to provide a reasonable estimate of the effect of climate change on streamflow in the Pinus River basin.

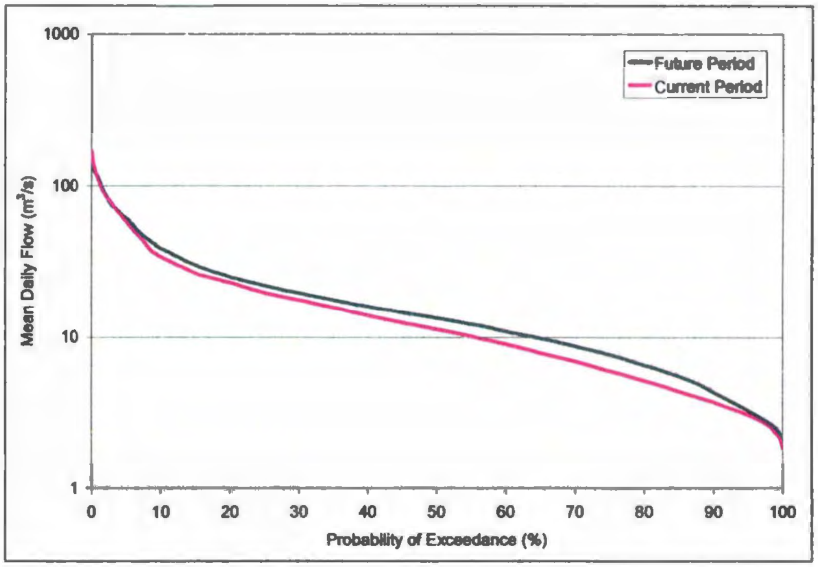

Figure 6.7 Flow Duration Curves under Current and Future Climate (CGCM3-CRCM bias-corrected climate)

6.4 Simulation with NCEP-CRCM Modeled Climate

Section 5.5 describes the comparison of NCEP-CRCM and CGCM3-CRCM temperature and precipitation inputs. As mentioned in that section, the reanalysis-driven RCM run (NCEP-CRCM) removes much of the error associated with the boundary conditions of the RCM since reanalysis data are more realistic than GCM model output. As a result, the NCEP-CRCM predicted temperature and precipitation are more accurate than those from the CGCM3-CRCM run, as shown in Section 5.5.

Figure 6.8 illustrates the monthly average observed and simulated streamflow based on both uncorrected CGCM3-CRCM and NCEP-CRCM inputs.

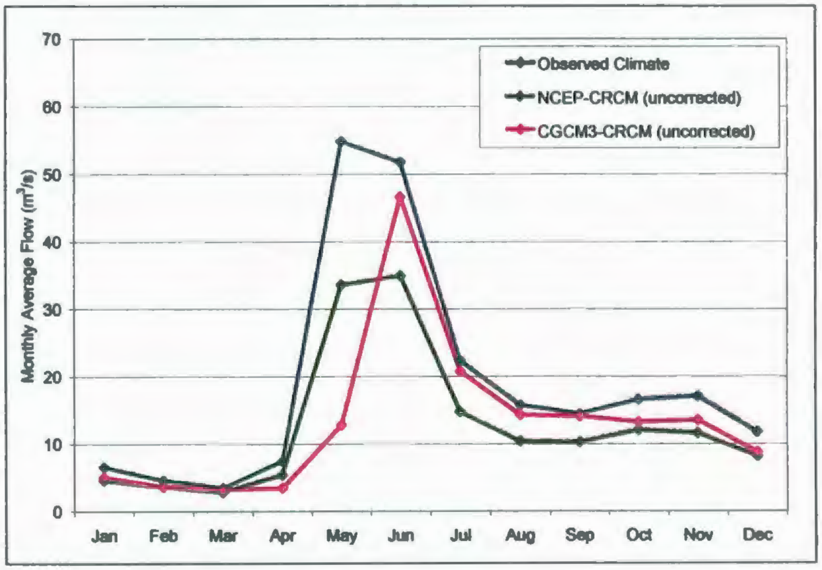

Figure 6.8 Simulated Pinus River Flow under Observed and Uncorrected RCM Climate (1980-2000)

As shown in Figure 6.8, the timing of the spring runoff is different in the two RCM cases. The timing of the NCEP-CRCM spring runoff appears to be in line with observed; however the CGCM3-CRCM spring runoff occurs later as a result of the underestimation of temperatures which is more severe in this case. The annual volume of runoff is underestimated in both RCM cases and this is a result of the underestimation of precipitation. The annual average flows based on observed, NCEP-CRCM and CGCM3-CRCM climates are 19.0 m^3/s, 12.7 m^3/s, and 13.2 m^3/s, respectively.

Figure 6.9 illustrates the monthly average observed and simulated flows based on bias-corrected CGCM3-CRCM and NCEP-CRCM inputs.

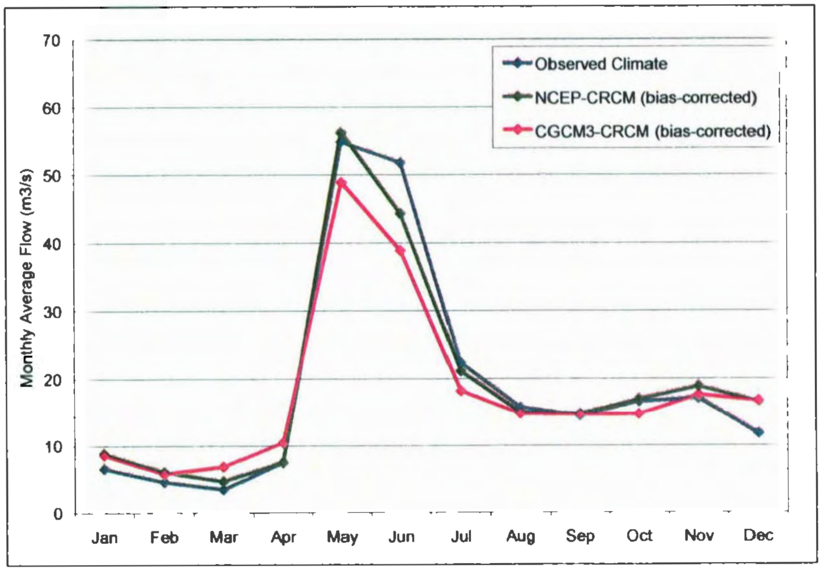

Figure 6.9 Simulated Pinus River Flow under Observed and Bias-Corrected RCM Climate (1980-2000)

As shown in Figure 6.9, the bias-corrections led to a significant improvement in the representation of observed streamflow in both RCM cases. The annual average flows based on observed, NCEP-CRCM and CGCM3-CRCM climates are 19.0 m^3/s, 19.3 m^3/s, and 17.9 m^3/s, respectively.

Chapter 7 Discussion

In 2008, Nalcor Energy initiated a program in partnership with Memorial University of Newfoundland to study the effects of climate change on the hydroelectric potential of the proposed Lower Churchill Project. The current research forms an early phase of this program. The objective of this thesis was not to provide a definitive answer to this complex climate change question, but rather to accumulate and assess some of the more recently available data sets and develop approaches that could be applied and extended in future as this research moves forward.

Many climate change impact assessments described in the literature use the change factor approach or statistical downscaling to transfer the results of GCMs to a scale appropriate for local impacts assessment. These methods are known to have several limitations but are used extensively due to their relative ease of application compared to dynamic downscaling with regional climate models. Dynamic downscaling is considered to be the most scientifically rigorous downscaling method and new data sources have allowed it to be examined here. In the current study, regionally downscaled climate were obtained through the North American Regional Climate Change Assessment program (NARCCAP), and an attempt was made to use these data directly to force a hydrological model to assess water resources impacts. Unfortunately, a limitation of the data available from NARCCAP at the time of this research was that only one emission scenario was used in the modeling. There is considerable variability in projected GHG emissions, and the SRES A2 scenario represents just one possible forecast based on estimates of the nature of future society. Many studies in the past have utilized a number of emission scenarios to understand the range of future impacts. It is interesting to note however, that the IPCC emission scenarios were originally developed in 2000 and there has been some concern expressed that many scenario emission rates are low compared to actual emissions observed over the past decade. The A2 scenario, used here, was one of the most pessimistic views of future emissions at the time of scenario development; it turns out that actual global emissions over the past decade have tracked more closely to this scenario than many of the others (Lines, 2010). While this is not good news for the planet, it does reinforce the choice of a pessimistic emission option and makes the use of studies based on more optimistic views of human behaviour less credible.

NARCCAP modellers are in the process of completing simulations for multiple RCMs nested within simulations from a number of different GCMs. At the time of this research, the matrix of simulations (presented in Table 3.3) to be completed was far from complete. New results continue to be posted on a regular basis. Some of the earliest data available through the NARCCAP program was output from Canadian models using the CRCM nested within the CGCM3. These data were used for this "proof-of-concept" study since results for the observed climate period looked more representative for the Labrador region than many of the other offerings. This appraisal was completely subjective but provided a means of moving forward knowing that other model combinations would be completed as part of future studies. No two climate models provide the same result and it is difficult to predict which model will provide the most accurate representation of climate in the region of interest. It has been suggested that an "ensemble" approach be applied whereby the results of a number of different climate models are used in climate change impacts analysis. Minville et al. (2008) suggest that impacts studies based on results from a single GCM should be interpreted with caution. As more and more results are assembled through NARCCAP, future studies for Nalcor will assess ensemble methodologies and probabilistic forecasts based on these predictions.

At the beginning of this research it was hoped that dynamically downscaled climate data could be used directly as input to the hydrological model. However, in this research comparisons between observed and modeled climate at Goose Bay revealed significant biases in both RCM output of temperature and precipitation, leading to unrealistic hydrographs for the current period. It was important for the work to use plausible streamflow results rather than report changes derived from unrealistic results; therefore, much of the research for this thesis was devoted to correcting these biases. Bias correction methods were researched and evaluated and a non-linear correction method was implemented. A major assumption of this bias-correction procedure is that the future RCM climate simulations suffer from the same problems as the current RCM climate simulations. Accordingly, the bias correction factors were applied equally (in both magnitude and in timing) to both current and future RCM output. While this is a plausible assumption, it ignores the possibility of changed seasonality of future climate. Consider, for example, that if the future winter period were shorter than the current winter period, it would be more appropriate to apply a bias-correction based on current winter conditions to this shorter period. In this study, corrections are applied based on a Julian day application criteria only; application of these corrections based on model condition may provide a more realistic result but would be complex to develop and apply in an unbiased way. As it is, the bias correction method considers contributions from a 65-day period and is applied separately for 73 5-day periods. As a result the correction method should be relatively immune to all but the largest shifts in seasonality.

Another interesting investigation of this research relates to the source of the above-noted biases between the two components of potential uncertainty (GCM and RCM). Investigation of the sources and relative magnitudes of uncertainty in climate forecasts are evident in the current literature. Through comparison of results from RCM simulations forced with reanalysis data, it was determined that the RCM was responsible for approximately 65 percent of the temperature bias and 83 percent of the precipitation bias. This result indicates that further work is warranted in the refining of regional climate modeling schemes.

The transfer of climate signals to streamflow was conducted using the hydrological model WATFLOOD. While this model neglects many of the detailed energetic processes associated with snowmelt and evapotranspiration, it has proven over time to give robust estimates of streamflow in current climates using a minimum of input data (only temperature and precipitation inputs were used in the current research). Since the Pinus River watershed has no measured atmospheric data available, it was decided to use a simple hydrological model that would at least provide acceptable results for the current period based on climate variables measured at a nearby gauge.

The current study has assessed the potential impacts of climate change on the flow in the Pinus River. It is assumed that similar changes might be expected throughout the entire Churchill River watershed; however this has not been investigated as part of this thesis.

The following section summarizes the major conclusions of this thesis as well as various aspects of the current research that could be extended in the future to provide a more robust estimate of the impacts of climate change on the hydroelectric potential of the Lower Churchill Project.

Chapter 8 Conclusions and Recommendations

8.1 Conclusions

The main findings of this research are provided as follows.

- Although there are no observed climate data available from within the Pinus River basin, an acceptable hydrological model calibration was achieved using Goose Bay climate (Nash-Sutcliffe coefficient of 0.80 and r^2 of 0.81).

- Monthly average precipitation at Goose Bay from the Adjusted Historical Canadian Climate Database (AHCCD) was between 7 and 37 percent higher than the original gauge precipitation. The use of AHCCD precipitation led to a significant improvement in the simulated hydrograph at the Pinus River gauge and was thus used as the observed precipitation data set in this study.

- Monthly average temperatures at Goose Bay from the AHCCD were within 0.2 degrees C of the original gauge temperatures. Since the difference was small and because hourly temperatures were not available from the AHCCD, the original gauge temperature data were used in this study.

- Significant temperature and precipitation biases were detected in CGCM3-CRCM output. Monthly average RCM temperature was between 2.3 and 7.0 degrees lower than observed; monthly average RCM precipitation was between 5 and 53 percent lower than observed, with the largest difference occurring in the winter.

- Monthly average temperature from reanalysis driven CRCM simulations was closer to observed than CGCM3-CRCM for all months with the exception of December. On average, the reanalysis driven RCM temperature was 35 percent closer to observed than the CGCM3-CRCM temperature.

- Monthly average precipitation from reanalysis driven CRCM simulations was closer to observed than CGCM3-CRCM for all months with the exception of August, September, October, and December. On average, the reanalysis driven RCM precipitation was 17 percent closer to observed than the CGCM3-CRCM precipitation.

- Under the A2 future emissions scenario, the bias-corrected CGCM3-CRCM output suggests a 2.4 degrees C increase in temperature and an 11 percent increase in precipitation at Goose Bay between the current climate period (1968-2000) and the future climate period (2038-2070).

* The current research resulted in a projected increase in runoff of approximately 13 percent. This is consistent with the IPCC figure presented in Section 1.1 which suggests an increase in runoff of between 10 and 20 percent based on an ensemble of GCM model output.

8.2 Recommendations

This thesis summarizes the work completed as an early phase of a broader research program being conducted at Memorial University. As such, this thesis presents various methods and data sets that may be extended by other researchers as this study continues. The following list presents some of the future work that is recommended to move towards a more robust understanding of the impacts of climate change on the hydroelectric potential of the Lower Churchill Project.

* A range of future emission scenarios should be considered, and updated scenarios should be used when they become available.

* Results from different climate model simulations should be used. There are currently data sets available through NARCCAP for several more GCM-RCM combinations.

* A hydrological model of the entire Churchill River basin should be developed. It would be extremely valuable to have additional climate and streamflow monitoring stations throughout the basin for calibration of such a model.

- If sufficient data can be obtained, consideration should be given to the use of a more sophisticated hydrological model to more accurately represent the energy balance and hence processes such as snowmelt and evapotranspiration.

- As additional years of streamflow data are collected, hydrological model verification should be completed.

- Based on the biases discovered in CRCM temperature and precipitation for Goose Bay, it would be advantageous to perform additional regional climate modeling focussed on the Labrador region to understand and correct the problems discovered in the CRCM.

- Consideration should be given to bias-correcting RCM data based on condition rather than timing as future climate predictions may include changes in seasonality of climate.

- Climate changed streamflow sequences should be input to a reservoir/ generation model to determine how a change in flow translates to a change in energy generation potential.

- Further research should be conducted to look into the effects of climate change on extreme flows (floods and droughts) in the Churchill River basin.

References

Bingeman, A. K., N. Kouwen, E. D. Soulis (2006). Validation of the Hydrological Processes in a Hydrological Model. Journal of Hydrologic Engineering 11:5, 451-463.

Castles, I. and D. Henderson (2003). The IPCC Emission Scenarios: An Economic-Statistical Critique. Energy and Environment 14(2&3):159-185.

Chow, V. T. Handbook of Applied Hydrology. New York: McGraw-Hill Book Company, 1964.

Christensen, J. H, F. Boberg, O. B. Christensen, P. Lucas-Picher (2008). On the need for bias correction of regional climate change projections of temperature and precipitation. Geophysical Research Letters 35(20).

Diaz-Nieto, J. and R. Wilby (2005). A Comparison of Statistical Downscaling and Climate Change Factor Methods: Impacts on Low Flows in the River Thames, United Kingdom. Climatic Change 69: 245-268.

Dibike, Y. B. and P. Coulibaly (2007). Validation of hydrological models for climate scenarios simulation: the case of Saguenay watershed in Québec. Hydrological Processes 21: 3123-3135.

Donald, J. R. (1992). Snowcover depletion curves and satellite snowcover estimates for snowmelt runoff modelling. Ph. D. Thesis, University of Waterloo, ON, Canada, 232 p.

Environment Canada (1981). Hydrometric Field Manual – Measurement of Streamflow. Inland Waters Directorate, Water Resource Branch. Ottawa, Canada, 40 p.

Gachon, P. and Y. Dibike (2007). Temperature change signals in northern Canada: convergence of statistical downscaling results using two driving GCMs. International Journal of Climatology 27: 1623-1641.

Giorgi, F. (2008). Regionalization of climate change information for impact assessment and adaptation. WMO Bulletin, April 2008. Available at: http://www.wmo.int/wcc3/bulletin/57_2_en/giorgi_en.html

Government of Newfoundland and Labrador (2007). Provincial Energy Plan. Department of Natural Resources. Available at: http://www.nr.gov.nl.ca/energyplan/

Government of Newfoundland and Labrador (2010). Industry Overview – Electricity. Department of Natural Resources, Mines and Energy Division. Available at: http://www.nr.gov.nl.ca/mines&en/industry/overview.stm

Graham, Andréasson, Carlsson (2007). Assessing climate change impacts on hydrology from an ensemble of regional climate models, model scales and linking methods – a case study on the Lule River basin. Climatic Change 81: 293-307.

Hargreaves, G., Z.A. Samani (1982). Estimating potential evapotranspiration. ASCE, Journal of Irrigation and Drainage Division 108: 225-230.

Hayakawa, Y. S., T. Oguchi, Z. Lin (2008). Comparison of new and existing global digital elevation models: ASTER G-DEM and SRTM-3. Geophysical Research Letters 35(17).

IPCC (2000). Special Report on Emissions Scenarios.

IPCC (2008). IPCC Technical Paper VI: Climate Change and Water.

IPCC (2010). http://sedac.ciesin.columbia.edu/ddc/sres/ Accessed May 1, 2010.

Jacob, D., L. Barring, O. B. Christensen, J. H. Christensen, M. de Castro, M. Déqué, F. Giorgi, S. Hagemann, M. Hirschi, R. Jones, E. Kjellström, G. Lenderink, B. Rockel, E. Sánchez, C. Schär, S. I. Seneviratne, S. Somot, A. van Ulden, B. van den Hurk. An inter-comparison of regional climate models for Europe: model performance in present-day climate. Climatic Change 81: 31-52.

Kouwen, N. (2009) WATFLOOD User's Manual.

Leander, R. and T. A. Buishand (2007). Resampling of regional climate model output for the simulation of extreme river flows. Journal of Hydrology 332: 487-496.

Lemmen, D.S, F.J. Warren, J. Lacroix, E. Bush, editors (2008). From Impacts to Adaptation: Canada in a Changing Climate 2007. Government of Canada, Ottawa, ON, 448 p.

Lines, G. Public Infrastructure Engineering Vulnerability Committee Workshop. St. John's, Canada. June 17, 2010.

Ludwig, R., I. May, R. Turcotte, L. Vescovi, M. Braun, J.-F. Cyr, L.-G. Fortin, D. Chaumont, S. Biner, I. Chartier, D. Caya, W. Mauser (2009). The role of hydrological model complexity and uncertainty in climate change impact assessment. Advances in Geosciences (21): 63-71.

Mékis, E., W. D. Hogg (1999). Rehabilitation and Analysis of Canadian Daily Precipitation Time Series. Atmosphere-Ocean 37(1): 53-85.

Minville, M., F. Brissette, R. Leconte (2008). Uncertainty of the impact of climate change on the hydrology of a nordic watershed. Journal of Hydrology 358: 70-83.

Minville, M., F. Brissette, R. Leconte (2008). Uncertainty of climate change impacts and consequences on the prediction of future hydrological trends. CEATI Water Management Interest Group 9th Annual Workshop. Montreal, QC, Canada.

Musy, A., B. Music, R. Roy (2008). The Impact of Climate Change on Hydro-Electricity Generation. CEATI Water Management Interest Group 9th Annual Workshop. Montreal, QC, Canada.

Nalcor Energy (2009). Lower Churchill Hydroelectric Generation Project Environmental Impact Statement.

NARCCAP (2010). http://www.narccap.ucar.edu/about/index.html Accessed April 16, 2010.

NASA Jet Propulsion Laboratory. http://www2.jpl.nasa.gov/srtm/ Accessed November 21, 2009.

National Research Council, Environment Canada (2007). EnSim Hydrologic Reference Manual (2007).

NOAA's office of Oceanic and Atmospheric Research (2010). Website http://www.oar.noaa.gov/climate/t_modeling.html. Accessed April 5, 2010.

Pierce, D. W., T. P. Barnett, B. D. Santer, P. J. Gleckler (2009). Selecting global climate models for regional climate change studies. Proceedings of the National Academy of Sciences of the United States of America 106 (21): 8441-8446.

Quilbé, R., A. N. Rousseau, J-S. Moquet, N. B. Trinh, Y. Dibike, P. Gachon, D. Chaumont (2008). Assessing the Effect of Climate Change on River Flod Using General Circulation Models and Hydrological Modelling – Application to the

Chaudière River, Québec, Canada. Canadian Water Resources Journal 33(1): 73-94.

Richter, Barnard, Pryse-Phillips (2004). Impact of Climate Change on Hydroelectric Generation in Newfoundland. CDA 2004 Annual Conference. Ottawa, ON, Canada.

Roberts, J., K. Snelgrove & M. Organ (2009). Hydropower and Climate Change: Dealing with an Uncertain Future. CTCC 2009. Hamilton, ON, Canada.

Snelgrove, K., J. Roberts & M. Organ (2008). Climate Change Studies for Newfoundland and Labrador Hydro. CEATI Water Management Interest Group 9th Annual Workshop. Montreal, QC, Canada.

Stadnyk, T. (2004). Validation of hydrological models using stable isotope tracers. International Workshop on the Application of Isotope Techniques in Hydrological and Environmental Studies, UNESCO. Paris, France.

Tebaldi, C., D. B. Lobell (2008). Towards probabilistic projections of climate change impacts on global crop yields. Geophysical Research Letters 35(8).

Terink, W., R. T. W. L. Hurkmans, P. J. J. F. Torfs, R. Uijlenhoet (2009). Bias correction of temperature and precipitation data for regional climate model application to the Rhine basin. Hydrology and Earth System Sciences Discussions 6: 5377-5413.

Thorne, O. M., R. A. Fenner (2009). Risk-based climate-change impacts assessment for the water industry. Water Science & Technology 59(3).

Toth, B., A. Pietroniro, F. M. Conly, N. Kouwen (2006). Modelling climate change impacts in the Peace and Athabasca catchment and delta: I – hydrological model application. Hydrological Processes 20: 4197-4214.

van Vuuren, D. P. and K. Riahi (2008). Do recent emission trends imply higher emissions forever? Climate Change 91: 237-248.

Vincent, L.A.(1998). A technique for the identification of inhomogeneities in Canadian temperature series. Journal of Climate (11): 1094-1104.

Wilby, R., C. W. Dawson, E. M. Barrow (2002). SDSM – a decision support tool for the assessment of regional climate change impacts. Environmental Modelling & Software 17: 147-159.

Wilby, R. (2008). Climate change, water & hydropower – Challenges for adaptation. CEATI Water Management Interest Group 9th Annual Workshop. Montreal, QC, Canada.

Appendix A

Summary of Research Data Sources

CLIMATE DATA

Original Observed

Daily Climate Data

Environment Canada (Gerard Morin at CLIMATE.ATLANTIC@EC.GC.CA)

Churchill Falls Automatic Station (8501130) - Not quality assured: Dec 1, 1992 to Jul 23, 2009
Goose Manual Station (8501900) - Not quality assured: Dec 1, 1992 to Jul 23, 2009

Churchill Falls Automatic Station (8501130) - Quality assured: Jan 1, 2006 to Dec 31, 2007
Churchill Falls Manual Station (8501132) - Quality assured: Nov 1, 1968 to Mar 31, 1993
Goose Manual Station (8501900) - Quality assured: Jan 1, 1953 to May 31, 2009

Hourly Climate Data

Environment Canada (Gerard Morin at CLIMATE.ATLANTIC@EC.GC.CA)

1. Churchill Falls Auto Station (8501130): Feb 1, 1994 to Jul 24, 2009
2. Churchill Falls Manual Station (8501132): Nov 11, 1968 to Mar 31, 1993
3. Goose Manual Station (8501900): Jan 1, 1953 to Jul 24, 2009

Tipping Bucket Rain Gauge Data (Hourly Rainfall)

Environment Canada (Gerard Morin at CLIMATE.ATLANTIC@EC.GC.CA)

1. Churchill Falls Manual Station (8501132): Feb 1, 1969 to Aug 1, 1992
2. Goose Manual Station (8501900): May 1, 1961 to Dec 1, 2007

Adjusted Observed

Adjusted Historical Canadian Climate Data - Daily Precipitation

Environment Canada (http://www.cccma.ec.gc.ca/hccd/index_e.shtml) - Eva Mekis (Eva.Mekis@ec.gc.ca)

1. Churchill Falls Manual Station (8501132): Jan 1, 1969 to Mar 31, 1993
2. Goose Manual Station (8501900): Jan 1, 1942 to Dec 31, 2008

Adjusted Historical Canadian Climate Data - Daily Temperature

Environment Canada (http://www.cccma.ec.gc.ca/hccd/index_e.shtml) - Lucie Vincent (Lucie.Vincent@ec.gc.ca)

1. Goose Manual Station (8501900): Dec 1, 1941 to Dec 31, 2008

(not available for Churchill Falls yet)

Downscaled

NARCCAP downscaled temperature and precipitation (3-hourly)

Apply for Data Access through Seth McGinnis (NARCCAP User Community Manager) at mcginnis@ucar.edu
Download data through Earth System Grid login (https://www.earthsystemgrid.org/security/loginout.htm?)

CGCM3-CRCM Current Period: Jan 1, 1968 to Nov 21, 2000
CGCM3-CRCM Future Period: Jan 1, 2038 to Nov 23, 2070

NCEP-CRCM Current Period: Jan 1, 1979 to Nov 30, 2003

FLOW DATA

Observed

Water Survey of Canada (http://www.wsc.ec.gc.ca/hydat/H2O/index_e.cfm?cname=main_e.cfm)
Pinus River (03OE011): Oct 3, 1998 to Dec 31, 2008
East Metchin River (03OD007): Sep 28, 1998 to Dec 31, 2008
Minipi River (03OE003): Jan 1, 1979 to Dec 31, 2008
Churchill River above Upper Muskrat Falls (03OE001): Jul 7, 1948 to Dec 31, 2008
Churchill River at Churchill Falls Powerhouse (03OD005): Jan 1, 1972 to Dec 31, 2008

TERRAIN/ MAPPING DATA

Basemapping

National Topographical Database (www.geogratis.ca)

Digital Elevation Data

Shuttle Radar Topographical Mission 3 arc sec
USGS National Map Seamless Server (http://seamless.usgs.gov/index.php)

Appendix B

Summary of Research Steps

Flow Chart of Steps Completed during Research

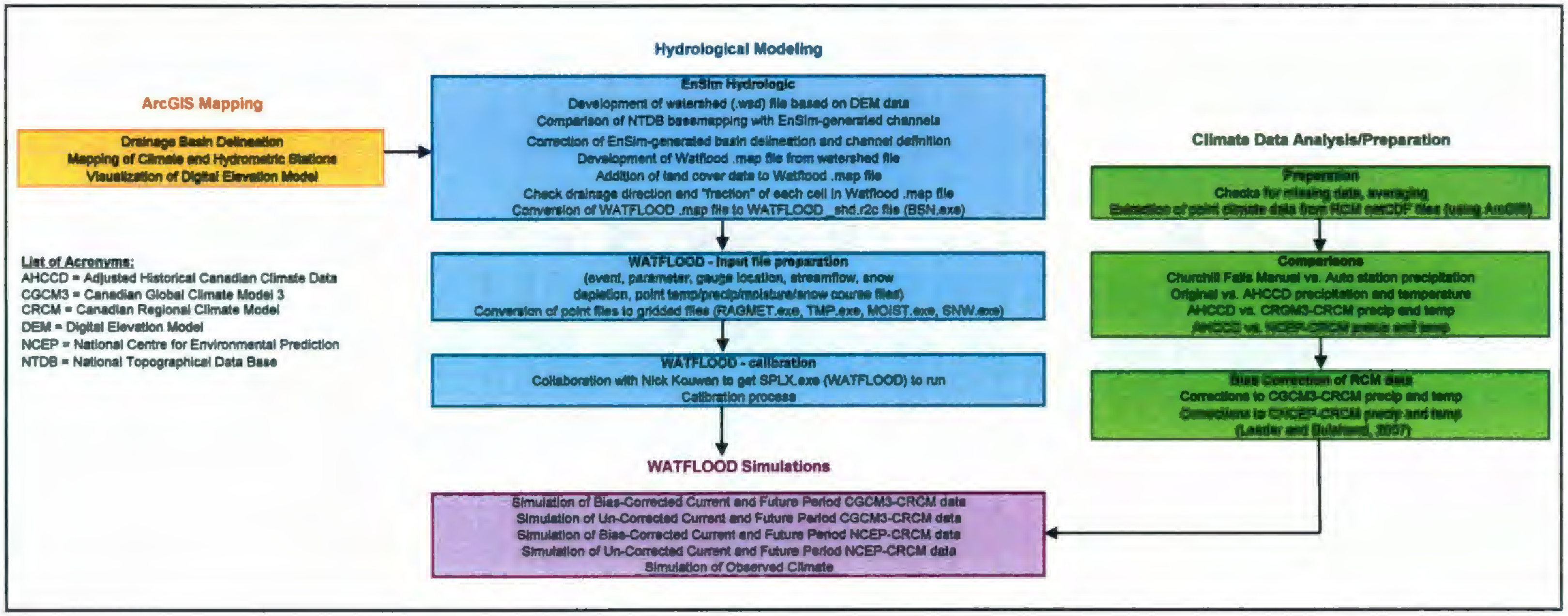

Appendix C

Monthly Temperature at Goose Bay

Appendix C - Monthly Temperature at Goose Bay (degrees C)

CGCM3-CRCM Current Period Temperature (Uncorrected)

	1968	1969	1970	1971	1972	1973	1974	1975	1976	1977	1978	1979	1980	1981	1982	1983	1984	1985	1986	1987	1988	1989	1990	1991	1992	1993	1994	1995	1996	1997	1998	1999	2000	avg
Jan	-18.8	-27.0	-26.3	-22.2	-19.7	-22.6	-26.2	-23.2	-20.3	-27.7	-25.2	-19.9	-28.0	-18.2	-19.5	-26.5	-19.9	-22.3	-23.3	-22.3	-25.2	-22.4	-28.5	-23.6	-27.3	-23.4	-20.8	-24.7	-24.8	-20.0	-20.9	-25.0	-15.0	-23.1
Feb	-23.7	-28.7	-25.1	-26.4	-22.4	-24.3	-16.9	-23.5	-19.9	-26.3	-17.8	-22.8	-27.3	-20.3	-18.7	-24.9	-24.1	-16.3	-21.0	-22.9	-21.5	-19.4	-24.4	-20.8	-23.5	-26.9	-18.6	-23.3	-20.2	-22.7	-22.5	-24.6	-19.2	-22.4
Mar	-17.1	-12.5	-16.6	-15.5	-14.5	-14.8	-13.5	-16.7	-16.9	-18.0	-8.9	-11.5	-13.3	-15.0	-12.8	-11.1	-12.8	-9.2	-16.8	-14.5	-13.5	-13.5	-18.5	-10.1	-16.1	-11.9	-6.5	-13.9	-13.7	-17.7	-16.3	-14.1	-12.2	-13.9
Apr	-7.8	-3.2	-7.2	-6.7	-8.3	-8.7	-6.3	-6.5	-9.7	-6.9	-8.6	-7.4	-7.4	-6.8	-5.4	-4.9	-6.1	-11.3	-2.5	-4.7	-4.8	-6.7	-7.6	-6.5	-8.7	-5.3	-6.1	-5.6	-5.0	-3.4	-9.5	-6.6	-4.0	-6.7
May	2.3	2.6	0.4	2.6	-1.2	2.7	1.1	2.6	-1.8	1.4	0.1	3.0	-0.7	0.7	1.0	-0.2	1.6	-1.9	-0.5	0.7	0.9	1.2	1.3	4.5	1.8	-0.8	1.6	0.3	-0.2	1.6	0.6	2.7	1.4	1.0
Jun	7.2	6.1	6.3	5.5	5.5	4.2	5.3	7.9	7.4	5.8	6.4	6.7	6.3	3.7	5.1	6.7	5.2	4.8	5.9	5.0	4.8	5.6	5.6	5.0	6.6	4.7	5.2	7.4	7.1	7.7	3.9	7.8	5.8	5.9
Jul	9.0	7.4	9.2	10.2	8.6	9.0	10.3	10.7	7.2	8.9	9.7	8.6	10.2	6.8	9.6	9.3	8.4	7.6	10.4	6.6	10.3	8.6	9.8	7.4	10.1	7.3	10.5	9.5	9.4	12.4	8.3	9.5	10.7	9.1
Aug	8.5	8.3	9.4	7.8	6.2	7.7	7.0	6.6	7.4	8.0	8.2	7.2	7.6	6.1	6.3	6.9	9.3	5.6	8.0	7.3	7.4	8.4	7.8	6.1	8.1	6.2	7.8	7.4	9.2	6.4	7.6	9.2	6.8	7.8
Sep	0.6	4.7	3.3	2.3	4.5	3.1	3.7	5.4	1.8	4.6	4.6	3.3	1.5	5.0	4.9	2.9	3.7	2.9	3.9	5.0	3.6	7.3	5.1	3.5	3.2	4.0	3.8	4.4	5.1	4.4	4.4	4.1	2.5	3.9
Oct	-5.4	0.3	-2.7	-2.5	-0.2	-3.0	-2.3	-2.9	-3.2	-2.5	-5.3	-1.5	-0.6	-1.9	1.6	-0.3	-4.7	-0.8	-0.4	-2.3	0.5	-0.8	-1.5	0.1	-1.9	-2.9	-0.8	0.8	-0.2	-1.3	-0.8	-1.1	-2.5	-1.6
Nov	-10.7	-10.4	-9.1	-12.8	-10.0	-11.4	-8.5	-6.4	-10.6	-8.0	-7.0	-9.7	-10.5	-14.7	-7.5	-5.9	-10.7	-8.7	-6.4	-9.2	-10.3	-11.2	-7.8	-10.0	-6.5	-8.1	-10.1	-11.5	-5.2	-7.9	-11.0	-9.6	-8.0	-9.2
Dec	-20.6	-12.9	-17.4	-17.4	-20.9	-21.5	-13.7	-15.8	-12.3	-20.1	-17.9	-19.3	-10.5	-15.6	-13.1	-12.0	-19.6	-16.2	-12.5	-9.8	-18.3	-15.7	-18.8	-21.6	-13.7	-18.5	-12.9	-9.5	-13.7	-13.1	-10.3	-16.4		-15.7

Annual Average -5.3

CGCM3-CRCM Current Period Temperature (Bias-Corrected)

	1968	1969	1970	1971	1972	1973	1974	1975	1976	1977	1978	1979	1980	1981	1982	1983	1984	1985	1986	1987	1988	1989	1990	1991	1992	1993	1994	1995	1996	1997	1998	1999	2000	avg
Jan	-13.9	-21.3	-20.7	-17.1	-14.8	-17.5	-20.6	-18.0	-15.3	-22.1	-19.7	-14.9	-22.1	-13.5	-14.6	-20.9	-14.9	-17.2	-18.0	-17.1	-19.6	-17.3	-22.5	-18.2	-21.7	-18.2	-15.6	-19.3	-19.3	-15.1	-15.8	-19.5	-10.5	-17.8
Feb	-17.7	-22.3	-19.0	-20.2	-16.5	-18.3	-11.5	-17.5	-14.3	-20.1	-12.4	-16.8	-21.0	-14.6	-11.4	-18.8	-18.1	-11.0	-15.3	-17.0	-15.7	-13.9	-18.4	-15.1	-17.6	-20.5	-13.1	-17.3	-14.6	-16.8	-16.7	-18.6	-13.6	-16.5
Mar	-11.7	-7.3	-11.3	-10.2	-9.2	-9.6	-8.3	-11.4	-11.5	-12.5	-3.9	-6.4	-8.1	-9.7	-7.6	-6.1	-7.6	-4.2	-11.4	-9.2	-8.3	-8.3	-13.1	-5.1	-10.8	-6.8	-1.7	-8.7	-8.4	-12.3	-11.0	-8.9	-7.1	-8.7
Apr	-2.9	1.4	-2.3	-1.9	-3.4	-3.8	-1.5	-3.6	-4.8	-2.0	-3.7	-2.6	-2.6	-2.1	-0.7	-0.2	-1.3	-6.2	2.1	0.0	-0.1	-1.9	-2.8	-3.6	-3.8	-0.5	-1.3	-0.9	-0.3	1.3	-4.5	-1.8	0.7	-1.9
May	6.9	7.3	4.7	7.0	3.3	7.1	5.5	6.9	2.9	5.9	4.7	7.5	3.7	5.1	5.5	4.3	5.9	2.6	4.0	5.0	5.3	5.5	5.8	9.1	6.1	3.6	5.9	5.0	4.3	6.1	5.1	7.3	5.9	5.6
Jun	12.8	11.4	11.6	10.7	10.6	9.0	10.4	13.7	13.1	11.0	11.8	12.1	11.7	8.5	10.3	12.3	10.3	9.9	11.3	10.1	9.8	10.8	10.8	10.1	12.0	9.6	10.4	13.1	12.8	13.5	8.6	13.6	11.0	11.2
Jul	15.8	13.8	16.0	17.4	15.3	15.8	17.5	18.0	13.6	15.8	16.8	15.4	17.5	12.9	16.6	16.3	15.1	14.0	17.6	12.7	17.5	15.3	16.9	13.8	17.1	13.6	17.8	16.5	16.3	20.3	14.9	16.6	18.1	16.0
Aug	15.5	15.3	16.5	14.7	12.8	14.5	13.7	13.2	14.1	14.9	15.1	13.9	14.5	12.7	12.8	13.6	16.4	12.0	14.8	14.0	14.2	15.3	14.6	14.9	15.0	12.8	14.6	14.2	16.3	13.0	14.4	16.2	13.4	14.4
Sep	5.8	10.3	8.8	7.6	10.3	8.6	9.3	11.1	7.2	10.4	10.3	8.7	6.8	10.7	10.6	8.3	9.3	8.5	9.6	10.7	9.1	13.4	10.8	8.9	8.7	9.6	9.3	10.1	10.9	10.0	10.0	9.8	7.9	9.4
Oct	-0.1	4.9	2.3	2.5	4.5	2.0	2.6	2.1	1.9	2.5	0.0	3.4	4.2	3.0	6.1	4.5	0.5	4.0	4.3	2.6	5.2	4.1	3.3	4.7	3.0	2.1	4.0	5.4	4.5	3.5	4.1	3.7	2.5	3.3
Nov	-6.7	-6.4	-4.9	-8.6	-6.0	-7.4	-4.5	-2.1	-6.4	-3.9	-2.8	-5.5	-6.5	-10.6	-3.3	-1.8	-6.6	-4.5	-2.2	-5.1	-6.3	-7.1	-3.8	-5.9	-2.4	-4.0	-6.1	-7.3	-1.0	-3.6	-7.0	-5.6	-3.9	-5.1
Dec	-16.5	-9.1	-13.5	-13.6	-16.7	-17.4	-9.9	-11.9	-8.6	-16.0	-13.8	-15.0	-7.0	-11.7	-9.5	-8.6	-15.4	-12.3	-9.0	-8.3	-14.3	-11.8	-14.8	-17.6	-10.2	-14.5	-9.3	-6.0	-10.0	-9.5	-6.6	-12.5		-11.8

Annual Average -0.1

CGCM3-CRCM Future Period Temperature (Uncorrected)

	2038	2039	2040	2041	2042	2043	2044	2045	2046	2047	2048	2049	2050	2051	2052	2053	2054	2055	2056	2057	2058	2059	2060	2061	2062	2063	2064	2065	2066	2067	2068	2069	2070	avg
Jan	-18.9	-17.7	-21.0	-23.3	-21.2	-15.4	-18.6	-18.6	-23.6	-20.8	-21.8	-20.4	-20.9	-18.1	-17.4	-20.8	-15.1	-23.5	-18.4	-16.7	-19.0	-17.4	-12.1	-21.9	-19.2	-22.6	-16.4	-21.4	-14.8	-7.8	-18.4	-20.2	-17.0	-18.8
Feb	-17.8	-13.5	-21.4	-18.1	-20.8	-18.7	-17.3	-21.4	-20.2	-20.7	-17.2	-22.4	-21.8	-18.3	-16.4	-18.4	-17.8	-18.4	-16.0	-21.9	-18.0	-22.4	-19.0	-21.6	-13.8	-23.9	-20.0	-20.4	-14.0	-13.2	-11.5	-17.4	-13.7	-18.4
Mar	-13.2	-13.4	-11.4	-16.3	-12.0	-12.1	-13.0	-6.7	-16.7	-12.6	-12.3	-14.8	-14.0	-13.0	-13.7	-10.4	-12.2	-10.5	-10.4	-14.9	-11.6	-16.4	-9.6	-8.5	-13.7	-3.2	-9.6	-13.1	-16.6	-7.4	-8.0	-5.8	-6.0	-11.6
Apr	-2.5	-2.3	-0.7	-7.2	-9.4	-1.7	-5.7	-5.4	-4.7	0.4	-6.8	-5.3	-2.8	-4.5	-6.5	-5.6	-4.5	-5.9	-7.7	-2.9	-8.5	-5.3	-3.5	-6.2	-3.6	-2.2	-6.7	-2.9	-6.3	-3.2	-1.2	-5.0	-2.5	-4.5
May	1.8	1.9	3.7	1.9	3.1	4.2	0.2	1.7	2.9	3.5	0.9	1.3	1.3	3.0	3.0	4.9	1.7	1.9	1.3	0.8	2.7	5.2	3.0	4.1	2.0	4.2	2.7	3.9	2.7	2.3	4.3	7.2	1.9	2.8
Jun	6.9	6.0	6.7	6.3	5.7	8.4	6.6	6.6	9.3	6.7	6.4	6.7	6.4	6.4	7.0	8.3	6.6	8.9	8.3	8.7	6.6	7.5	9.6	7.7	6.9	8.5	8.0	6.7	8.5	6.9	9.9	7.9	5.9	7.4
Jul	9.9	9.3	11.8	9.4	11.0	12.5	10.7	9.1	11.0	13.0	10.5	9.9	10.2	9.1	10.8	10.8	10.5	11.6	10.2	11.4	11.5	11.9	11.2	9.1	9.1	12.3	12.4	11.2	11.9	12.2	13.9	12.9	12.0	11.0
Aug	8.8	10.3	7.4	9.1	9.7	7.6	8.7	10.2	8.9	10.9	10.5	9.0	9.2	9.4	9.9	9.0	9.8	10.1	9.0	10.5	11.1	9.2	8.9	10.2	9.1	9.8	10.2	11.5	9.0	8.8	10.3	12.7	11.1	9.7
Sep	5.5	4.5	6.6	5.0	4.2	3.2	5.7	4.7	2.9	5.2	4.4	5.6	5.5	6.1	7.8	6.0	6.9	4.9	5.5	7.4	5.6	4.3	5.5	6.2	6.3	6.4	9.4	6.7	6.2	5.3	5.2	6.4	7.4	6.7
Oct	1.1	1.9	-1.9	-3.4	-1.4	-0.6	-0.5	2.8	-1.3	-0.1	-0.9	-0.3	-0.5	-1.5	0.3	2.4	-1.2	3.8	-0.4	1.5	1.1	1.1	-0.2	2.0	0.9	1.5	0.5	0.3	0.7	-0.3	-0.4	-0.6	2.7	0.3
Nov	-5.1	-9.3	-6.8	-6.5	-10.2	-10.0	-5.2	-6.2	-7.6	-4.1	-6.4	-4.9	-6.1	-6.9	-6.6	-6.5	-5.8	-5.1	-8.5	-7.4	-6.4	-8.1	-8.5	-12.0	-4.4	-5.1	-3.9	-4.3	-6.8	-7.7	-8.1	-5.4	-2.3	-6.6
Dec	-8.9	-18.8	-16.3	-16.6	-17.7	-14.6	-12.7	-17.9	-13.0	-16.7	-17.2	-12.5	-13.2	-15.2	-13.6	-13.0	-15.8	-11.6	-14.4	-11.3	-16.4	-11.8	-9.0	-12.9	-13.7	-6.8	-16.8	-10.3	-13.8	-11.8	-12.3	-14.5		-13.8

Annual Average -3.0

CGCM3-CRCM Future Period Temperature (Bias-Corrected)

	2038	2039	2040	2041	2042	2043	2044	2045	2046	2047	2048	2049	2050	2051	2052	2053	2054	2055	2056	2057	2058	2059	2060	2061	2062	2063	2064	2065	2066	2067	2068	2069	2070	avg
Jan	-14.0	-13.0	-16.0	-18.0	-16.2	-11.0	-13.9	-13.9	-18.3	-15.9	-16.6	-15.6	-15.9	-13.5	-12.7	-15.8	-10.8	-18.2	-13.7	-12.2	-14.3	-12.8	-8.0	-16.7	-14.3	-17.4	-11.9	-16.3	-10.5	-4.0	-13.6	-15.2	-12.4	-14.0
Feb	-12.4	-8.5	-15.6	-12.7	-15.1	-13.2	-12.0	-15.7	-14.6	-15.1	-11.8	-16.6	-16.0	-12.8	-11.1	-13.0	-12.4	-12.9	-10.7	-16.1	-12.6	-16.5	-13.6	-15.8	-8.7	-17.9	-14.4	-14.8	-9.0	-8.2	-6.7	-12.1	-8.6	-12.9
Mar	-8.1	-8.2	-6.3	-10.9	-6.9	-7.0	-7.9	-1.8	-11.3	-7.4	-7.3	-9.5	-8.8	-7.8	-8.5	-5.4	-7.0	-5.4	-5.4	-9.8	-6.5	-11.1	-4.6	-3.6	-8.6	1.4	-4.6	-7.9	-11.2	-2.5	-3.0	-1.0	-1.2	-6.5
Apr	2.1	2.2	3.7	-2.3	-4.5	2.8	-1.0	-0.6	-0.1	4.8	-1.9	-0.6	1.7	0.1	-2.0	-0.9	0.2	-1.1	-2.9	1.6	-3.6	-0.6	1.1	-1.4	0.9	2.4	-1.9	1.7	-1.6	1.4	3.3	-0.3	2.1	0.1
May	6.3	6.3	8.1	6.4	7.7	8.8	4.8	6.1	7.5	7.9	5.4	5.9	5.7	7.3	7.3	9.4	6.0	6.5	5.9	5.2	7.2	9.8	7.5	8.5	6.3	8.7	7.2	8.4	7.2	6.7	8.7	11.8	6.3	7.2
Jun	12.5	11.4	12.3	11.8	10.9	14.3	12.1	12.0	15.5	12.2	11.9	12.3	11.8	11.8	12.7	14.3	12.1	15.1	14.2	14.8	12.1	13.3	16.0	13.5	12.4	14.6	13.8	12.2	14.5	12.4	16.3	13.8	11.2	13.1
Jul	17.1	16.2	19.4	16.4	18.4	20.4	18.1	16.0	18.3	21.0	17.8	17.0	17.3	15.9	18.1	18.2	17.8	19.2	17.4	18.9	19.2	19.5	18.7	15.9	16.1	20.2	20.2	18.8	19.6	20.0	22.2	20.9	19.7	18.5
Aug	15.8	17.6	14.2	16.2	16.8	14.5	15.7	17.5	15.9	18.3	17.9	16.0	16.2	16.6	17.1	16.0	17.0	17.4	16.1	17.9	18.6	16.3	15.9	17.4	16.2	17.0	17.5	19.0	16.0	15.8	17.7	20.4	18.5	16.9
Sep	11.4	10.2	12.5	10.8	9.9	8.6	11.6	10.4	8.5	11.1	9.9	11.4	11.3	12.0	14.0	11.9	12.9	10.6	11.3	13.4	11.4	10.0	11.3	11.9	12.2	12.3	15.7	12.7	12.2	11.1	10.8	12.5	13.7	11.6
Oct	5.7	6.4	2.9	1.7	3.4	4.2	4.0	7.2	3.6	4.6	3.9	4.5	4.2	3.3	5.0	6.8	3.6	8.1	4.4	6.0	5.6	5.7	4.5	6.6	5.4	6.0	5.1	5.0	5.4	4.5	4.4	4.2	7.1	4.9
Nov	-1.1	-5.0	-2.6	-2.2	-6.1	-5.9	-1.0	-2.1	-3.6	-0.1	-2.4	-0.8	-1.9	-2.7	-2.3	-2.5	-1.7	-1.0	-4.4	-3.3	-2.3	-4.3	-4.3	-7.9	-0.2	-0.9	0.1	-0.2	-2.6	-3.6	-4.0	-1.2	1.9	-2.5
Dec	-5.6	-14.7	-12.2	-13.0	-13.7	-11.0	-9.1	-14.0	-9.3	-13.0	-13.2	-8.9	-9.8	-11.4	-9.9	-9.3	-11.9	-8.1	-10.9	-7.8	-12.4	-8.3	-5.7	-9.2	-10.0	-3.6	-13.0	-6.8	-10.2	-8.2	-8.6	-10.6		-10.1

Annual Average 2.3

Appendix C - Monthly Temperature at Goose Bay (degrees C)

Environment Canada Observed Temperature

	1968	1969	1970	1971	1972	1973	1974	1975	1976	1977	1978	1979	1980	1981	1982	1983	1984
Jan	-16.9	-10.9	-16.2	-14.9	-21.7	-18.3	-23.1	-22.4	-18.9	-12.9	-17.9	-12.5	-13.4	-15.6	-16.8	-18.4	-23.0
Feb	-10.9	-7.7	-14.9	-16.8	-19.6	-17.7	-14.5	-17.7	-18.5	-13.6	-9.0	-15.8	-14.6	-7.2	-20.1	-18.2	-14.8
Mar	-11.1	-5.4	-6.3	-5.6	-12.9	-7.7	-12.4	-8.8	-13.1	-4.1	-13.1	-6.6	-7.4	-3.4	-11.9	-9.7	-9.9
Apr	0.4	-6.7	-1.8	0.0	-4.7	-1.1	-4.7	-2.9	-2.4	-0.9	-2.4	0.7	-0.8	-2.2	-3.8	0.9	-3.2
May	4.8	4.4	4.5	5.8	1.3	7.3	3.3	4.0	6.1	4.1	4.3	9.4	5.1	6.0	3.8	4.6	5.8
Jun	10.0	12.0	10.3	10.6	10.4	12.4	12.5	11.0	12.2	12.3	9.1	14.7	9.1	10.0	9.7	11.9	9.6
Jul	15.5	15.5	17.1	16.0	16.0	18.5	15.2	18.5	16.1	14.8	15.7	16.0	14.8	15.5	15.9	16.2	16.6
Aug	11.7	13.6	15.9	14.1	12.5	14.7	13.9	14.0	14.2	13.5	13.5	14.2	14.4	14.3	13.9	14.0	17.0
Sep	11.7	7.3	8.7	9.8	7.7	9.8	8.9	9.8	7.8	6.7	6.7	8.5	8.4	11.0	9.1	9.4	8.7
Oct	5.5	0.4	4.8	4.0	0.8	2.9	0.3	2.9	1.5	3.1	1.0	2.1	2.6	3.9	0.9	2.7	2.2
Nov	-4.2	-0.2	-3.6	-3.0	-5.8	-3.4	-3.4	-5.6	-5.1	0.2	-7.2	-3.6	-2.6	-2.1	-4.1	-4.7	-3.2
Dec	-8.3	-7.0	-15.4	-18.7	-21.3	-7.8	-11.3	-16.0	-14.9	-12.2	-12.4	-12.1	-16.0	-8.0	-17.3	-15.2	-16.6

	1985	1986	1987	1988	1989	1990	1991	1992	1993	1994	1995	1996	1997	1998	1999	2000	2001
Jan	-15.7	-15.7	-17.7	-18.2	-19.0	-19.2	-24.5	-17.0	-18.5	-20.5	-20.0	-17.5	-14.4	-15.9	-16.8	-16.4	-17.7
Feb	-14.0	-14.0	-11.0	-18.2	-17.7	-21.4	-16.3	-21.5	-20.5	-19.7	-18.9	-12.3	-19.0	-12.3	-12.7	-14.7	-16.4
Mar	-8.9	-12.4	-7.9	-8.0	-11.3	-11.1	-6.7	-10.0	-13.6	-9.2	-11.3	-7.8	-12.3	-9.4	-3.2	-5.8	-4.8
Apr	-2.8	1.0	2.6	0.5	-0.1	-2.2	-3.3	-3.8	-1.5	-3.0	-0.2	2.4	-2.5	-0.3	-0.2	-0.2	-2.1
May	2.7	6.0	6.7	7.3	6.5	3.3	3.8	3.8	3.8	4.4	6.3	4.2	4.3	5.9	9.0	4.3	8.5
Jun	11.1	9.4	11.7	9.1	14.0	10.9	8.7	10.1	9.6	12.1	11.2	11.0	11.0	13.6	14.0	12.2	12.2
Jul	15.5	13.3	16.0	15.8	15.0	14.4	13.5	12.9	13.9	16.5	16.1	13.7	13.6	16.0	16.0	15.8	13.7
Aug	14.7	15.4	14.0	16.0	12.9	14.7	14.7	13.4	16.0	13.6	15.3	17.2	14.2	15.5	15.6	17.4	16.8
Sep	10.0	7.8	10.0	9.3	10.2	8.8	9.4	10.7	9.4	9.6	9.9	9.7	10.8	9.6	12.0	10.4	10.4
Oct	1.9	0.5	4.2	3.4	2.7	2.5	3.6	3.2	1.4	4.8	4.5	2.4	3.4	3.1	1.4	2.2	4.9
Nov	-4.8	-10.0	-4.1	-2.8	-6.1	-3.6	-3.0	-7.2	-6.2	-1.9	-3.9	-2.2	-4.1	-3.3	-4.6	-2.6	-2.7
Dec	-14.0	-14.1	-10.8	-17.7	-13.0	-15.4	-17.8	-14.7	-11.9	-12.8	-11.2	-9.0	-10.6	-11.8	-11.4	-10.0	-7.0

	2002	2003	2004	2005	2006	2007	2008	avg
Jan	-20.3	-14.2	-12.5	-21.1	-14.4	-13.9	-18.2	-17.4
Feb	-16.8	-17.4	-14.2	-12.1	-15.8	-13.3	-16.6	-15.6
Mar	-10.9	-13.1	-9.2	-7.4	-4.4	-10.0	-12.5	-9.0
Apr	-2.3	-2.8	-0.4	0.9	2.8	-2.3	1.2	-1.3
May	4.2	6.9	4.9	8.5	9.7	4.0	6.8	5.4
Jun	11.2	12.9	11.0	13.1	15.5	13.5	12.0	11.4
Jul	16.1	16.0	17.6	17.5	16.9	17.5	18.7	15.8
Aug	14.2	16.3	16.3	14.5	14.6	14.9	16.2	14.7
Sep	11.3	15.0	9.6	11.2	11.2	9.4	11.1	9.7
Oct	3.7	5.6	5.4	4.8	4.5	3.8	4.7	3.0
Nov	-5.5	-2.1	-4.3	-1.7	-1.7	-4.1	-2.2	-3.8
Dec	-11.9	-8.9	-12.7	-11.5	-10.2	-15.2	-15.6	-12.9
						Annual Average		0.1

NCEP-CRCM Temperature (Uncorrected)

	1979	1980	1981	1982	1983	1984	1985	1986	1987	1988	1989	1990	1991	1992	1993	1994	1995	1996	1997	1998	1999	2000	2001	2002	2003	avg
Jan	-16.1	-17.8	-19.8	-21.1	-21.1	-24.4	-22.7	-20.5	-21.5	-21.1	-23.8	-21.6	-26.6	-20.9	-22.2	-28.1	-21.5	-22.1	-19.9	-22.4	-21.8	-22.3	-22.6	-23.5	-20.9	-21.9
Feb	-18.8	-17.5	-9.7	-24.0	-18.8	-17.8	-17.1	-18.7	-17.8	-20.6	-22.8	-24.4	-19.2	-24.1	-22.5	-23.2	-23.9	-14.4	-23.6	-16.6	-16.7	-20.2	-20.9	-22.5	-25.3	-20.0
Mar	-9.8	-10.7	-8.0	-15.7	-13.3	-13.0	-12.9	-15.2	-12.3	-9.1	-16.0	-13.7	-9.5	-12.9	-14.5	-13.2	-14.4	-11.1	-15.8	-12.2	-6.5	-9.9	-7.7	-13.9	-13.2	-12.2
Apr	-2.5	-5.2	-3.2	-3.9	0.3	-3.3	-5.4	-0.6	0.6	-2.4	-4.0	-3.3	-4.0	-6.5	-2.0	-3.8	-4.2	-1.1	-3.9	-4.7	-2.1	-3.3	-3.6	-4.7	-5.5	-3.3
May	6.6	3.2	3.2	3.6	4.7	4.6	1.3	5.2	3.5	5.5	6.3	2.0	2.5	2.3	3.8	3.2	3.6	2.6	2.0	4.3	7.4	2.8	6.8	1.5	4.0	3.8
Jun	11.5	7.1	8.9	9.3	9.9	9.3	9.8	5.8	7.6	7.7	10.5	7.7	6.7	9.6	6.8	9.9	8.9	7.7	7.5	10.8	12.0	8.7	8.8	7.5	8.2	8.7
Jul	14.0	11.0	12.7	12.0	12.9	13.2	12.7	10.4	11.3	12.6	11.2	11.8	10.6	10.3	11.4	12.9	12.6	11.6	11.3	13.2	12.3	12.7	11.3	13.9	12.1	12.1
Aug	11.3	12.1	10.8	9.9	10.6	12.9	11.4	11.4	9.7	11.5	10.2	12.6	11.4	10.5	11.4	11.4	11.5	12.6	10.4	11.4	12.3	12.2	12.6	11.7	12.2	11.4
Sep	6.0	4.3	8.7	5.8	5.7	5.3	6.6	4.2	7.3	6.0	7.8	6.8	5.7	7.8	6.5	7.1	5.0	7.1	7.8	6.4	10.5	6.7	8.2	7.9	11.2	6.9
Oct	-0.4	-1.8	0.4	-0.2	0.1	-2.2	-1.1	-2.0	1.6	1.9	-0.8	0.9	1.8	-1.4	-2.2	2.3	1.4	-1.5	0.1	0.0	-1.8	-0.1	2.3	-0.7	2.9	0.0
Nov	-7.8	-9.7	-7.6	-9.7	-9.0	-8.1	-10.0	-13.3	-10.0	-7.2	-8.9	-9.2	-8.1	-12.0	-11.9	-8.5	-7.2	-7.4	-6.4	-8.9	-10.8	-7.8	-7.2	-10.6	-6.6	-9.0
Dec	-16.3	-21.4	-12.5	-19.1	-18.2	-20.2	-17.8	-19.3	-14.7	-19.8	-18.3	-17.1	-21.0	-20.3	-15.8	-18.1	-15.7	-12.5	-15.9	-15.5	-18.4	-16.3	-12.4	-15.8		-17.2
																							Annual Average			-3.3

NCEP-CRCM Temperature (Bias-Corrected)

	1979	1980	1981	1982	1983	1984	1985	1986	1987	1988	1989	1990	1991	1992	1993	1994	1995	1996	1997	1998	1999	2000	2001	2002	2003	avg
Jan	-12.6	-14.0	-15.7	-16.9	-16.9	-19.8	-18.2	-16.4	-17.2	-16.9	-19.2	-17.3	-21.6	-16.7	-17.9	-22.9	-17.3	-17.6	-15.8	-18.1	-17.5	-18.0	-18.2	-18.9	-16.7	-17.5
Feb	-15.1	-14.0	-7.0	-19.6	-15.1	-14.2	-13.7	-14.9	-14.1	-16.6	-18.6	-20.0	-15.4	-19.7	-18.3	-18.9	-19.5	-11.1	-19.3	-13.1	-13.3	-16.3	-16.9	-18.3	-20.8	-16.2
Mar	-7.2	-8.1	-5.6	-12.6	-10.4	-10.1	-10.0	-12.1	-9.4	-6.5	-12.8	-10.7	-7.0	-10.0	-11.4	-10.3	-11.4	-8.3	-12.7	-9.3	-4.2	-7.3	-5.3	-10.9	-10.2	-9.4
Apr	-0.4	-3.1	-1.2	-1.8	2.2	-1.3	-3.2	1.3	2.4	-0.4	-1.9	-1.2	-1.9	-4.3	0.0	-1.7	-2.0	0.9	-1.8	-2.6	-0.1	-1.3	-1.5	-2.6	-3.3	-1.2
May	8.7	5.1	5.2	5.5	6.8	6.6	3.2	7.2	5.4	7.5	8.4	3.9	4.4	4.3	5.8	5.2	5.5	4.5	3.9	6.2	9.4	4.8	8.8	3.5	6.0	5.8
Jun	14.4	9.3	11.4	11.9	12.7	11.9	12.5	8.0	9.9	10.2	13.3	10.1	9.0	12.2	9.1	12.7	11.5	10.1	9.8	13.7	15.1	11.3	11.3	10.0	10.7	11.3
Jul	17.6	14.2	16.1	15.3	16.4	16.7	16.1	13.5	14.5	16.0	14.5	15.0	13.7	13.3	14.6	16.3	16.1	14.9	14.6	16.8	15.7	16.2	14.5	17.5	15.4	15.4
Aug	14.9	15.8	14.3	13.4	14.2	16.6	15.1	15.1	13.2	15.2	13.8	16.3	15.0	14.0	15.1	15.0	15.1	16.4	14.0	15.0	16.0	15.9	16.4	15.4	15.9	15.1
Sep	9.3	7.7	12.1	9.1	9.0	8.7	9.9	7.5	10.6	9.4	11.2	10.2	9.0	11.2	9.9	10.5	8.4	10.5	11.2	9.7	14.0	10.1	11.6	11.3	14.6	10.3
Oct	3.2	1.9	3.9	3.3	3.6	1.6	2.6	1.8	4.9	5.1	2.8	4.3	5.1	2.3	1.5	5.5	4.8	2.2	3.7	3.5	2.0	3.5	5.5	2.9	6.0	3.5
Nov	-3.6	-5.2	-3.3	-5.3	-4.6	-3.7	-5.6	-8.3	-5.4	-3.0	-4.6	-4.7	-3.8	-7.1	-7.0	-4.3	-3.1	-3.2	-2.3	-4.4	-6.1	-3.6	-3.1	-5.9	-2.4	-4.5
Dec	-11.8	-16.5	-8.3	-14.4	-13.6	-15.3	-13.2	-14.6	-10.3	-15.0	-13.5	-12.5	-16.1	-15.4	-11.3	-13.4	-11.3	-8.3	-11.4	-11.0	-13.7	-11.8	-8.2	-11.4		-12.6
																							Annual Average			0.1

Appendix D

Monthly Precipitation at Goose Bay

Appendix D - Monthly Precipitation at Goose Bay (mm)

CGCM3-CRCM Current Period Precipitation (Uncorrected)

	1968	1969	1970	1971	1972	1973	1974	1975	1976	1977	1978	1979	1980	1981	1982	1983	1984	1985	1986	1987	1988	1989	1990	1991	1992	1993	1994	1995	1996	1997	1998	1999	2000	avg
Jan	82.5	30.3	36.1	32.8	36.8	32.6	44.2	34.8	45.9	26.5	47.9	56.6	17.9	44.7	69.3	26.0	59.2	45.4	72.0	51.8	50.1	32.9	61.5	82.1	38.4	34.4	55.1	87.2	29.5	52.1	52.9	19.5	106.5	48.3
Feb	33.5	9.2	49.8	13.3	63.1	61.5	56.5	59.9	51.5	13.2	31.3	27.9	11.5	20.8	54.9	38.3	51.8	27.3	33.8	49.9	16.6	70.7	11.1	42.2	48.8	33.4	38.5	44.9	63.2	49.6	33.3	29.9	41.8	38.9
Mar	71.5	30.0	37.0	34.6	42.0	43.7	88.8	14.5	51.7	48.4	32.2	56.4	36.2	31.5	17.6	39.4	37.8	80.8	35.0	38.6	35.0	41.0	26.3	70.2	41.8	82.9	32.7	55.0	39.5	20.2	44.0	37.9	86.1	44.9
Apr	74.3	49.2	29.6	69.2	25.9	56.8	50.6	107.0	55.6	73.0	48.4	32.8	47.8	51.6	47.0	44.1	78.3	55.7	26.9	42.0	109.0	48.9	25.0	69.8	46.1	30.5	81.0	41.6	60.5	17.4	29.4	58.0	49.1	52.5
May	94.4	41.3	81.9	54.2	63.0	55.4	21.8	38.0	49.8	68.6	49.8	64.1	106.8	75.8	65.1	62.0	87.1	65.9	78.1	77.9	47.6	87.8	43.8	56.0	70.2	53.2	76.8	74.6	22.4	50.6	76.8	30.4	77.8	64.0
Jun	117.4	36.5	106.9	84.0	92.4	159.8	56.3	89.6	63.8	57.0	84.2	61.3	74.0	54.5	66.7	44.7	81.3	53.1	90.2	66.8	72.8	81.3	60.8	41.1	77.6	100.2	102.0	113.8	67.2	54.9	79.1	89.2	65.7	77.2
Jul	95.8	72.1	24.8	88.5	64.5	102.1	72.6	146.8	68.4	132.2	87.3	122.0	95.8	76.4	75.9	157.6	39.6	124.8	92.7	130.4	86.5	69.9	68.6	100.3	78.2	124.6	156.3	85.4	76.3	127.3	137.4	225.9	125.9	101.0
Aug	56.6	70.5	52.1	123.0	96.6	80.8	126.5	126.9	82.8	122.9	111.4	73.9	109.4	111.6	113.5	85.6	123.6	38.1	254.1	120.9	110.6	53.1	62.8	128.9	93.6	102.9	114.5	93.4	149.4	113.2	102.9	125.5	71.5	103.1
Sep	67.6	76.4	121.3	131.7	42.2	115.1	79.0	53.1	60.6	87.2	59.1	134.8	114.5	67.1	60.9	120.8	81.8	59.8	120.8	83.3	113.4	29.9	69.1	74.6	72.6	47.8	132.5	82.8	121.3	103.3	48.3	66.8	63.2	83.7
Oct	54.6	43.7	123.8	64.7	98.2	26.3	85.0	88.6	48.9	82.8	81.0	86.4	42.1	99.7	60.3	119.4	35.1	64.9	96.9	72.7	56.6	107.3	44.3	118.9	56.2	99.8	95.3	125.5	45.2	117.6	92.4	21.9	113.3	77.9
Nov	78.1	104.4	85.3	45.5	71.7	90.3	55.3	46.3	57.6	61.2	54.2	35.7	48.6	37.8	73.4	82.5	60.9	112.1	106.8	21.7	80.7	41.7	53.2	61.7	96.0	109.6	77.6	67.3	41.2	71.4	68.6	106.2	52.6	68.4
Dec	58.6	88.4	48.4	80.7	36.8	15.7	65.3	89.0	68.4	57.1	48.2	62.8	70.2	101.1	93.6	74.4	44.2	82.8	40.2	101.7	107.7	68.0	32.6	75.8	119.6	50.9	113.4	70.6	44.3	65.4	123.5	74.5		71.0

Annual Average 830.8

CGCM3-CRCM Current Period Precipitation (Bias-Corrected)

	1968	1969	1970	1971	1972	1973	1974	1975	1976	1977	1978	1979	1980	1981	1982	1983	1984	1985	1986	1987	1988	1989	1990	1991	1992	1993	1994	1995	1996	1997	1998	1999	2000	avg
Jan	153.1	56.7	63.9	60.4	69.2	81.3	83.3	63.8	81.4	48.6	88.2	105.9	34.6	83.1	126.2	48.7	110.8	80.5	134.3	97.2	93.1	61.6	111.8	153.4	72.4	64.6	102.7	153.1	54.4	95.1	99.0	35.7	195.0	89.2
Feb	67.0	19.4	99.4	27.5	124.7	121.2	113.2	117.9	102.9	27.3	63.3	57.0	23.9	42.9	107.8	76.8	103.8	55.6	67.3	99.2	34.0	141.4	23.3	85.7	97.1	67.3	76.2	89.5	125.9	98.8	67.2	61.3	83.5	77.9
Mar	136.0	61.1	71.7	70.0	85.0	87.3	170.9	29.7	101.2	96.0	64.0	111.7	71.1	64.2	35.9	78.3	74.9	158.4	69.4	77.2	72.4	80.7	52.4	140.2	82.1	161.2	65.7	110.2	78.6	40.4	87.7	77.6	166.6	88.9
Apr	119.2	73.1	44.7	106.8	37.6	85.9	82.4	165.2	92.8	116.3	78.0	49.9	73.4	80.6	74.4	73.6	118.3	86.8	44.2	63.8	175.9	77.0	38.8	103.3	72.4	45.1	128.2	61.2	90.8	25.3	45.0	92.9	73.6	81.8
May	121.8	53.5	104.2	68.5	82.4	70.6	26.1	48.0	62.8	88.1	83.6	82.2	140.9	100.2	84.2	106.1	112.4	110.5	100.3	99.6	61.6	112.1	55.6	74.7	92.0	88.7	97.9	94.6	27.9	64.1	97.9	39.0	98.8	82.1
Jun	149.6	41.2	132.8	103.6	115.9	205.1	67.3	112.4	75.9	67.2	100.8	73.8	90.2	64.0	80.6	51.6	98.9	64.6	114.2	81.2	90.9	98.1	75.0	46.5	94.1	127.8	131.5	137.9	78.7	64.5	96.3	108.6	77.1	94.6
Jul	110.8	83.2	24.8	101.7	71.3	118.7	79.8	186.1	75.7	161.5	98.5	142.9	110.9	83.8	86.5	196.9	39.6	145.6	105.3	162.7	97.5	78.8	74.0	115.7	87.2	152.0	190.3	95.7	91.1	148.1	166.9	294.3	145.5	118.9
Aug	59.2	75.7	52.8	139.2	106.9	85.1	147.0	140.8	91.2	139.3	122.6	80.3	124.5	122.4	129.5	95.0	151.1	37.4	314.5	136.0	122.0	58.9	65.5	149.7	102.4	111.6	125.4	101.7	173.5	131.2	116.6	142.5	75.9	116.0
Sep	76.4	87.6	142.4	159.1	47.3	135.9	90.0	59.0	67.3	100.0	86.3	158.6	133.4	76.2	68.1	141.9	92.9	67.3	141.9	94.3	133.8	31.5	79.7	84.1	83.4	51.8	155.9	94.7	146.6	122.1	53.8	75.8	69.5	96.6
Oct	65.4	51.4	156.7	81.4	127.0	30.2	107.3	107.3	57.7	100.3	99.0	106.7	50.5	125.5	74.3	150.7	40.3	79.3	118.5	88.4	67.9	132.3	53.3	149.0	69.1	123.2	117.1	155.4	53.3	147.8	114.0	24.9	139.7	95.9
Nov	96.7	133.0	105.8	55.4	88.9	113.5	67.0	54.9	73.2	76.3	65.2	42.6	58.4	44.5	94.0	104.8	74.5	141.6	135.3	24.4	100.9	49.6	64.9	75.1	118.6	138.6	97.3	81.8	49.7	87.1	85.2	139.1	63.5	84.9
Dec	88.1	131.6	71.5	122.8	54.2	22.8	96.5	137.4	101.0	84.9	72.0	93.4	106.7	157.0	144.1	111.4	63.3	125.5	58.8	151.6	165.4	101.1	46.8	113.5	184.9	75.7	170.9	103.6	65.7	100.9	187.9	112.6		107.0

Annual Average 1133.7

CGCM3-CRCM Future Period Precipitation (Uncorrected)

	2038	2039	2040	2041	2042	2043	2044	2045	2046	2047	2048	2049	2050	2051	2052	2053	2054	2055	2056	2057	2058	2059	2060	2061	2062	2063	2064	2065	2066	2067	2068	2069	2070	avg
Jan	45.6	65.1	45.9	33.3	33.0	84.0	61.7	39.4	26.3	93.9	33.2	68.0	33.2	45.5	32.7	23.8	59.8	21.8	21.5	55.6	110.4	77.2	88.6	67.3	77.1	32.8	71.1	55.9	100.1	80.0	60.0	40.3	30.9	55.0
Feb	64.6	60.8	43.3	84.2	41.1	46.7	30.4	45.8	26.8	68.3	52.6	37.7	24.5	30.3	27.4	31.3	63.3	22.7	110.0	61.0	63.4	39.2	17.8	39.2	44.6	25.3	47.8	58.6	60.0	70.3	113.5	43.4	59.8	50.2
Mar	52.2	43.4	54.3	75.1	55.9	31.5	77.4	86.6	65.0	25.9	61.0	15.0	85.3	18.5	42.0	55.3	79.7	56.6	58.1	69.4	44.1	87.3	65.6	70.8	91.5	110.8	65.0	78.9	46.9	36.5	41.8	54.7	70.9	60.4
Apr	36.0	62.7	23.4	46.4	78.2	25.2	34.1	70.8	117.7	54.6	60.2	111.6	61.1	7.4	39.0	41.9	153.4	33.1	70.3	74.3	106.5	77.8	55.6	58.7	62.4	44.5	43.4	35.0	58.6	83.7	62.9	48.3	98.4	61.6
May	91.8	82.3	99.6	79.4	95.7	58.6	82.8	101.9	106.3	50.0	91.6	42.4	48.6	36.0	73.6	67.1	74.1	41.7	29.8	31.2	21.8	84.4	51.8	51.2	87.2	51.7	79.2	77.5	46.4	57.8	105.3	57.8	105.9	68.6
Jun	93.0	89.9	49.5	78.7	115.7	91.7	82.4	124.4	68.9	190.7	97.6	65.9	58.8	94.5	74.5	48.2	69.7	88.1	102.7	95.4	61.0	115.1	76.8	91.5	133.2	122.1	73.2	71.7	95.0	105.4	61.5	111.3	88.9	90.5
Jul	75.0	84.3	119.6	90.9	73.8	93.9	84.6	150.3	94.8	94.9	73.1	68.1	69.8	87.4	152.0	149.2	55.0	149.4	61.3	45.6	86.8	86.0	104.2	120.0	98.5	92.9	114.1	108.7	100.3	198.9	174.5	137.7	133.6	103.9
Aug	107.2	102.9	91.2	101.9	73.4	116.0	175.3	91.8	123.7	105.8	97.1	149.5	104.2	107.5	61.5	79.1	117.3	154.1	88.0	152.1	148.2	139.1	104.3	66.1	110.8	49.4	92.4	101.1	111.1	120.4	140.9	93.0	64.4	107.3
Sep	80.5	115.0	92.8	94.2	68.9	101.2	119.8	87.6	131.6	112.7	63.7	82.3	97.0	59.2	57.2	132.5	129.0	71.3	62.0	97.4	153.6	63.2	88.0	134.0	116.2	146.6	73.0	74.5	141.0	91.6	187.6	116.1	89.0	100.9
Oct	94.2	88.1	83.3	85.8	54.2	97.6	69.8	45.0	88.7	48.9	61.6	77.2	71.4	93.2	81.2	100.8	116.2	91.7	55.2	63.8	152.4	109.5	103.2	110.1	73.0	73.8	35.7	34.7	64.9	59.2	96.6	63.2	47.5	78.5
Nov	45.7	65.2	70.3	103.1	43.7	55.4	99.2	69.2	48.3	89.1	56.0	55.8	73.9	70.8	135.4	99.2	182.4	79.2	87.9	78.5	93.5	56.4	44.1	63.3	67.8	123.2	64.5	69.8	59.0	69.5	64.9	62.7	38.2	75.3
Dec	71.9	52.6	48.7	33.0	48.7	23.5	74.9	65.1	70.3	29.4	56.8	49.3	61.6	53.0	66.7	42.3	84.7	73.1	49.7	105.5	73.3	70.9	51.0	54.6	72.7	86.4	65.6	91.4	60.0	59.6	66.4	59.6		61.6

Annual Average 913.8

CGCM3-CRCM Future Period Precipitation (Bias-Corrected)

	2038	2039	2040	2041	2042	2043	2044	2045	2046	2047	2048	2049	2050	2051	2052	2053	2054	2055	2056	2057	2058	2059	2060	2061	2062	2063	2064	2065	2066	2067	2068	2069	2070	avg
Jan	86.3	120.0	85.9	61.8	59.5	156.3	113.8	71.6	47.5	171.2	61.2	124.2	61.1	83.0	62.2	44.0	111.1	41.3	38.9	102.9	197.1	140.8	161.0	124.7	142.4	60.8	131.0	98.7	178.5	151.2	107.8	72.2	59.5	100.9
Feb	129.4	121.3	85.7	164.8	83.2	92.5	62.4	91.7	53.8	134.5	104.8	75.4	49.1	60.2	55.6	83.6	125.7	46.7	215.6	122.0	124.1	78.5	36.5	79.4	89.0	51.2	95.6	114.7	118.9	135.9	222.1	86.8	120.1	99.7
Mar	103.2	82.9	108.8	142.4	109.3	62.3	152.5	168.2	165.6	53.7	121.4	31.1	164.3	36.0	84.7	110.9	156.3	110.1	117.1	137.9	84.3	168.2	132.4	140.3	179.8	217.6	129.1	151.7	94.2	74.4	82.9	103.0	136.4	118.6
Apr	56.1	99.9	35.2	71.5	123.8	37.4	52.0	108.1	190.5	83.8	93.7	170.1	92.7	11.5	63.2	66.3	254.2	49.8	105.0	115.8	162.5	128.3	89.4	93.2	93.5	70.1	65.8	52.0	87.7	133.5	102.8	81.8	150.0	96.7
May	118.5	105.6	128.4	103.4	123.6	73.9	105.5	131.1	139.5	62.6	116.8	53.6	61.4	44.4	93.0	86.2	95.3	51.6	37.3	38.9	28.4	108.4	65.3	65.4	113.2	65.9	101.4	100.8	60.2	72.9	134.7	73.6	136.7	87.9
Jun	114.7	110.1	57.5	97.3	145.9	110.6	98.9	153.6	81.9	248.7	123.0	77.8	69.8	113.8	87.6	56.6	83.7	107.5	127.0	117.8	71.5	146.3	93.0	111.1	167.5	150.0	87.4	87.7	116.7	129.1	71.9	137.9	106.0	110.9
Jul	86.0	97.7	146.1	104.2	79.9	107.8	98.4	187.7	111.3	111.1	80.5	73.7	76.0	101.9	189.8	185.9	57.3	177.4	65.8	49.1	97.7	95.2	119.8	142.1	118.7	108.5	134.9	127.7	114.2	254.6	216.1	166.3	164.2	122.7
Aug	117.5	113.3	100.8	113.5	76.1	130.1	211.2	100.6	142.4	120.2	108.9	178.0	113.8	117.7	65.1	82.9	129.5	182.4	96.4	178.6	172.0	159.1	116.5	69.1	128.8	51.3	99.5	112.0	125.0	136.8	164.0	99.0	67.6	120.7
Sep	91.7	135.2	106.7	110.9	77.3	118.2	144.7	99.8	153.3	133.0	71.6	94.7	112.8	66.2	63.1	155.7	150.4	78.4	69.7	112.4	190.9	70.8	100.5	158.4	142.3	177.6	84.8	84.1	167.5	107.6	233.4	135.8	102.0	118.2
Oct	115.8	106.9	104.2	107.5	64.3	124.7	85.1	53.6	109.5	56.9	74.5	93.8	87.5	113.7	97.4	126.6	146.6	115.6	65.9	76.2	194.8	133.8	126.2	137.3	89.2	91.3	41.2	40.1	78.1	74.1	118.9	75.1	55.6	96.5
Nov	55.1	87.8	88.0	128.3	53.2	67.6	127.8	85.3	59.0	111.8	66.5	89.4	94.5	87.4	179.5	123.1	242.1	96.1	111.1	97.0	120.7	68.9	54.2	77.2	85.2	164.1	78.7	88.1	71.6	85.8	78.8	76.5	44.8	94.7
Dec	109.5	78.2	69.8	48.2	73.9	36.2	114.0	98.4	104.7	43.9	84.9	71.9	94.6	78.8	97.6	61.8	129.3	109.7	75.1	161.0	110.1	106.9	77.0	80.6	110.6	128.9	105.0	140.7	89.6	87.0	100.5	87.0		92.7

Annual Average 1260.1

Appendix E

RCM Data Gridpoint Extraction Code

1) After the netCDF file is downloaded from NARCCAP, GRADS must be informed of how the data is structured. Here an example control file for prNOW:

```
DSET ^pr_CRCM_cgcm3_%ch010103.nc
CHSUB     1  8760  1968                  !these CHSUB lines open a new
file as time increases
CHSUB  8761 23360  1971
CHSUB 23361 37960  1976
CHSUB 37961 52560  1981
CHSUB 52561 67160  1986
CHSUB 67161 81760  1991
CHSUB 81761 96112  1996
DTYPE netcdf
OPTIONS template 365_day_calendar
UNDEF 1.e+20  FillValue
XDEF 140 linear 1 1
YDEF 115 linear 1 1
ZDEF 1   linear 1 1
TDEF 96112 linear 03z01jan1968 180mn

VARS 3
   lon=>lon1     0 y,x longitude
   lat=>lat1     0 y,x latitude
   pr=>pr1      0 t,y,x Precipitation
ENDVARS
```

2) Here's a GRADS script that extracts netCDF data from the file and created a raw binary file (taFUT example):

```
"reinit"
"open taFUT.ctl"     !alter this line for pr ta NOW FUT NCP combination
"set t 1 last"
"set gxout fwrite"
"set fwrite -le -st -cl ta.FUT"    !alter this line for pr ta NOW FUT
NCP combination
#Goose Bay(117,87)
"set x 117"
"set y 87"
"d tas1"        !alter these tas1 lines to pr1 lines for pr files
#Pinus(116,86)
"set x 116"
"set y 86"
"d tas1"
#Churchill Falls(113,85)
"set x 113"
"set y 85"
"d tas1"
"disable fwrite"
```

3) GRADS won't easily output ascii data so I wrote a short piece of fortran code that reads the GRADS binary file and writes the ascii files you have (taFUT example here):

```
PROGRAM bin2ascii

IMPLICIT NONE
INTEGER, PARAMETER             :: isize=96112, jsize=3
!uncomment this line for FUT NOW
c      INTEGER, PARAMETER             :: isize=72800, jsize=3 !uncomment
this line for NCP
CHARACTER(LEN=2)               :: var  = 'ta' !alter this line for pr ta
CHARACTER(LEN=3)               :: time = 'FUT' !alter this line for NOW
FUT NCP
REAL, DIMENSION(isize,jsize)  :: binData
INTEGER                        :: i,j

OPEN(10,File=var//'.'//time,
1          Form='BINARY',Access='SEQUENTIAL')
READ(10) binData

OPEN(11,File=var//time//'.txt',
1          Form='FORMATTED',Access='SEQUENTIAL')
WRITE(11,'(3(a15))')  'Goose Bay','Pinus','Churchill Falls'
WRITE(11,'(3(e15.6)') ((binData(i,j),j=1,jsize),i=1,isize)

STOP
END PROGRAM bin2ascii
```

Appendix F

Monthly Pinus River Flow

Appendix F - Monthly Pinus River Flow (m^3/s)

Simulated Flows - CGCM3-CRCM Current Period (Uncorrected RCM Inputs)

	1968	1969	1970	1971	1972	1973	1974	1975	1976	1977	1978	1979	1980	1981	1982	1983	1984	1985	1986	1987	1988	1989	1990	1991	1992	1993	1994	1995	1996	1997	1998	1999	2000	avg
Jan	3.7	3.9	1.9	3.8	4.2	4.2	3.3	3.8	4.6	2.9	4.4	5.1	3.6	6.0	3.3	3.1	14.1	3.3	3.9	7.2	4.1	5.4	3.8	2.6	4.3	4.7	5.3	5.0	4.0	4.4	7.6	4.9	3.3	4.8
Feb	2.8	3.0	1.6	3.0	3.3	3.3	3.1	3.5	3.5	2.2	3.4	3.6	2.8	3.8	2.6	2.5	5.3	2.6	3.0	6.3	3.2	4.0	2.8	2.1	3.4	3.6	4.4	3.8	3.2	3.4	5.1	3.4	2.7	3.3
Mar	2.3	2.6	1.4	2.5	2.7	2.7	2.6	2.6	2.8	1.8	2.7	2.6	3.1	3.0	2.2	2.1	4.0	2.2	2.5	4.0	2.6	3.2	2.3	1.8	2.7	2.8	9.3	3.0	2.6	2.7	3.9	2.8	2.2	2.9
Apr	2.7	7.5	1.2	2.0	2.2	2.2	1.9	2.1	2.3	1.6	2.3	2.2	3.4	2.5	1.8	1.8	3.1	1.8	2.8	4.8	15.6	2.6	3.1	1.5	2.3	2.4	3.5	2.4	2.2	2.5	4.0	3.9	1.9	3.0
May	20.5	23.7	4.1	21.2	2.0	32.9	7.3	18.7	4.7	9.0	4.6	31.6	12.1	11.5	4.1	2.5	21.0	1.9	11.8	18.3	6.5	16.6	10.4	37.8	19.8	3.8	27.8	5.6	3.4	19.3	19.4	9.5	4.3	13.6
Jun	39.8	8.5	64.7	44.9	55.9	42.9	49.3	41.8	54.9	49.5	51.6	19.1	39.3	36.9	62.3	46.7	46.7	52.2	42.8	32.7	39.5	48.2	29.4	29.8	47.3	47.7	38.8	83.8	64.8	23.0	32.6	47.0	85.5	45.6
Jul	17.7	5.6	19.5	12.0	21.3	19.1	15.9	20.3	12.9	12.6	12.2	9.8	17.9	11.1	21.5	35.6	12.8	32.5	25.8	21.5	17.2	18.6	8.9	11.8	11.8	41.9	23.5	23.4	17.0	10.5	18.1	23.6	28.0	18.5
Aug	8.2	4.9	6.7	10.8	12.8	13.4	13.6	13.2	7.6	17.9	11.1	9.5	12.1	10.9	17.0	17.1	9.5	11.2	27.0	13.0	10.5	8.2	5.2	14.8	12.2	15.8	18.5	11.9	14.2	9.0	18.5	25.1	15.9	12.9
Sep	7.8	5.7	10.8	20.9	7.3	12.3	11.0	12.6	8.5	15.5	9.2	17.6	17.7	12.1	9.6	18.2	14.5	7.2	30.9	15.7	17.4	6.0	5.6	9.6	10.2	10.9	20.5	11.3	20.8	16.8	11.3	16.4	9.9	13.1
Oct	8.0	5.9	15.1	15.1	9.9	13.1	11.5	13.5	8.6	15.4	11.8	13.4	12.7	11.0	8.4	19.9	12.4	7.7	26.3	14.9	13.1	11.7	5.4	15.1	8.4	11.6	20.2	15.7	12.3	13.0	9.5	9.5	16.5	12.6
Nov	14.3	4.5	12.2	12.2	16.5	6.2	16.7	13.4	5.4	13.2	13.3	8.8	9.1	6.8	7.7	18.1	6.9	16.2	24.1	11.1	19.2	10.3	8.0	15.3	12.9	19.8	13.5	10.3	8.9	23.4	15.9	6.9	16.7	12.7
Dec	8.2	2.6	6.9	7.5	6.7	4.3	5.4	7.5	5.3	6.2	7.8	5.2	13.3	4.3	4.4	12.8	4.7	8.4	15.6	5.6	9.5	6.1	4.8	6.2	13.3	10.0	7.3	5.5	8.7	16.4	12.0	4.4		7.7

Annual Average 12.5

Simulated Flows - CGCM3-CRCM Current Period (Bias-Corrected RCM Inputs)

	1968	1969	1970	1971	1972	1973	1974	1975	1976	1977	1978	1979	1980	1981	1982	1983	1984	1985	1986	1987	1988	1989	1990	1991	1992	1993	1994	1995	1996	1997	1998	1999	2000	avg
Jan	3.7	4.4	6.7	7.0	5.8	6.7	3.7	6.1	8.6	7.8	5.4	9.8	6.9	9.8	4.4	6.6	19.7	5.2	6.5	9.5	7.3	7.0	7.4	3.3	6.1	18.4	9.2	7.3	5.4	7.1	10.8	16.0	4.4	7.7
Feb	2.8	3.4	4.0	5.0	4.3	4.8	3.1	6.0	5.3	4.9	5.9	7.8	4.7	6.0	3.3	4.7	8.6	3.8	4.7	11.2	5.0	5.0	4.4	2.5	4.5	6.0	12.2	4.6	4.7	4.2	8.0	8.0	3.6	5.4
Mar	2.2	2.9	3.6	4.2	3.3	3.7	3.1	4.6	4.0	3.9	7.3	5.3	13.1	4.2	2.7	3.9	7.1	5.7	3.6	5.4	3.8	4.1	3.5	5.8	3.5	11.7	32.9	11.2	3.5	3.3	4.8	5.6	2.7	6.8
Apr	3.9	23.4	5.0	3.1	3.0	3.0	2.8	2.9	3.1	7.1	7.2	7.0	28.3	4.6	3.1	8.2	5.7	3.2	8.5	8.9	49.9	3.0	6.9	2.9	2.8	10.8	26.5	5.5	4.1	13.1	3.7	14.0	3.6	8.7
May	56.0	36.5	49.3	57.3	18.1	70.3	40.3	62.8	18.5	44.3	32.0	53.9	23.5	48.5	43.2	43.1	77.7	18.6	62.2	59.3	43.8	69.0	41.0	79.0	76.9	47.5	30.4	42.5	25.5	37.1	54.7	44.3	55.6	47.3
Jun	54.0	5.9	31.8	23.7	81.3	41.4	58.1	28.2	81.3	24.8	43.3	15.8	16.3	26.5	67.3	41.3	28.5	70.8	39.1	20.1	15.8	49.4	10.8	24.2	33.5	33.3	26.7	87.2	65.7	11.9	33.8	14.1	96.8	39.5
Jul	24.4	6.3	14.5	11.6	19.4	22.4	12.9	26.8	14.9	12.8	12.1	10.9	15.6	9.3	12.6	21.2	11.8	22.9	15.3	26.0	14.5	15.0	8.9	13.8	11.7	31.4	22.6	25.9	16.4	10.8	24.0	29.0	20.2	17.2
Aug	9.7	5.2	5.9	10.0	12.7	13.2	14.4	14.8	8.6	18.4	11.2	9.4	11.7	9.5	16.5	16.5	11.4	10.6	32.6	12.7	9.3	8.0	4.9	16.1	11.6	13.7	18.3	13.7	14.7	9.5	20.7	30.2	14.9	13.3
Sep	8.8	5.5	10.8	23.9	6.7	12.3	10.8	13.6	8.7	16.1	9.4	20.0	18.2	10.9	9.0	18.7	15.2	7.0	37.0	15.5	17.0	5.5	5.7	10.0	9.8	9.0	22.0	11.8	24.0	18.9	11.9	17.8	9.1	13.7
Oct	9.4	5.6	18.7	18.2	11.4	14.0	13.8	16.0	8.8	16.8	14.3	15.4	12.8	12.4	8.5	22.3	12.1	7.7	31.2	15.7	13.2	13.4	5.3	17.2	8.8	13.0	23.2	19.1	13.9	14.8	11.5	10.0	18.5	14.2
Nov	14.7	7.6	30.3	17.3	22.8	8.3	20.0	14.8	6.5	14.4	15.3	15.6	10.5	12.0	14.9	27.2	11.9	19.8	30.2	11.5	21.5	10.3	7.5	21.6	14.3	25.5	19.2	16.9	10.2	27.7	22.2	13.6	17.4	16.8
Dec	9.4	27.9	13.2	10.4	14.5	5.7	12.1	15.4	23.9	7.5	13.9	17.3	18.5	8.4	15.9	27.1	13.9	17.8	18.7	22.4	15.1	15.3	9.3	10.9	19.1	20.9	14.4	10.4	12.7	20.1	33.0	7.3		15.7

Annual Average 17.2

Simulated Flows - CGCM3-CRCM Future Period (Uncorrected RCM Inputs)

	2038	2039	2040	2041	2042	2043	2044	2045	2046	2047	2048	2049	2050	2051	2052	2053	2054	2055	2056	2057	2058	2059	2060	2061	2062	2063	2064	2065	2066	2067	2068	2069	2070	avg
Jan	3.7	6.2	5.0	5.4	3.1	3.7	3.3	7.3	3.9	7.1	4.2	3.2	3.8	4.4	3.8	5.2	6.1	7.5	6.2	2.9	6.5	7.2	7.1	8.9	3.9	6.9	8.4	3.0	10.1	14.2	4.7	9.5	4.4	5.8
Feb	2.8	3.4	3.7	4.0	2.6	2.9	2.7	5.2	3.6	4.6	3.3	2.5	3.0	3.4	3.2	3.9	4.5	5.3	4.4	2.3	3.8	5.2	4.6	4.8	3.1	4.7	4.3	2.4	3.9	11.3	4.0	11.7	3.7	4.2
Mar	2.2	2.7	2.9	3.2	2.5	2.1	2.2	4.0	2.7	3.6	2.6	2.1	2.7	2.7	2.9	3.3	3.5	5.8	3.9	2.0	3.2	3.9	3.0	3.7	2.5	18.5	3.3	2.1	3.1	9.5	4.7	9.6	5.3	4.0
Apr	2.7	2.3	6.0	3.5	1.8	3.6	1.9	3.6	3.9	5.1	2.2	4.0	3.9	2.3	2.0	3.8	3.3	7.4	2.7	1.7	2.1	3.1	2.8	3.6	2.8	9.4	2.6	1.7	3.0	7.7	5.8	16.1	3.0	4.0
May	12.8	18.1	38.5	9.4	20.5	35.3	7.5	14.2	30.1	38.2	16.0	8.4	10.7	21.3	25.7	34.1	13.3	16.3	4.5	4.0	5.6	44.3	23.4	43.5	21.6	25.6	19.1	31.8	23.3	30.5	50.3	17.2	14.4	22.1
Jun	29.9	52.7	19.7	59.9	65.7	20.0	65.1	61.9	55.0	31.2	53.6	54.3	42.9	18.5	30.2	13.1	60.1	37.7	65.3	60.3	67.7	48.7	39.5	12.5	74.1	18.7	48.3	44.0	42.8	19.7	26.7	12.4	61.1	42.8
Jul	7.7	15.6	11.6	14.7	20.7	8.4	17.7	29.7	14.1	22.0	16.1	8.1	8.6	10.7	15.9	18.4	22.0	14.4	13.4	13.4	17.2	18.2	13.1	16.8	27.5	11.7	17.3	11.1	11.9	18.6	17.1	14.9	22.4	16.8
Aug	10.3	9.9	10.5	11.1	10.0	11.2	16.7	13.9	12.0	13.8	10.7	17.9	7.9	9.1	9.2	8.6	12.7	22.3	8.8	16.6	15.0	18.3	13.5	8.4	14.2	5.9	10.0	12.6	13.1	25.3	19.0	9.0	10.3	12.7
Sep	10.6	13.7	10.8	11.4	9.0	12.1	18.9	15.6	18.3	13.1	7.4	11.6	11.3	6.7	6.8	13.3	15.2	15.8	6.5	12.2	25.0	12.6	10.6	13.2	14.1	12.0	8.3	8.2	19.7	14.1	28.0	12.7	10.8	13.0
Oct	13.3	15.0	10.8	10.3	9.4	13.1	21.3	9.3	19.1	14.1	8.2	13.5	12.8	13.4	9.1	13.7	17.9	12.5	8.0	12.0	24.2	13.0	14.6	16.2	21.5	13.2	7.2	6.8	13.2	13.8	33.6	12.7	7.7	13.8
Nov	11.3	11.4	15.6	10.0	7.6	8.0	17.3	12.1	13.8	11.5	9.8	9.3	11.3	10.7	11.7	23.0	34.2	18.6	9.7	11.6	22.4	15.8	12.5	9.6	12.4	13.0	8.7	7.5	12.8	14.5	18.2	12.7	7.0	13.2
Dec	7.5	10.4	12.0	4.4	5.1	4.4	19.6	5.8	16.3	5.9	4.6	5.2	10.8	5.3	21.5	12.1	16.3	9.4	4.1	6.8	18.9	9.1	10.0	5.3	16.4	19.4	4.4	13.8	9.1	8.8	19.4	7.1		10.3

Annual Average 13.6

Simulated Flows - CGCM3-CRCM Future Period (Bias-Corrected RCM Inputs)

	2038	2039	2040	2041	2042	2043	2044	2045	2046	2047	2048	2049	2050	2051	2052	2053	2054	2055	2056	2057	2058	2059	2060	2061	2062	2063	2064	2065	2066	2067	2068	2069	2070	avg
Jan	3.7	16.0	10.4	7.1	7.6	9.0	7.3	10.6	5.1	11.2	5.4	4.9	4.4	5.6	5.8	9.0	12.6	13.6	10.4	4.1	15.4	11.5	20.9	11.7	5.0	11.8	24.9	3.5	17.7	30.6	9.5	12.8	6.9	10.5
Feb	3.0	7.2	7.4	5.0	5.7	5.6	4.7	6.8	3.8	6.5	4.5	3.3	3.4	4.3	4.2	6.2	7.3	8.2	7.8	3.8	5.9	7.3	14.1	5.7	3.8	6.1	12.3	2.8	5.9	28.4	9.6	18.3	6.9	7.2
Mar	2.7	7.6	6.2	4.0	9.4	3.0	3.5	13.0	3.0	4.7	3.4	2.6	3.6	3.4	4.1	10.9	5.3	12.4	15.9	3.0	4.6	5.3	9.2	4.3	3.0	60.0	10.7	2.3	4.3	33.8	16.2	22.4	36.8	10.1
Apr	27.0	29.0	37.5	6.6	5.3	15.8	2.9	43.7	11.5	24.4	2.6	13.6	23.0	4.2	3.8	10.1	7.1	40.8	5.1	9.8	3.1	14.1	16.5	3.3	10.7	31.0	7.6	12.8	3.4	32.8	44.8	39.4	42.0	17.7
May	43.6	53.4	37.7	36.1	62.9	47.7	40.3	52.1	91.6	62.8	65.7	46.7	57.4	48.0	54.9	46.9	75.8	21.6	47.2	74.0	57.8	89.7	48.1	84.1	107.3	16.9	65.5	87.8	76.4	18.9	55.8	16.0	38.9	55.4
Jun	16.1	23.5	13.3	71.9	35.4	16.4	60.9	35.5	40.4	34.5	51.2	35.4	15.4	13.8	21.5	10.8	55.3	14.3	47.0	37.6	70.8	43.4	14.6	20.5	52.6	21.6	22.1	31.0	41.9	19.7	20.5	15.5	27.1	31.9
Jul	9.4	15.2	12.9	16.4	21.3	8.5	14.0	35.3	16.3	27.0	16.2	8.6	7.8	11.5	20.8	24.1	13.6	13.8	16.1	12.7	18.3	23.2	12.7	21.5	30.3	12.9	18.2	13.0	15.0	22.8	19.2	19.3	23.4	17.3
Aug	10.7	9.7	10.5	11.5	9.8	11.4	18.2	15.5	13.6	14.7	11.2	19.5	7.5	9.1	9.9	8.9	12.3	25.1	9.6	18.2	17.2	21.5	13.4	9.8	14.9	5.6	10.0	13.5	15.2	31.6	21.9	10.4	10.6	13.7
Sep	11.5	14.2	11.5	12.1	8.9	13.0	23.3	16.5	21.4	14.1	7.1	12.1	10.6	6.5	7.0	14.7	15.3	16.9	6.9	13.1	32.7	13.7	10.4	15.3	15.6	14.4	8.2	8.4	23.8	15.7	35.6	14.7	11.6	14.5
Oct	15.7	17.2	12.0	15.3	8.9	17.4	24.2	9.9	22.3	15.7	9.5	15.1	14.1	15.1	9.9	16.0	21.1	14.2	8.1	13.6	29.9	14.7	16.4	20.1	26.6	15.8	7.5	7.2	15.8	17.7	42.5	14.6	8.1	16.1
Nov	12.9	15.9	18.1	26.4	9.2	24.8	20.5	15.7	15.4	15.2	12.2	11.1	13.4	12.3	20.4	29.9	48.6	22.8	15.5	17.7	31.4	19.5	14.2	16.4	15.0	19.2	10.0	8.3	17.7	17.0	21.6	15.2	7.6	17.9
Dec	15.6	19.4	15.9	15.7	12.9	9.8	26.1	9.9	24.6	10.7	8.4	7.5	12.9	15.0	29.0	20.3	37.1	17.9	7.2	15.3	30.9	21.5	13.3	8.0	20.3	36.6	5.7	17.2	13.1	19.3	29.0	12.9		17.5

Annual Average 19.2

Appendix F - Monthly Pinus River Flow (m^3/s)

Simulated Flows - Observed Climate Inputs

	1968	1969	1970	1971	1972	1973	1974	1975	1976	1977	1978	1979	1980	1981	1982	1983	1984
Jan	3.7	6.0	10.7	6.3	6.2	4.3	5.9	6.4	3.8	13.1	6.6	5.3	5.5	8.0	10.8	5.9	5.6
Feb	4.9	6.4	8.1	3.4	4.5	3.3	3.5	4.5	3.0	5.6	4.0	11.2	4.0	6.1	7.0	4.0	4.1
Mar	3.0	4.1	4.2	2.7	4.5	2.7	2.8	6.2	2.4	4.1	3.1	4.6	3.1	4.8	5.0	3.1	3.2
Apr	3.6	2.8	3.5	5.3	3.2	2.3	2.3	8.2	3.7	4.1	2.5	6.8	2.5	3.3	3.8	11.2	2.6
May	63.1	44.6	58.7	67.4	7.2	69.7	31.5	34.1	54.8	63.1	53.7	82.5	71.5	65.6	27.9	100.5	55.1
Jun	10.4	58.1	46.5	42.0	90.4	22.5	54.7	27.8	50.8	42.5	76.4	20.8	75.6	68.3	94.4	40.0	124.2
Jul	15.1	17.3	18.2	19.5	16.1	16.5	11.1	8.1	10.2	10.9	28.1	17.3	40.7	31.6	22.1	22.0	29.5
Aug	15.5	17.6	19.8	12.6	19.8	11.1	8.7	6.6	19.3	16.3	15.9	21.0	18.4	23.5	13.0	12.7	14.2
Sep	17.4	17.4	16.5	18.3	12.2	5.4	5.2	9.5	27.0	16.8	13.0	20.3	18.0	14.8	16.4	9.9	14.6
Oct	15.1	21.4	11.9	13.5	15.1	8.9	12.1	8.3	22.4	23.0	22.2	17.4	20.0	23.5	10.8	14.2	11.7
Nov	22.5	17.3	9.7	20.6	10.0	10.6	12.5	11.4	25.1	12.7	13.1	16.7	24.0	28.5	12.7	22.3	9.7
Dec	9.1	20.9	6.6	15.4	7.7	13.1	18.2	8.4	13.4	10.1	6.8	8.6	17.1	24.9	10.7	10.9	9.6

	1985	1986	1987	1988	1989	1990	1991	1992	1993	1994	1995	1996	1997	1998	1999	2000	2001
Jan	4.2	6.9	4.5	5.8	4.7	6.6	4.6	4.5	4.7	6.9	5.4	14.0	9.8	7.0	5.1	7.6	6.9
Feb	3.2	6.2	3.5	4.3	3.6	4.8	3.5	3.5	3.5	4.5	4.1	7.1	5.6	5.0	3.9	5.1	3.1
Mar	2.6	3.3	2.8	3.3	2.9	3.7	3.3	2.8	2.8	4.2	3.2	4.0	4.1	3.9	3.1	3.8	2.5
Apr	2.2	23.8	31.5	4.9	13.0	2.9	2.4	2.3	3.9	5.2	12.1	9.8	3.8	4.4	2.5	8.6	2.1
May	10.7	37.4	55.2	58.8	43.3	19.2	32.3	29.9	44.4	56.6	73.3	65.9	72.1	85.6	103.0	43.8	71.4
Jun	157.2	15.1	17.0	26.9	13.2	81.9	38.0	81.5	50.4	22.2	13.8	16.8	25.1	34.3	26.7	64.8	20.5
Jul	57.7	12.8	11.6	17.7	16.1	22.3	23.4	15.0	9.0	11.4	15.8	22.0	22.8	13.1	20.5	32.0	21.1
Aug	45.6	12.2	9.4	7.0	21.7	13.6	11.7	17.9	6.6	13.2	6.7	15.3	20.2	6.7	27.1	13.6	16.1
Sep	27.6	17.2	7.4	7.4	26.9	13.0	8.2	14.0	8.0	16.3	9.1	11.2	23.1	11.9	19.4	9.3	10.1
Oct	22.8	19.7	17.2	11.5	22.0	10.8	13.8	14.7	19.6	10.1	10.2	22.3	18.7	16.8	30.3	7.1	14.2
Nov	15.1	11.6	12.1	15.9	22.7	13.6	14.6	13.4	14.9	20.9	16.2	22.1	16.3	17.6	23.5	10.0	22.8
Dec	9.2	6.3	15.0	9.8	11.1	13.1	6.7	6.9	13.3	8.1	11.4	14.3	14.6	8.3	13.7	5.4	10.4

	2002	2003	2004	2005	2006	2007	2008	avg
Jan	6.9	7.9	5.7	4.4	6.3	10.2	5.7	6.6
Feb	4.5	4.9	4.0	3.4	4.6	4.4	4.2	4.7
Mar	3.5	3.8	3.1	2.7	3.6	3.4	3.3	3.5
Apr	2.8	6.1	6.8	2.6	21.2	3.1	7.7	6.3
May	37.5	64.1	59.0	71.2	70.6	47.5	63.6	58.3
Jun	47.4	25.1	28.4	11.4	17.8	28.6	22.2	44.7
Jul	15.3	15.7	11.9	8.6	17.3	13.3	14.4	18.9
Aug	22.0	8.2	17.9	13.8	13.5	11.3	8.8	16.3
Sep	18.1	6.8	11.7	11.8	6.1	16.4	12.1	14.0
Oct	16.6	8.5	15.7	14.0	6.1	15.5	12.5	15.7
Nov	16.1	18.9	9.8	15.4	11.1	20.0	13.0	16.3
Dec	14.9	10.5	8.7	14.1	9.5	8.8	13.2	11.4
						Annual Average		17.8

Simulated Flows - NCEP-CRCM RCM Inputs (Uncorrected)

	1979	1980	1981	1982	1983	1984	1985	1986	1987	1988	1989	1990	1991	1992	1993	1994	1995	1996	1997	1998	1999	2000	2001	2002	2003	avg
Jan	8.4	3.7	4.4	6.2	6.6	4.8	3.6	4.6	3.1	4.2	4.7	4.0	3.7	4.5	3.1	6.8	3.9	6.8	5.8	5.4	3.6	2.9	7.9	8.8	4.1	5.0
Feb	8.6	2.8	4.8	4.4	4.1	4.1	3.5	2.8	2.5	3.2	3.6	3.2	3.7	3.5	2.6	4.3	3.0	5.3	3.9	4.2	3.2	2.4	3.6	3.4	3.8	3.8
Mar	5.9	2.3	3.3	3.5	2.7	3.1	2.6	2.3	2.1	2.8	2.9	2.6	3.1	3.1	2.0	3.4	2.5	4.9	2.5	3.8	2.4	2.1	2.9	3.4	2.6	3.0
Apr	10.0	1.9	2.4	2.8	18.9	2.4	2.0	5.0	25.7	2.2	2.5	4.4	2.9	3.6	9.1	9.5	2.4	5.0	4.2	2.6	2.0	1.9	2.4	3.2	2.1	5.2
May	35.2	20.9	9.3	49.7	55.5	37.4	13.5	58.0	29.7	45.3	36.2	17.7	15.8	14.3	40.8	38.0	28.9	34.7	25.9	43.5	76.4	13.5	46.2	8.7	25.0	32.8
Jun	14.5	52.6	72.3	14.5	16.3	36.4	39.7	26.2	11.8	36.8	12.7	34.8	50.5	53.1	16.6	23.0	37.7	21.7	45.1	35.2	29.5	67.5	18.3	47.3	45.9	34.4
Jul	12.7	13.9	18.4	14.9	16.2	14.0	11.7	23.6	12.0	20.3	8.2	14.5	13.5	8.8	14.1	13.0	12.0	10.1	20.0	14.5	12.4	22.9	15.8	12.7	13.8	14.6
Aug	17.5	9.3	18.0	6.8	11.9	7.8	9.2	12.8	11.0	14.0	7.6	9.4	13.3	5.9	7.0	12.8	8.1	8.3	15.1	10.4	7.8	11.1	16.8	10.6	8.7	10.8
Sep	9.3	10.0	11.9	7.7	13.5	7.2	6.3	10.9	8.6	11.7	7.7	13.6	10.3	11.5	10.3	9.0	7.3	7.2	19.4	8.6	8.7	14.2	9.0	10.8	9.1	10.2
Oct	7.9	18.1	12.1	6.9	14.9	15.4	8.0	11.0	7.9	12.7	10.6	14.4	19.5	10.0	14.9	15.4	8.6	9.9	11.0	11.5	9.9	10.0	9.5	14.9	9.0	11.8
Nov	9.2	13.5	12.0	14.7	12.6	10.2	14.1	6.0	15.1	14.5	13.2	7.6	12.7	7.4	14.5	10.6	11.7	9.7	12.2	11.9	7.8	11.0	8.6	11.6	17.5	11.6
Dec	6.8	7.7	19.3	10.1	8.5	5.3	5.7	4.0	8.5	10.5	6.4	5.4	6.6	4.0	19.1	5.2	6.0	9.2	13.8	4.9	4.2	7.3	7.4	5.7		8.0
																							Annual Average			12.6

Simulated Flows - NCEP-CRCM RCM Inputs (Bias-Corrected)

	1979	1980	1981	1982	1983	1984	1985	1986	1987	1988	1989	1990	1991	1992	1993	1994	1995	1996	1997	1998	1999	2000	2001	2002	2003	avg
Jan	14.7	6.6	12.4	11.0	15.8	9.1	6.1	6.9	4.1	7.2	6.3	5.6	6.0	6.9	4.1	14.3	7.6	18.1	14.6	9.7	5.9	4.8	15.3	16.8	10.2	9.7
Feb	14.5	4.1	11.8	6.7	8.2	6.9	4.3	4.5	3.1	5.1	5.7	4.2	5.5	4.9	3.2	7.4	5.4	13.2	7.1	8.2	4.1	3.6	5.2	6.6	6.8	6.4
Mar	8.6	3.2	8.0	4.9	4.7	4.4	3.4	3.1	2.6	3.8	4.3	3.3	4.6	4.4	2.9	5.3	3.9	13.7	4.1	7.0	3.2	3.2	4.5	5.9	4.0	4.8
Apr	14.2	2.6	5.8	3.7	22.3	3.3	2.7	8.8	31.6	3.2	5.1	4.6	3.7	4.3	9.7	12.4	3.7	13.6	6.4	3.6	2.7	4.2	4.4	5.2	3.9	7.4
May	57.6	35.9	36.8	71.4	62.9	68.0	27.0	91.2	49.7	66.6	47.7	26.5	33.7	31.2	60.3	57.4	54.7	54.9	59.7	65.2	121.1	33.8	71.9	25.5	42.0	55.1
Jun	23.8	61.5	59.9	21.1	25.2	36.8	59.5	40.0	16.9	53.3	15.7	57.3	59.0	65.4	30.7	32.4	33.8	13.6	44.7	55.2	45.4	83.0	26.0	45.9	51.1	43.1
Jul	20.0	22.7	21.3	21.3	24.1	21.0	18.8	34.2	16.8	30.2	11.4	20.2	17.5	12.8	19.7	18.0	15.5	12.6	27.5	23.7	16.8	35.0	23.6	16.4	19.4	20.9
Aug	27.8	13.5	24.1	9.4	16.2	11.5	14.7	16.5	15.1	21.0	11.0	12.6	18.9	7.8	9.8	19.5	11.2	11.5	21.0	16.8	11.8	16.8	27.0	14.3	12.4	15.8
Sep	14.5	14.4	16.6	10.0	19.3	9.7	8.4	15.4	12.6	16.6	11.1	19.2	14.1	17.2	15.4	13.5	10.2	10.1	28.0	13.3	13.0	20.8	13.7	15.3	13.5	14.6
Oct	12.1	24.4	17.0	9.8	21.1	22.1	12.0	14.5	11.3	17.3	14.9	19.8	26.9	14.3	20.7	22.0	11.5	13.8	16.1	16.7	14.4	14.0	13.8	20.5	12.9	16.6
Nov	12.9	33.1	19.3	19.7	22.9	14.8	19.5	10.0	23.0	23.3	18.9	11.7	23.3	11.5	21.1	27.0	16.4	12.4	15.9	18.6	17.3	15.2	16.3	18.5	29.7	18.9
Dec	11.7	27.2	28.1	21.5	21.7	14.6	8.8	5.6	17.6	21.2	9.6	15.9	12.9	5.8	28.5	11.8	15.9	20.0	22.7	11.0	10.5	11.3	17.3	18.1		16.2
																							Annual Average			19.2

Appendix F - Monthly Pinus River Flow (m^3/s)

Measured Flows

	1998	1999	2000	2001	2002	2003	2004	2005	2006	2007	2008	avg
Jan		5.8	5.0	3.2	7.4	4.4	4.6	4.6	7.3	6.0	2.7	5.1
Feb		4.4	3.8	2.2	3.4	3.0	3.4	3.4	4.7	3.8	2.0	3.4
Mar		3.7	4.2	2.1	2.6	2.2	2.9	2.9	3.2	2.9	1.6	2.8
Apr		4.3	5.0	2.5	3.6	5.1	6.5	7.0	5.2	2.3	3.0	4.6
May		81.0	42.6	71.3	36.5	70.3	74.6	66.4	75.3	48.1	59.3	62.6
Jun		32.6	52.7	26.5	52.5	25.7	51.4	12.1	14.2	38.7	18.3	32.5
Jul		20.9	29.3	23.1	13.0	18.7	13.2	5.6	20.4	15.0	15.7	17.5
Aug		22.4	10.6	16.8	25.5	7.6	19.3	7.6	14.3	5.9	12.1	14.2
Sep		14.5	4.6	12.7	16.1	8.4	9.9	13.3	6.4	20.6	8.3	11.5
Oct		14.4	6.8	23.0	26.8	12.8	12.1	13.3	7.7	21.6	11.1	15.0
Nov	18.3	20.0	7.5	18.4	15.3	14.1	8.5	15.4	19.6	18.8	14.8	15.6
Dec	8.6	8.0	4.7	12.0	7.3	7.7	6.1	20.0	17.3	5.2	9.1	9.6
										Annual Average		16.3

Appendix G

WATFLOOD Parameter File

```
# runtime    12:16:28
# rundate  2009-11-13
ver        9.300     parameter file version number
iopt           1     debug level
itype          0     type of valley (0=floodplain, 1=no flood
numa           0     optimization 0=no 1=yes
nper           0     1=delta 0=absolute
kc             5     no of times delta halved
maxn        1001     max no of trials
errfl          0     0=rms 1=correl 2=Dv
itrc           4     tracer no GW=100,3-comp=4,6-comp=5
iiout          0
typeo          4     no of land classes optimized(part 2)
nbsn           1     no of river classes optimized (part 2)
mndr    -999.999
a2         1.000     Manning's corection for instream lakes
a3      -999.999     min water fraction for slope adjustment
a4      -999.999     river slope for water area
a5         0.984     API hourly reduction value (optimized)
a6       900.000     Minimum routing time step in seconds
a7         0.900     weighting factor - old vs. new sca value
a8         0.135     min temperature time offset
a9         0.300     max heat deficit to swe ratio
a10        1.000     uz discharge function exponent
a11        0.010     min h() for bare ground
a12        0.500     min precip rate for smearing
      riverclas
lzf   0.100E-06
pwr   0.250E+01
R1n   0.120E+00
R2n   0.280E-01
mndr  0.100E+01
aa2   0.110E+01
aa3   0.100E-01
aa4   0.100E+01
theta 0.263E+00
widep 0.300E+02
kcond 0.612E-02
      forest    wetland   wetland   water     impervious
ds    0.100E+02 0.100E+10 0.100E+10 0.000E+00 0.100E+01
dsfs  0.200E+02 0.100E+10 0.100E+10 0.000E+00 0.100E+01
rec   0.100E+01 0.100E+01 0.100E+01 0.100E+01 0.100E+01
ak    0.120E+01 0.500E+00 0.500E+00-0.100E+00 0.100E-10
akfs  0.120E+01 0.500E+00 0.500E+00-0.100E+00 0.100E-10
retn  0.100E+03 0.100E+03 0.100E+03 0.100E+00 0.100E+00
ak2   0.100E+00 0.140E-00 0.140E-00 0.140E-01 0.200E-01
ak2fs 0.200E-01 0.840E+00 0.840E+00 0.840E+00 0.200E-01
r3    0.381E+02 0.898E+01 0.898E+01 0.400E+01 0.400E+01
R3fs  0.381E+02 0.898E+01 0.898E+01 0.400E+01 0.400E+01
r4    0.100E+02 0.100E+02 0.100E+02 0.100E+02 0.100E+02
ch    0.900E+00 0.900E+00 0.900E+00 0.700E+00 0.700E+00
mf    0.220E+00 0.220E+00 0.220E+00 0.200E+00 0.200E+00
base -0.244E+01-0.250E+01-0.250E+01-0.250E+01-0.250E+01
nmf   0.200E+00 0.200E+00 0.200E+00 0.100E+01 0.200E+00
```

```
UADJ  0.000E+00 0.000E+00 0.000E+00 0.000E+00 0.000E+00
TIPM  0.200E+00 0.200E+00 0.200E+00 0.200E+00 0.200E+00
RHO   0.333E+00 0.333E+00 0.333E+00 0.333E+00 0.333E+00
WHCL  0.350E-01 0.350E-01 0.350E-01 0.350E-01 0.350E-01
fmadj     0.300
fmlow     0.600
fmhgh     1.000
gladj     0.000
rlaps     0.000
elvrf     0.000
flgev      2.00 1 = pan; 2 = Hargreaves; 3 = Priestley-Taylor
albed      0.11
aw-a       0.11       0.18       0.18       0.15       0.18
fpet       3.56       3.50       3.50       1.00       1.00
ftal       0.70       0.70       0.70       0.65       0.65
flint        1.         1.         1.         0.         1.
fcap       0.20       0.20       0.20       0.20       0.20
ffcap      0.10       0.10       0.10       0.10       0.10
spore      0.30       0.30       0.30       0.30       0.30
sublm        0.         0.         0.         0.         0.
tempa        0.
temp3      500.
tton       500.
lat.        53.
mxmn  10.4 11.3 11.7  9.9 10.8 11.6 11.2 10.9  9.4  7.7  7.3  8.9
humid 63.4 60.1 60.8 61.0 55.1 55.8 57.0 57.1 60.8 64.4 71.0 69.3
pres  95.1 95.1 95.1 95.1 95.1 95.1 95.1 95.1 95.1 95.1 95.1 95.1
ti2    jan  feb  mar  apr  may  jun  jul  aug  sep  oct  nov  dec
h1    0.51 0.51 0.51 1.31 1.31 1.51 1.61 1.61 1.61 1.61 1.11 0.51
h2    0.51 0.51 0.51 1.31 1.31 1.51 1.61 1.61 1.61 1.61 1.11 0.51
h3    0.51 0.51 0.51 1.31 1.31 1.51 1.61 1.61 1.61 1.61 1.11 0.51
h4    0.01 0.01 0.01 0.01 0.01 0.01 0.01 0.01 0.01 0.01 0.01 0.01
h5    0.01 0.01 0.01 0.01 0.01 0.01 0.01 0.01 0.01 0.01 0.01 0.01
ti3       delta        low        high parameter
ak      -0.200E+00   0.500E+00   0.400E+01   0.120E+01
ak      -0.200E+00   0.500E+00   0.400E+01   0.500E+00
ak      -0.200E+00   0.500E+00   0.400E+01   0.500E+00
ak      -0.200E+00   0.500E+00   0.400E+01  -0.100E+00
akfs    -0.200E+00   0.500E+00   0.400E+01   0.120E+01
akfs    -0.200E+00   0.500E+00   0.400E+01   0.500E+00
akfs    -0.200E+00   0.500E+00   0.400E+01   0.500E+00
akfs    -0.200E+00   0.500E+00   0.400E+01  -0.100E+00
rec     -0.200E+00   0.500E+00   0.400E+01   0.100E+01
rec     -0.200E+00   0.500E+00   0.400E+01   0.100E+01
rec     -0.200E-01   0.200E-01   0.200E+00   0.100E+01
rec     -0.200E-01   0.200E-01   0.200E+00   0.100E+01
r3      -0.200E-01   0.200E-01   0.200E+00   0.381E+02
r3      -0.200E-01   0.200E-01   0.200E+00   0.898E+01
r3      -0.200E-01   0.200E-01   0.200E+00   0.898E+01
r3      -0.200E-01   0.500E+01   0.500E+02   0.400E+01
fpet     0.500E-01   0.500E+00   0.500E+01   0.356E+01
fpet    -0.500E-01   0.500E-01   0.500E+01   0.350E+01
fpet    -0.500E-01   0.500E-01   0.500E+01   0.350E+01
fpet    -0.500E-01   0.500E-01   0.500E+01   0.100E+01
```

ftal	0.500E-01	0.100E+00	0.500E+01	0.700E+00
ftal	-0.500E-01	0.700E+00	0.500E+01	0.700E+00
ftal	-0.500E-01	0.700E+00	0.500E+01	0.700E+00
ftal	-0.500E-01	0.700E+00	0.500E+01	0.650E+00
mf	-0.200E-01	0.500E-01	0.250E+00	0.220E+00
mf	-0.200E-01	0.500E-01	0.250E+00	0.220E+00
mf	-0.200E-01	0.500E-01	0.250E+00	0.220E+00
mf	-0.200E-01	0.500E-01	0.250E+00	0.200E+00
base	-0.100E+00	-0.500E+01	0.500E+01	-0.244E+01
base	-0.100E+00	-0.500E+01	0.500E+01	-0.250E+01
base	-0.100E+00	-0.500E+01	0.500E+01	-0.250E+01
base	-0.100E+00	-0.500E+01	0.500E+01	-0.250E+01
nmf	-0.100E-03	-0.400E+01	0.000E+00	0.200E+00
nmf	-0.100E-03	-0.400E+01	0.000E+00	0.200E+00
nmf	-0.100E-03	-0.400E+01	0.000E+00	0.200E+00
nmf	-0.200E-01	0.100E+00	0.200E+00	0.100E+01
retn	0.500E+00	0.100E+01	0.200E+03	0.100E+03
retn	-0.200E-01	0.100E+00	0.200E+00	0.800E+02
retn	-0.200E-01	0.100E+00	0.200E+00	0.800E+02
retn	-0.200E-01	0.100E+00	0.200E+00	0.100E+00
ak2	0.100E-01	0.100E-01	0.400E+01	0.100E+00
ak2	-0.200E+00	0.500E+00	0.400E+01	0.140E-01
ak2	-0.200E+00	0.500E+00	0.400E+01	0.140E-01
ak2	-0.200E+00	0.500E+00	0.400E+01	0.140E-01
ak2fs	-0.200E+00	0.500E+00	0.400E+01	0.200E-01
ak2fs	-0.200E+00	0.500E+00	0.400E+01	0.840E+00
ak2fs	-0.200E+00	0.500E+00	0.400E+01	0.840E+00
ak2fs	-0.200E+00	0.500E+00	0.400E+01	0.840E+00
lzf	-0.100E-07	0.100E-08	0.100E-04	0.100E-06
pwr	-0.500E-01	0.200E+00	0.400E+01	0.250E+01
r2n	-0.500E-02	0.500E-02	0.200E+01	0.280E-01
theta	-0.100E-01	0.100E-01	0.500E+00	0.263E+00
kcond	-0.100E-03	0.500E-02	0.500E-01	0.612E-02
a5	-0.200E+00	0.500E-01	0.200E+00	0.984E+00